POLARIZATION OBSERVATIONS OF 3C RADIO SOURCES

AND

GALACTIC FARADAY ROTATION

thesis by

William Edwin Wright

In Partial Fulfillment of the Requirements

for the Degree of

Doctor of Philosophy

California Institute of Technology

Pasadena, California

1973

(Submitted April 3, 1973)

ACKNOWLEDGMENTS

Although not directly concerned with the production of this thesis, there are three people without whose help and encouragement at crucial junctures the author would never have finished or even begun the present work. My most sincere appreciation is extended to Professor J.A. Cowen of the Department of Physics, Michigan State University, to Captain R.M. Marshall, USN, and to Commander K.B. McGee, USN.

Practically everyone connected with the Owens Valley Radio Observatory has had some influence upon the researches described here. Particular thanks go to Dr. G.A. Seielstad, research advisor for the thesis, for his suggestion of the topic and considerable help given throughout the years. Professor A.T. Moffet has also been instrumental in my work at CalTech and has provided useful suggestions many times. As well as helping with some of the data analysis problems, Dr. G.L. Berge has served as a sounding board for many ideas still in the formative stages.

The project could not have been completed without the skilled help of the Owens Valley Observatory crew headed by Wayne Hutton. Their speed and competence in preparing and maintaining the necessary equipment enabled 77 days of observations to be completed with less than one day of down time, an outstanding record. Special thanks must go to C.L. Spencer for many weekends and evenings spent making recalcitrant electronics behave.

Many have assisted with the observations. My gratitude has truly been earned by Mark Allen, John Bieging, Kwong Chu, Eric Greisen, John

Huchra, Doug Jones, Dan Packman, Jay Cee Pigg, George Purcell, Bruce Schupler, and Carol Walton, as well as by Drs. Berge and Seielstad. Faye DeWindt and Alice Fisher have made the production of this work, in all its stages, far easier through their willing help and advice on secretarial matters.

B.D. Mulhall and Ka Bing Yip of the Jet Propulsion Laboratory have proved most helpful in furnishing geomagnetic field and ionosphere information. The ionospheric data so willingly and quickly provided by A.V. da Rosa of the Stanford Electronics Laboratory is greatly appreciated.

Gordon J. Stanley, Director of the Owens Valley Radio Observatory, has provided the observing time, for which I am most grateful and have tried to repay with observations worthy of the time and funds invested. The work was supported by National Science Foundation grant GP 30400-X1 and by the Office of Naval Research contract N00014-67-A-0094-0019. The author has been partially supported by a National Science Foundation Predoctoral Fellowship accepted under the terms of the Navy Scholarship Program, SECNAVINST 1500.4C. The United States Navy has my profound appreciation for providing the opportunity for completing my work at CalTech.

For my parents, who deserve this and more,

and for Juley, who is my light.

ABSTRACT

The linear polarization properties of 206 radio sources from the 3CR Catalogue have been measured--in most cases at 21, 18 and 6 cm. The observing scheme also allowed the establishement of upper limits for the degree of circular polarization. The Owens Valley Radio Observatory 90' interferometer was used for these observations, and it operated with the many advantages of a crossed-feed interference polarimeter over a single-dish system.

With the use of all available data, the Faraday rotation measures of 354 radio sources, mostly extragalactic, have been computed with careful attention to ambiguities and uncertainties; a novel quality grading system has been employed. These rotation measures constitute a powerful probe of the magnetic field structure and electron density of the local spiral arm. If the electrons in the local regions of the galaxy form a disk 200 pc in thickness and 2 kpc in radius, then there is a uniform, linear component of the galactic field in the direction $l = 94° \pm 3°$, $b = -8° \pm 8°$ with a strength of $n_e B = 0.12$ electrons-cm^{-3}-μgauss, or $B = 2.0$ μgauss for $n_e = 0.06$ cm^{-3}. Distributions of the differences between this model and the actual rotation measures show that regions of magnetic loops and field reversals or electron concentrations of 100 to 200 pc in size have values of $n_e B$ two to three times that of the average linear field of the model, implying a high degree of disorder. Most of the very large rotation measures seem to be produced by small-scale structure in the galaxy, although a very few may be intrinsic to

the source. The linear field model compares well with hydrogen line Zeeman splitting, pulsar dispersion and rotation measures, and other magnetic field data. The apparent discrepancy with field structures given by stellar polarization can be resolved by differences in the distributions of electrons and dust and by the large-scale loops and field reversals.

Searches for correlations between rotation measure and source type, depolarization, or redhsift have all led to negative results. The upper limit for a uniform, linear component of the intergalactic magnetic field, based on the failure of the last correlation, is $n_e B < 2 \times 10^{-13}$ cm^{-3} gauss.

CONTENTS

CHAPTER I

INTRODUCTION TO FARADAY ROTATION

A. Introduction

Magnetic fields play important roles in the dynamics and evolution of many astrophysical phenomena; indeed, they can be the dominate forces. The spiral structure is doubtlessly closely linked with the intensity and form of the associated magnetic field. Whether there was a field existing before the epoch of galaxy formation or such fields were created or greatly intensified by the evolution of such large-scale concentrations of matter is a question of prime importance to one studying the mechanics of galactic structure and cosmology. If magnetic field strengths of a few microgauss exist throughout the galaxy, then the mean energy density of the fields is on the order of 10^{-12} ergs/cm^3, which is identical with the energy density of cosmic rays (Spitzer, 1968), an order of magnitude greater than the total energy density of starlight (Spitzer, 1968) and the 3° K microwave background radiation, two orders of magnitude greater than the thermal energy of H I regions (based on data from Spitzer, 1968), but four orders of magnitude less than the galactic gravitational binding energy of the average mass density in the solar neighborhood (based on data from Schmidt, 1965b). Thus, while the overall structure of the galaxy will be largely determined by gravitational effects, magnetic fields will be at least as important as other phenomena in determining the energetics and evolution of the system.

Therefore, a sound knowledge of the magnetic fields is a prerequisite to a detailed understanding of galactic structure.

Faraday rotation of the polarized radiation from extragalactic radio sources constitutes a powerful probe for examining magnetic field structures and electron distributions. The plane of polarization of linearly polarized radiation passing through a region containing both magnetic fields and charged particles is rotated by an angle directly proportional to the line-of-sight integral of the product of the field strength and particle density and proportional to the square of the wavelength of the radiation. This phenomenon is termed "Faraday rotation" in honor of its discoverer.

If observations of the position angle of the polarized radiation from a radio source were available at several different frequencies, the idealized plot of the position angle versus the square of the wavelength would be a straight line. The slope of the line in units of rad/m^2 is defined as the "rotation measure". A positive rotation measure indicates a field directed towards the observer for negatively charged particles; a negative value, a field away from the observer. The magnitude provides the product of the magnetic field strength and the electron density. Prior to the present work many such measurements of the Faraday rotation of galactic and extragalactic radio sources have been made.

By 1963 enough data had been collected to enable Gardner and Whiteoak (1963) to demonstrate the dependence of the magnitude of the rotation measure upon the galactic latitude of the radio source. Figure 1-1 shows this dependence for the data known in 1966. Since sources closer to the

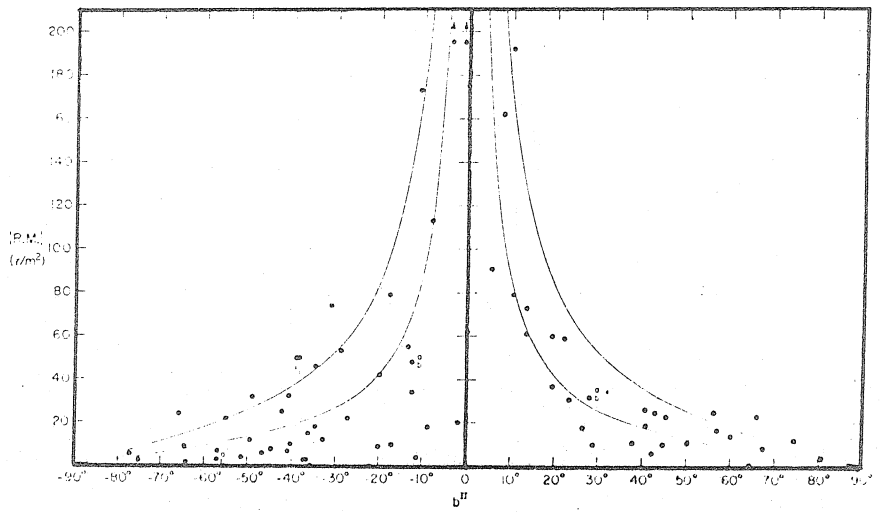

Fig. 1-1.--Dependence of the absolute values of the rotation measures on galactic latitude. The curves are given by $|RM| = 30|\cot b|$ and $|RM| = 15|\cot b|$. From Berge and Seielstad (1967).

galactic plane tended to have greater rotation measures, the probability of some, if not all, of the Faraday rotation's taking place within our galaxy seemed to be high.

By 1964 enough polarization data had been accumulated to enable the calculation of the rotation measures for 37 sources. Morris and Berge (1964a) were able to show that, on the basis of these data, a somewhat loose dependence of rotation measure upon galactic longitude existed. This dependence seemed to indicate a field directed along the local spiral arm above the galactic plane, and in the opposite direction below the plane. This was later supported by Berge and Seielstad (1967) on the basis of approximately 80 sources. As Hornby (1966) indicated, these observations could be explained by a highly sheared helical field of small pitch angle with axis directed along the arm. This was reassuring since the interstellar polarization of starlight caused by mag-

netically aligned dust grains could also be explained in terms of a similar helical field (Mathewson, 1969). Figure 1-2 shows the data of Berge and Seielstad (1967) plotted on galactic coordinates.

Unfortunately there was no unanimity among interpreters of the polarization data. Gardner and Davies (1966) offered an alternate interpretation based upon data yielding 86 rotation measures, some of which were considered by Berge and Seielstad (1967) to be questionable on the basis of additional data. For their 86 sources, Gardner and Davies postulated a linear field directed towards $l = 95°$ at latitudes lower than 20°.[1] This is supposed to be a linear field along the spiral arm extending 100 pc above and below the plane. At intermediate latitudes the field points in the opposite direction; there are other complicating features which are rather difficult to justify on the basis of the extremely limited data.

In 1969 Gardner, Morris, and Whiteoak (1969a) published the results of a very extensive survey of the polarization properties of Parkes radio sources at several frequencies. Using these new data, they derived rotation measures for more than 200 sources and interpreted (Gardner, Morris and Whiteoak, 1969b) the galactic distribution of these as being due to a linear field along the local arm with a loop in the neighborhood of the north galactic spur. Figure 1-3 shows the plot of their data and indicates that things were becoming fairly complicated by this time.

---

[1]New galactic coordinates, l^{II} and b^{II}, are used throughout this paper. The 'II' has been deleted.

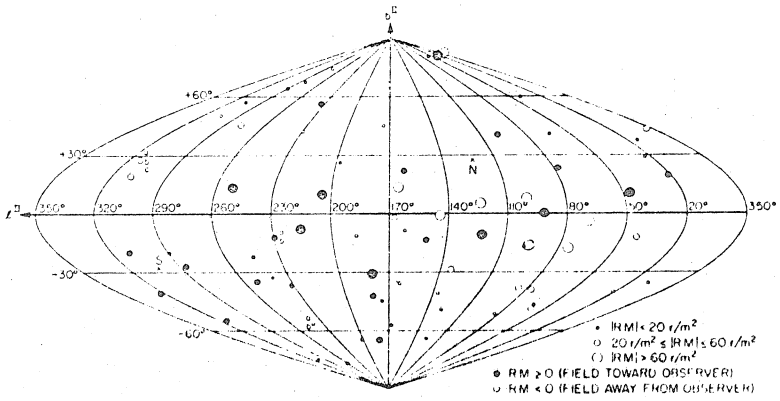

Fig. 1-2.--Galactic distribution of the rotation measures of extragalactic radio sources. From Berge and Seielstad (1967).

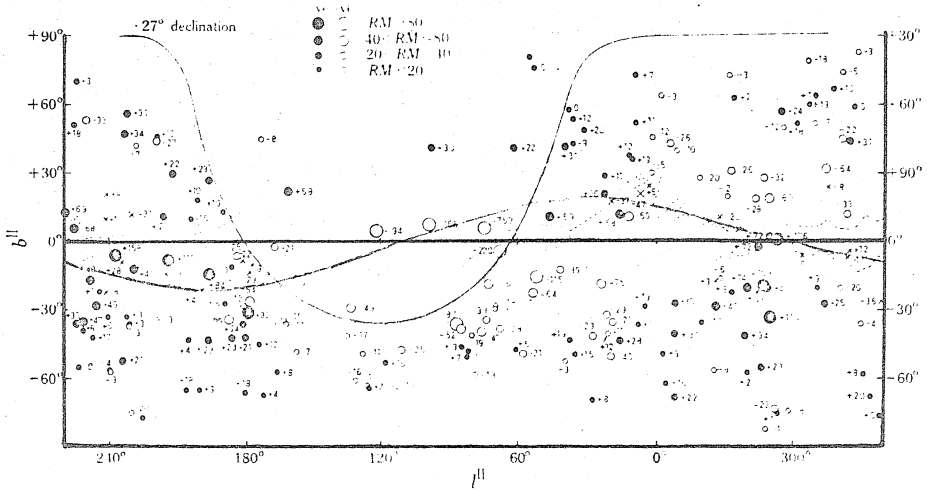

Fig. 1-3.--Galactic distribution of the rotation measures of extragalactic radio sources. Also shown are the +27° declination limit of the Parkes data, contours of neutral hydrogen and Gould's Belt. From Gardner, Morris and Whiteoak (1969b).

At this time very little information was available for northern hemisphere sources, and the quality, as well as the quantity, of the data was not sufficient for the degree of interpretation taking place. The data shown in figure 1-3 include many sources for which polarization data at only two frequencies existed. Since an individual polarization measurement is always ambiguous by any multiple of 180°, the position angles taken were those yielding the smallest possible absolute value of the rotation measure. Even some of the rotation measures based upon three or more polarization measurements were similarly ambiguous. Since the method used for deciding the proper rotation measure required the value to match the neighboring points as closely as possible, the map is no longer quite so imposing. However, if rotation measures which were ambiguous were eliminated from the plot, there no longer remained sufficient data to allow the determination of very much about the structure of the field in the local arm.

The present work was conceived as an effort to close the gap in the data in the northern hemisphere and to upgrade the quality of the "known" rotation measures in the hopes of resolving the local magnetic field structure. For that purpose, plans were made to measure the polarization parameters of as many new sources as possible in the northern hemisphere and to include observations of some sources for which the present data were not sufficient to obtain reliable rotation measures.

At the time of the inception of this project, some new interpretations of the rotation measures were put forth. While almost all of the Faraday rotation observed in an average source was felt to be caused

by our own galaxy, there was enough scatter in the data for some to suspect that some rotation originated either within the source or within the intergalactic medium. Sofue, Fujimoto and Kawabata (1969) and later Reinhardt and Thiel (1970) believed that they had obtained a correlation of rotation measure with redshift. Reinhardt and Thiel felt the evidence supported a uniform, linear component of an intergalactic magnetic field running from $l = 280°$, $b = +30°$ to $l = 100°$, $b = -30°$ with a magnitude less than 1 to 3 x 10^{-7} gauss. These deductions were based on somewhat unreliable rotation measures, as described above. If the unreliability of the data is disregarded, the statistics or the correlation are still marginal. The existence of such a field is of such cosmological importance, however, that this method of detecting intergalactic magnetism ought to be very carefully examined.

This possible correlation provided a very sound reason to restrict the polarization observations to that group of sources for which more redshifts are known than for any other--the 3CR survey sources. The number of these sources for which no adequate data were available was sufficient to occupy the entire observing program.

Since the initiation of the program, several other papers have appeared on the subject of the rotation measures of extragalactic and have set forth some novel interpretations. The need for more reliable data and increased skepticism for the methods of deciding upon the proper rotation measures has become very apparent.

B. Polarization Notation

The polarization characteristics of any electromagnetic wave may be described in several fashions, some of which are particularly useful for the present purposes. The most common way to present polarization data is to specify the fraction, p, and position angle, ψ, of the linearly polarized component, the fraction (including sign) of the circularly polarized component, and the total flux density. These four parameters completely specify the polarization state of the electromagnetic waves, and are useful in comparisons with physical properties of the source and in calculating the Faraday rotation parameters. This scheme is not, however, particularly convenient for understanding the origins of the polarization, the propagation of the wave through a magneto-plasma, or the method of observing the polarization.

To gain a better understanding of polarization processes, it is useful to consider two orthogonal directions, x and y, in a plane perpendicular to the path of the radiation. For the polarized portion of the radiation only, the electric field can be expressed as

$$\underline{E} = E_1 \sin(\omega t)\,\hat{x} + E_2 \sin(\omega t + \delta)\,\hat{y} \qquad (1\text{-}1)$$

where $\hat{x}$ and $\hat{y}$ are unit vectors, ω is the circular frequency of the radiation, and E_1, E_2 and δ are constants. For $\delta = 0$, the electric vector is that of linearly polarized radiation with position angle $\psi = \tan^{-1}(E_2/E_1)$, and $\psi = \tan^{-1}(-E_2/E_1)$ for $\delta = \pi$. For $\delta = \pi/2$ and $E_1 = E_2$, the wave is circularly polarized in the right-hand sense, i.e., clockwise rotation when viewed in the direction of propagation. The left-hand sense is given by $\delta = 3\pi/2$. Any other combination of these three constants yields

an electric vector which follows an elliptical path with time; and, of course, the situations detailed above are but special cases of elliptical polarization.

The fourth constant which must be specified in this notation is the amount of unpolarized radiation present. The electric vector for this radiation may be written as

$$\underline{E}_{unpol} = E_a(t) \sin[\omega t + \delta_1(t)]\, \hat{x} + E_b(t) \sin[\omega t + \delta_2(t)]\, \hat{y} \qquad (1\text{-}2)$$

where E_a, E_b, δ_1 and δ_2 are independent, randomly varying functions of time. The r.m.s. value of $\underline{E}_{unpol}$ is sufficient to specify the unpolarized radiation. Although these four constants, E_1, E_2, $\langle E^2_{unpol} \rangle$, and δ, illustrate the structure of the wave quite well, they are not the most convenient for analysis.

The Stokes parameters are a set of four constants based upon the time-averaged electric vectors:

$$\begin{aligned} I &= \langle E_x^2 \rangle + \langle E_y^2 \rangle \\ Q &= \langle E_x^2 \rangle - \langle E_y^2 \rangle = Ip \cos 2\psi \\ U &= \langle 2E_x E_y \rangle \cos \delta = Ip \sin 2\psi \\ V &= \langle 2E_x E_y \rangle \sin \delta \end{aligned} \qquad (1\text{-}3)$$

where E_x and E_y are the instantaneous components of the total electric field, polarized and unpolarized:

$$\begin{aligned} E_x &= E_1 \sin(\omega t) + E_a(t) \sin[\omega t + \delta_1(t)] \\ E_y &= E_2 \sin(\omega t + \delta) + E_b(t) \sin[\omega t + \delta_2(t)] \end{aligned} \qquad (1\text{-}4)$$

I is the total intensity, Q and U determine the linear polarization, and V determines the circular. The utility of these parameters will be made clear in the section dealing with the observing method and data reduction.

One final notation that will be useful in examining the linearly polarized emission of radio sources is the complex polarization

$$P = p \exp(2i\psi) = \frac{Q + iU}{I} \qquad (1\text{-}5)$$

which expresses the linear polarization only.

All of these notations are in common usage. For more detailed information consult Kraus (1966) or Gardner and Whiteoak (1966).

C. Faraday Rotation and Depolarization Mechanisms

This section presents a description of the origins of Faraday rotation and the various depolarization mechanisms, largely without derivations. For a detailed examination of many aspects of the polarization of radio sources, the review article by Gardner and Whiteoak (1966) is excellent. The paper by Burn (1966) provides sound information on the subject of Faraday depolarizations, and the series of papers by Pacholczyk and Swihart (1967, 1970, 1971 and 1973) covers many topics for careful readers.

The normal modes for propagation of electromagnetic waves within a magneto-ionic medium are determined by the relative values of the frequency of the wave, the plasma frequency, $\omega_p^2 = 4\pi ne^2/m$, the electron gyro frequency, $\omega_B = eB/mc$, and the collisional frequency, ν_c, where gaussian units are used throughout. Typical values for media of present interest are given in Table 1-1. In every case the collisional frequency is so much smaller than the others (ν_{obs} is always greater than 400 MHz) that collisions may be neglected. The real part of the index

TABLE 1-1

PARAMETERS FOR SELECTED MAGNETO-IONIC MEDIA

	Neutral H Region	H II Region	Ionosphere
T	10^2 °K.	10^4 °K.	10^2-10^3 °K.
n_e	10^{-2} cm^{-3}	1 cm^{-3}	10^6 cm^{-3}
ν_c	10^{-7} Hz	10^{-4} Hz	10^2-10^3 Hz
B	10^{-5}-10^{-6} g.	10^{-5}-10^{-6} g.	0.5 g.
ω_B	10-100 s^{-1}	10-100 s^{-1}	10^7 s^{-1}
ω_p	10^3 s^{-1}	10^4 s^{-1}	10^7 s^{-1}
θ_{400}	10^{-2} rad.	10^{-2} rad	10^{-2} rad.

of refraction for the magneto-ionic medium can then be expressed as the $\nu_c = 0$ approximation of the Appleton formula (see Davies, 1966, for a derivation and more complete explanation of the following treatment):

$$\mu^2 = 1 - \frac{2X(1-X)}{2(1-X) - Y_T^2 \pm \sqrt{Y_T^4 + 4(1-X)^2 Y_L^2}} \qquad (1\text{-}6)$$

where $X \equiv \omega_p^2/\omega_o^2$, $Y_L \equiv C(\omega_B/\omega_o)\cos\theta$, $Y_T \equiv c(\omega_B/\omega_o)\sin\theta$, ω_o is the circular frequency of the wave, and θ is the angle between the line-of-sight and the direction of the magnetic field. In all the cases of Table 1-1, the media are so tenuous that B and H are equivalent.

Two normal modes of propagation are permitted here and are called the "ordinary wave" and the "extraordinary wave". Their exact compo-

sitions are difficult to derive so that in practice one of two approximations is made. Either the "quasi-longitudinal" solution or the "quasi-transvers" solution will often apply. The criteria for determining which approximation is appropriate are

$$\begin{aligned} &\text{Quasi-longitudinal} \quad Y_L \ll 4(1-X)^2 Y_L^2 \\ &\text{Quasi-transverse} \quad Y_T \gg 4(1-X)^2 Y_L^2 \end{aligned} \tag{1-7}$$

In Table 1-1, θ_{400} is the maximum value of $|\theta-\pi/2|$ for which the quasi-longitudinal (QL) case does not apply at 400 MHz. As can be seen, the QL solution is sufficient for almost all possibilities except when the magnetic field lies exactly at right angles to the line-of-sight, a vanishingly slight probability.

For QL propagation, the two normal modes are plane-waves with opposite senses of circular polarization. The ordinary wave is that with right-hand polarization for a wave traveling in the direction of $\underline{B}$. The indices of refraction for the two waves are given by

$$\mu = \left(1 - \frac{X}{1 \pm Y_L}\right)^{1/2} \tag{1-8}$$

This causes a difference in phase for the two circularly polarized waves as they traverse the medium; and, since a linear polarization can be represented as the sum of the two circular polarizations with relative phase determining the position angle, the phase differential causes a rotation of the plane of linear polarization. For all cases of Table 1-1 μ is very close to unity so that the expansion

$$\mu \simeq 1 - \frac{1}{2} X(1 \mp Y_L) \tag{1-9}$$

is valid. This yields

$$\Delta\mu = \mu_+ - \mu_- \simeq XY_L = XY \cos\theta \qquad (1\text{-}10)$$

so that the position angle of a linearly polarized wave is given by

$$\psi = \psi_o + RM \cdot \lambda^2 \qquad (1\text{-}11)$$

where RM is the "rotation measure" and is given by

$$RM = K \int n\underline{B} \cdot d\hat{l} \qquad (1\text{-}12)$$

where the integral is along the line-of-sight. Notice that the sense is such that RM is positive for propagation in the direction of the magnetic field. An observer sees positive rotation measures when looking against the field and negative ones when looking along the field. The "intrinsic position angle", ψ_o, is the position angle of the polarization of the wave before it entered the magneto-ionic medium. The constant K is 2.62×10^{-13} for c.g.s.-gaussian units throughout, except that RM is expressed in rad/m^2. For astrophysical purposes, it is convenient to take $K = 8.12 \times 10^5$ for n in electrons/cm^3, B in gauss, and l in pc. This derivation has assumed that the negatively-charged electrons cause all the rotation. Positive protons cause rotation in the opposite sense, but the factor of $1/m^2$ makes such rotation only 10^{-6} that of the electron.

As long as the region of Faraday rotation is external to the source of polarized radiation and is uniform across the angular extent of the source, the rotation has no effect upon the degree of polarization.

When these conditions are not met different portions of the emitting region experience differing degrees of Faraday rotation. Therefore, at progressively longer wavelengths, the polarization vectors of small sections of the source will diverge more and more, yielding a lower net degree of polarization. This is the source of Faraday depolarization.

Burn (1966) defines the rotation depth for emission from a point $\underline{r}$ as

$$\phi(\underline{r}) \equiv K \int_0^r n\underline{B}\cdot\hat{d\underline{r}} \qquad (1\text{-}13)$$

so that the position angle, as seen by the observer, of the emission from point $\underline{r}$ is

$$\psi(\underline{r},\lambda) = \alpha(\underline{r}) + \phi(\underline{r})\lambda^2 \qquad (1\text{-}14)$$

where $\alpha(\underline{r})$ and $\phi(\underline{r})$ are the intrinsic position angle and rotation depth for the radiation emitted in the volume element at $\underline{r}$. This formulation allows the complex linear polarization of the integrated source to be expressed simply as

$$P(\lambda^2) = \frac{\iint \varepsilon(\underline{r},\lambda)\ p(\underline{r})\ \exp\{2i[\alpha(\underline{r}) + \phi(\underline{r})\lambda^2]\}dv}{\iint \varepsilon(\underline{r},\lambda)\ dv} \qquad (1\text{-}15)$$

where $\varepsilon(\underline{r},\lambda)$ is the volume emissivity at the point $\underline{r}$ and wavelength λ in the direction of the observer. This integration can be performed for simple models, the most illustrative of which is the case in which the emitting region consists of a slab at right angles to the line-of-sight. The emission (from relativistic electrons) and the Faraday rotation (from thermal electrons) are assumed to be uniformly distributed. The magnetic field is also assumed to be uniform. Figure 1-4 illustrates

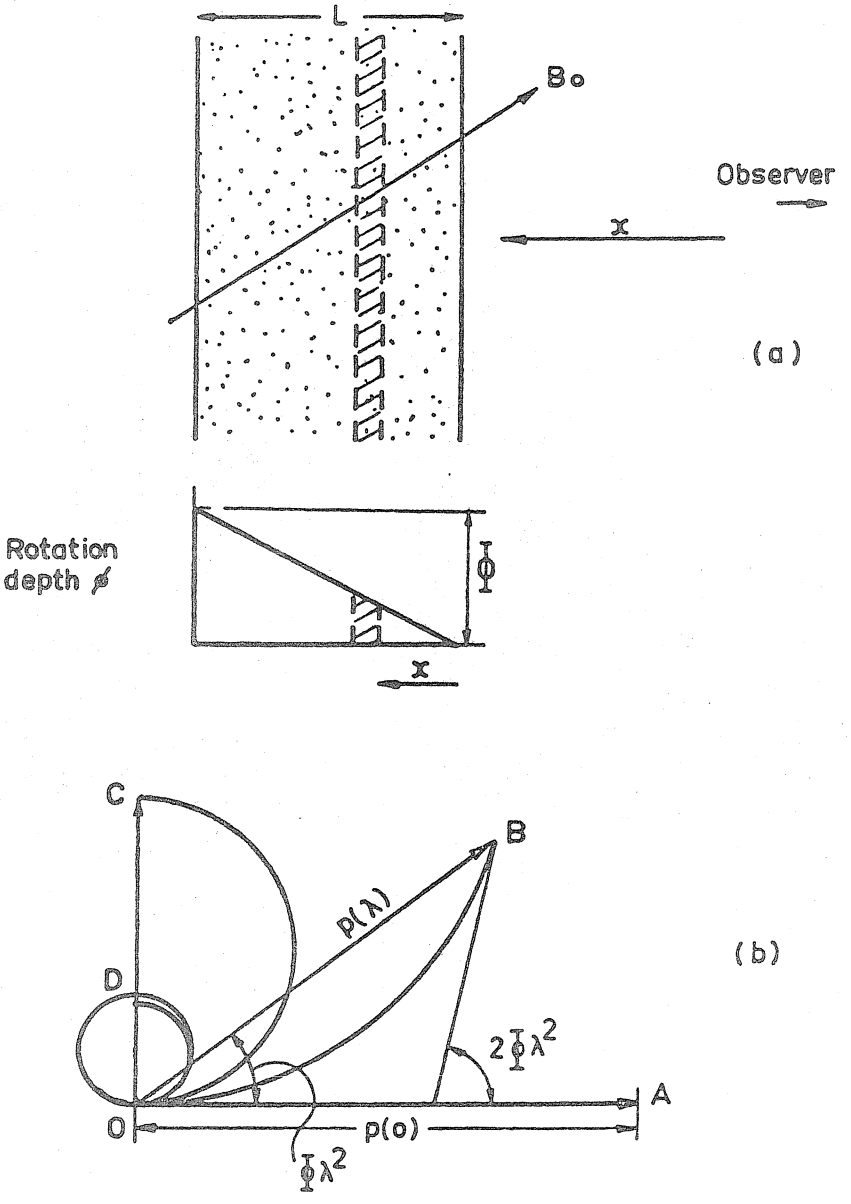

Fig. 1-4.--(a) Illustrates the uniform slab described in the text. The resultant Fraunhofer vector diagram is shown in (b). From Gardner and Whiteoak (1966).

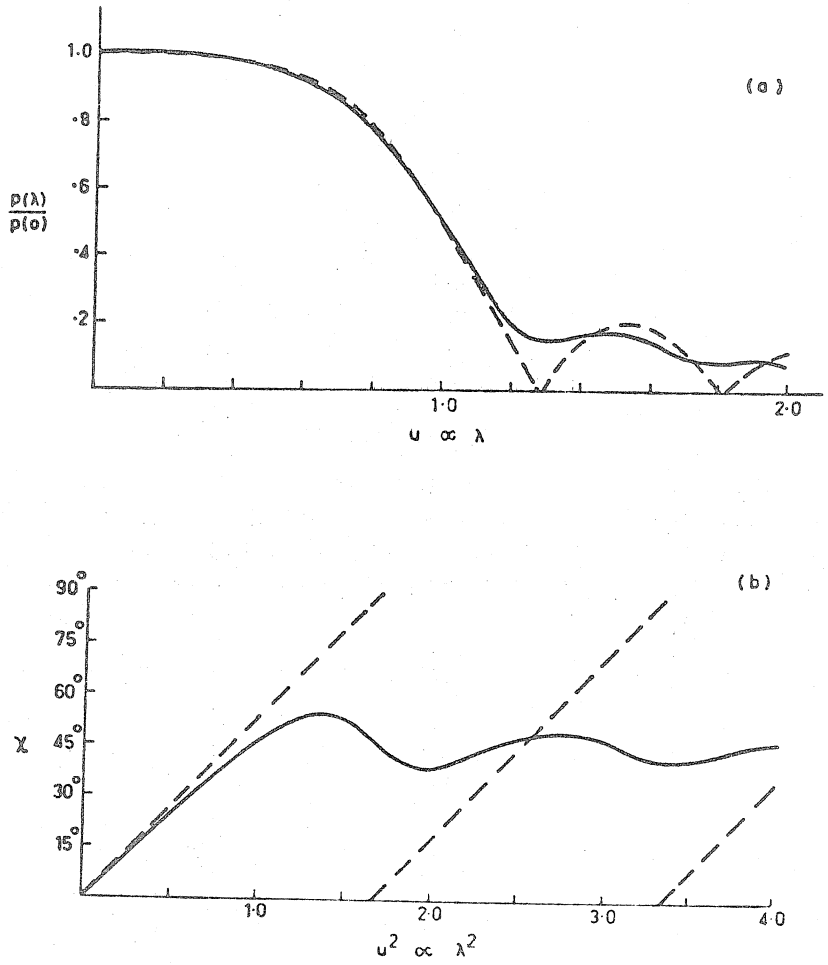

Fig. 1-5.--The relative degree of polarization for the rectangular slab of Figure 1-4 is shown in (a). The broken line gives the result for the slab while the solid line shows the result for a uniform sphere. The position angles for the two cases are shown in (b). From Gardner and Whiteoak (1966).

this situation. Relativistic electrons would also contribute to the Faraday rotation with K replaced by K/γ^2, but this lowered value of K and the fact that thermal electrons are usually considerably more populous mean that the rotation due to the relativistic electrons is generally insignificant. In the case indicated by Figure 1-4, equation 1-15 yields $P(\lambda^2)$ as shown in Figure 1-5. The complex polarization for a uniform spherical emission/rotation region is also shown. Further examples are given by Gardner and Whiteoak (1966) for distributions which differ for thermal and relativistic electrons. The important facts to consider here are that Faraday depolarization always leads to a degree of polarization which eventually decreases with increasing wavelength and that the position angle of the integrated polarized radiation is usually expected to be linear with λ^2 only at wavelengths shorter than that at which the source has depolarized to one-half to one-third the maximum. Polarization curves which show plateaus at high or low frequencies can be explained by Faraday depolarization as well as by other means.

There are other mechanisms of depolarization. An obvious one would affect a source that has two or more components with differing degrees of polarizations and power spectra. Such a source could either decrease or increase in degree of polarization with wavelength, or could be nearly constant but have a non-linear position angle curve. Both Burn (1966) and Gardner and Whiteoak (1966) discuss this possibility. The Pacholcsyk and Swihart papers have explored the effects of other phenomena such as synchrotron self-absorbtion, which can lead to a nearly con-

stant, non-zero polarization after the initial depolarization. At present it is difficult to separate these various processes since several may lead to exactly the same wavelength dependence for the polarization and since they may all be contributing to a single source. This topic will be further discussed in Chapter IV. The basic fact that the rotation curve ought to be nearly linear until the source is 50% or more depolarized can, however, provide clues to the nature of the sources and the constitution of the intervening medium.

CHAPTER II

THE OBSERVATIONS

A. Selection of Sources and Frequencies

Selection of sources requires that the objectives of the project be clearly stated. The primary purpose of this research was to obtain as many reliable and previously unknown rotation measures of the integrated polarization of radio sources as possible in order to probe possible galactic and intergalactic magnetic fields. Secondary goals were to increase the knowledge of the integrated polarization parameters of the 3CR list of radio sources, preferably making complete a survey of all 3CR sources down to a given limit of the flux density of polarized radiation, and to confirm certain previously measured polarization parameters. Although not an original objective, a search for circular polarization was a by-product since the observing scheme was sensitive to all Stokes parameters.

Polarization observations of the 3CR sources were quickly discovered to be far from complete. In fact, the 3CR sources for which reliable rotation measures could not be calculated on the basis of existing data were sufficient almost the whole of the observing list. These sources are particularly interesting due to the high percentage of known identifications and redshifts. All 3CR sources for which adequate data were felt to exist were discarded from the list as were sources showing structure greater than three minutes of arc in the east-west

direction so that resolution effects would not be significant at 100' E-W spacing and 5000 MHz. Only two sources observed were partially resolved. The only source discarded from the list on the basis of low flux density was 3C318.1, which has an unusually steep spectrum. As the observations progressed, additional selection criteria were used to eliminate some of the sources from the later observing sessions, as will be explained shortly.

Although some time was spent in determining the best possible set of frequencies to allow the unambiguous determination of the rotation measure, the actual selection of the observing frequencies was dictated by the available receivers. In particular, the 18 and 21 cm parametric receivers had the best sensitivity, stability and reliability of those available. The ideal third frequency for unambiguous Faraday rotation determinations would have been between 10 and 13 cm, but low-noise equipment was not available in that range. With three weeks of observations at each of 18 and 21 cm, and with about 200 sources, an ultimate r.m.s. noise level of about 0.003 flux units could be expected. An hour of observation for each of the two senses of polarization would provide this level based on the parameters given in Table 2-2 with a 10 MHz bandwidth. In practice uncertainties in excess of 10° in the measured position angle of the polarization cause multiple ambiguities to enter the rotation measure calculations, and measurements with standard errors greater than 20° are virtually worthless. Many of the sources are only one or two flux units at 18 and 21 cm. Such a source with a 2% linear polarization could then yield an unambiguous rotation measure calculation.

Excellent parametric receivers for 8000 MHz were available, but most sources are so weak at this frequency that a polarization in excess of 10 to 15% would be required to obtain adequate results within the observing time allotted. The 6 cm paramps, with a noise temperature of about 150° K., were finally selected by Hobson's choice. As explained in Chapter III, this selection of frequencies would give no ambiguities in the rotation measure determination under ±250 rad/m^2 assuming uncertainties of 5 to 10° in position angle. Also, a 0.5 fu source with 5% linear polarization could be expected to provide satisfactory results, because the observing time could be increased. Many of the sources already had 6 cm polarization data supplied by Gardner, Morris and Whiteoak (1969b) and others, so that they could be deleted from the source list. Additionally, no calibrating sources would be observed at 6 cm, as described in the section on instrumental polarization. This provided more time. Finally the last selection criterion came into effect; those sources which had shown insufficient polarization at 18 or 21 cm could be dropped.

B. Equipment and Observing Method

The Owens Valley Radio Observatory interferometer consists of two 90' parabolic antennas mounted on two tracks at right angles permitting spacings as large as 2200' E-W or 1600' N-S. This interferometer has been described in detail by Read (1963) and many others. In addition, there is a 130' parabolic antenna 3500' east of the intersection of the two interferometer tracks. This antenna may be used separately or as an

element of the interferometer in conjunction with one or both of the 90' antennas.

Many of the difficulties of single-dish polarimetry, notably the highly polarized ground spillover and the galactic background radiation, can be eliminated by the use of an interferometer, the elements of which have feeds of opposite senses of polarization. Since the objective of the observations was to measure the polarization parameters of the integrated radiation from radio sources, the higher resolution of the interferometer would be a handicap, not an advantage. Therefore, the ideal instrument for polarization studies would be the 90' interferometer with the antennas set at 100' E-W, the closest spacing possible. The N-S spacings would be impractical due to the shadowing of the north dish by the south for low declination sources. The 100' E-W spacing prohibits the tracking of sources for more than $1^h\ 40^m$ either side of transit, but this proved no handicap with the proposed observing scheme.

Although, for resolution purposes, the 100' spacing would have been ideal, solar radiation was found to interfere severely with the observations at 21 cm during the hours when the sun was near the zenith. In order to reduce this effect, the spacing was changed for some of the low frequency observations to 200' E-W so that the sun would be more completely resolved. This provided considerable relief and did not affect the observations in any way since sources were generally less than 3' in diameter.

The focus of each antenna contained the parametric receiver

packages with linearly polarized feed horns attached. The entire receiver package was mounted in a rotating ring with remote control and readout in the observing room. Each feed could be independently rotated through an arc of 360°. The readout was in hundredths of degrees and was repeatable, as checked with a sensitive level, to about 0.02°. The zero reference of the readout was fixed and did not vary at any time during the entire year during which observations were made. The physical orientation of the feed horns was compared with the indicator by means of a level whenever the receiver packages were newly mounted.

Figure 2-1 is a block diagram for the interferometer as used for the polarization observations. The receivers worked double sideband, single conversion to an intermediate frequency of 10 MHz with a bandpass of approximately 5 MHz located 10 MHz either side of the local oscillator frequency. The local oscillator was generated in the base of each antenna by phase-locking an oscillator one MHz above the appropriate harmonic of a 30 to 31 MHz signal, which was adjusted to obtain the desired L.O. frequency. Both the 30 MHz and 1 MHz references were generated in the observing room, with the 1 MHz line to one antenna running through a phase-shifter. This phase-shifter was computer-driven to create an artificial fringe rate of 1/60 Hz.

The response of such an interferometer to a distribution of unpolarized radiation has been described by Moffet (1962). Following the notation of Morris, Radhakrishnan and Seielstad (1964), the response is given by

$$\underline{R}(t) = \frac{1}{2} G(t)\, A\, S_I'\, \underline{\beta}_I(s_x, s_y) \exp\left[i(-2\pi\, s_x\, \Omega\, t + \psi(t)\right] \qquad (2\text{-}1)$$

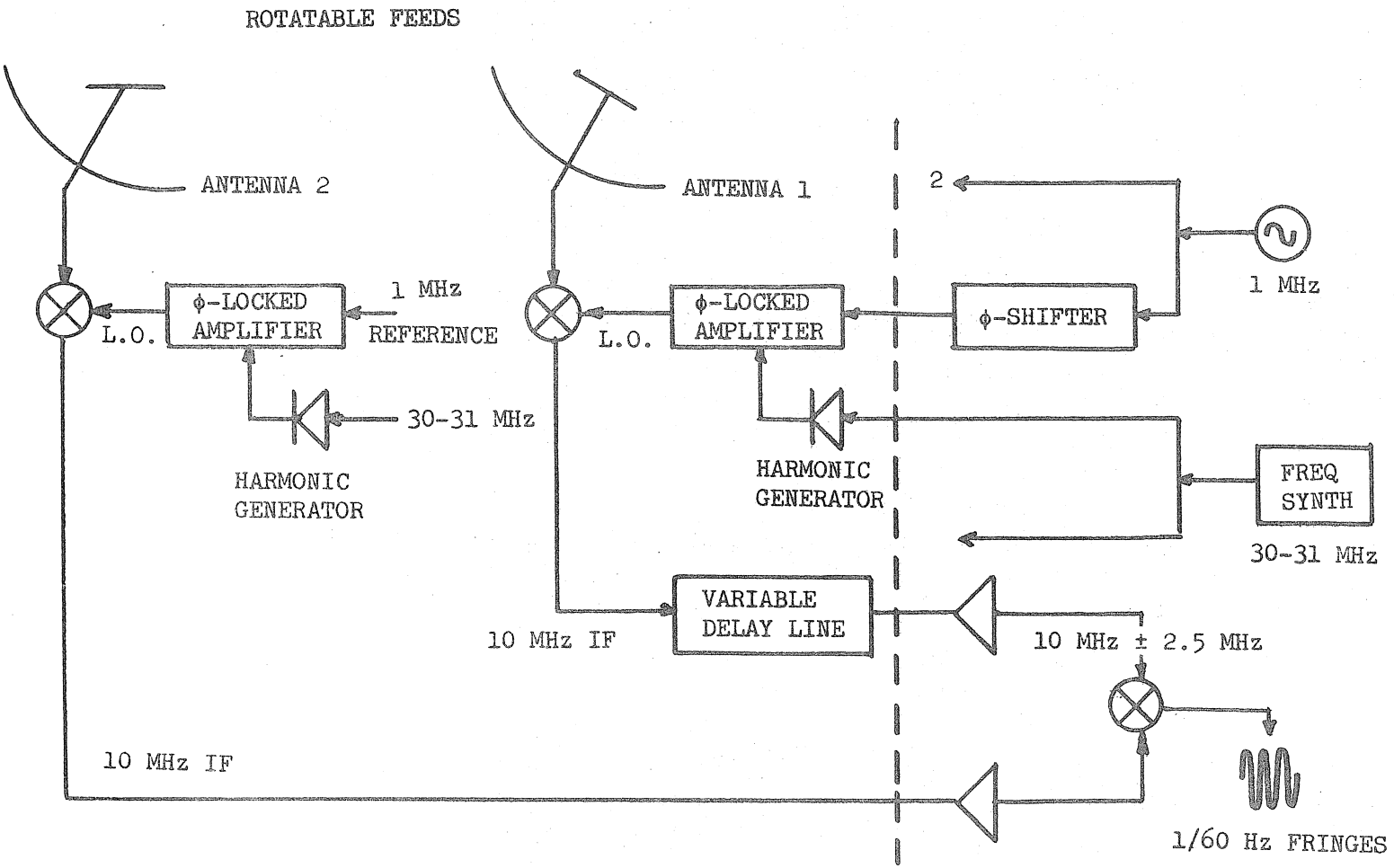

Fig. 2-1.--Block diagram of the interferometric polarimeter. The components to the right of the broken line are located in the observing room. The west antenna is number 1.

where $A = \sqrt{A_1 A_2}$, the geometric mean of the antenna areas, S'_I is the integrated flux of I, the total intensity, and $\underline{\beta}_I(s_x,s_y)$ is the complex visibility function for the distribution of I. The components of the interferometer spacing in wavelengths are given by s_x and s_y, while G(t) and $\psi(t)$ are the receiver gain and instrumental phase, respectively. These last two are, in practice, slowly varying functions of time. They will be considered as constants for the rest of this discussion; the effects of their variability will be examined in the next section.

The distributions of the Stokes parameters can be treated separately, and the resultant response to a polarized source distribution will be a function of all four. Morris, Radhakrishnan and Seielstad (1964) give the total response of the interferometer as

$$\begin{aligned}\underline{R}(t) = \frac{1}{2} k \{ & \underline{I} [\cos(\phi_1-\phi_2)\cos(\theta_1-\theta_2) + i \sin(\phi_1-\phi_2)\sin(\theta_1+\theta_2)] \\ & + \underline{Q} [\cos(\phi_1+\phi_2)\cos(\theta_1+\theta_2) + i \sin(\phi_1+\phi_2)\sin(\theta_1-\theta_2)] \\ & + \underline{U} [\sin(\phi_1+\phi_2)\cos(\theta_1+\theta_2) - i \cos(\phi_1+\phi_2)\sin(\theta_1-\theta_2)] \\ & + \underline{V} [\cos(\phi_1-\phi_2)\sin(\theta_1+\theta_2) + i \sin(\phi_1-\phi_2)\cos(\theta_1-\theta_2)]\}\end{aligned} \tag{2-2}$$

where $\underline{I} = S'_I \underline{\beta}_I(s_x,s_y)$. $\underline{Q}$, $\underline{U}$ and $\underline{V}$ are similarly defined for the distributions of the remaining Stokes parameters, and k is given by GA exp $[-i(2\pi s_x \Omega t + \psi)]$ and is assumed to be known. The polarizations of the two antennas are given by ϕ_1, θ_1 and ϕ_2, θ_2 where ϕ is the orientation of the major axis of the polarization ellipse and θ is the ellipticity. This is the general formula for the response of an interference polarimeter. The project undertaken here allows several simplifying assumptions to be made.

The first assumption is that $\theta_1 = \theta_2 = 0$, that is, that the antennas are both linearly polarized. This has been found to be not strictly true since there is some ellipticity of the feed-dish combination and therefore some crosstalk between linear and circular modes. Since no sources have been found to be strongly circularly polarized, and the primary purpose of this paper is not to examine circular polarizations, the effects of this departure from strict linearity is not terribly important and will be discussed later. The assumption will be treated as exact.

Next, all the sources examined are essentially point sources for the relatively short baselines used. This allows the substitution of $I = S'_I$ for $\underline{I}$, and similarly for the other Stokes parameters. That is, we are no longer dealing with complex distributions, but only with a single real value, the integrated Stokes parameter. Two errors can be introduced by this assumption: some sources are at least partially resolved, and uncertainties in the position of the centroid of the source can affect the calculation to a small degree. These problems will also be discussed in the following section.

Finally, the observing scheme utilized only those combinations of ϕ_1 and ϕ_2 involving feeds parallel or at right angles. For parallel feeds, $\phi_1 = \phi_2 \equiv \phi$, equation (2-2) reduces to

$$\underline{R}(t) = R(t) = \frac{k}{2} (I + Q\cos 2\phi + U\sin 2\phi) \qquad (2\text{-}3)$$

and is wholly real with R(t) defined as the real part of $\underline{R}(t)$. Note that the total intensity, I, may be obtained by adding any two observations with orthogonal ϕ's, as might be expected. If there is an

error, ε, in the orientations of the feeds (so that they are no longer parallel), the response is unchanged to first order in ε.

For orthogonal feeds the response reduces to

$$\underline{R}(t) = \frac{k}{2} (-Q \sin 2\phi_1 + U \cos 2\phi_1 - iV) \qquad (2\text{-}4)$$

for $\phi_2 = \phi_1 + \pi/2$, which is the case for all observations in this paper. For $\phi_1 = 0^\circ$, the real part of the response gives U and the imaginary gives V. The value of Q may be obtained by setting $\phi_1 = 45^\circ$. In this instance, the introduction of an error in the setting of the feeds does enter the response in first order. The response is now

$$\begin{aligned}\underline{R}(t) &= \frac{k}{2} [I \sin(\varepsilon_2-\varepsilon_1) - Q \sin(2\phi_1+\varepsilon_1-\varepsilon_2) + U \cos(2\phi_1+\varepsilon_1-\varepsilon_2) \\ &\qquad - iV \cos(\varepsilon_2-\varepsilon_1)] \\ &= \frac{k}{2} \{I (\varepsilon_2-\varepsilon_1) - Q [\sin 2\phi_1 + (\varepsilon_1-\varepsilon_2)\cos 2\phi_1] \\ &\qquad + U [\cos 2\phi_1 - (\varepsilon_1-\varepsilon_2)\sin 2\phi_1] - iV\} \qquad (2\text{-}5)\end{aligned}$$

to first order in ε_1 and ε_2, where ϕ_1 is mistakenly set at $\phi_1 + \varepsilon_1$; and ϕ_2, at $\phi_2 + \varepsilon_2$. The change in the Q and U terms is due to the effective rotation of the axes. Typically ε_1 and ε_2 were less than 1° so that the effect of these terms was fairly insignificant, especially when compared with the magnitude of the I term. The fractional values of Q and U (Q/I and U/I) were usually a few percent. If $(\varepsilon_1-\varepsilon_2) = 1^\circ$, then $\sin(\varepsilon_1-\varepsilon_2) \simeq 0.018$ and the I term could easily have dominated the others. Considerable effort was required to keep the value of $(\varepsilon_1-\varepsilon_2)$ as low as possible.

The observing system used to separate Q, U and V was the one used at the Owens Valley Radio Observatory by Berge and Seielstad (1972). The types of observations and the resulting responses are listed in

TABLE 2-1

INTERFEROMETER RESPONSES FOR VARIOUS

FEED ANGLE COMBINATIONS

Code	Feed Angles ϕ_1	Feed Angles ϕ_2	Interferometer Response
1	0°	0°	$\frac{k}{2}$ (I + Q)
2	0	90	$\frac{k}{2}$ (U - iV)
3	45	45	$\frac{k}{2}$ (I + U)
4	45	135	$\frac{k}{2}$ (-Q - iV)
5	90	90	$\frac{k}{2}$ (I - Q)
6	90	180	$\frac{k}{2}$ (-U - iV)
7	135	135	$\frac{k}{2}$ (I - U)
8	135	225	$\frac{k}{2}$ (Q - iV)

Table 2-1.

The actual observation of an individual source usually consisted of the sequence of codes 1-2-5-6-3-4-7-8-1, with 20 minute records for the crossed-horn positions and 4 minutes for the parallel. The parallel horn records on either side of the crossed-horn record were used to calibrate the instrumental phase and gain--recall that k(t) is actually a slowly varying function of time. Codes 2 and 4 would have been sufficient to determine the polarization completely, but codes 6 and 8 were added in order to have some check on the various calibrating procedures. This redundancy improved confidence in the entire procedure and partic-

ularly in the calibration method detailed later.

No attempt was made to obtain an absolute system gain calibration. Therefore, only three of the Stokes parameters were obtainable, the fractional values Q/I, U/I and V/I. The extra observing time required to make an absolute flux determination for each source would have degraded the polarization observations, and new flux determinations were hardly called for for the sources on the observing list. The only flux value presented is that obtained by assuming that the gain remained constant throughout the entire session and determining a fixed fringe amplitude to flux ratio from the few calibrators that were observed.

The values for ϕ_1 in Table 2-1 are those read directly from the readout in the observing room. As discussed before, the correspondence between these values and the physical orientation of the feed horn was determined by means of a level. The correlation between the physical orientation and the actual polarization ellipse is discussed in the next section. The values for ϕ_2 were not exactly those listed in the table, but differed slightly due to mechanical differences in the mountings of the receiver packages and to various electrical differences. The required value of ϕ_2 was determined by making a series of observations of ORI A, CAS A, and CYG A and determining the orientation, within 0.01°, giving the minimum interferometer response. This method assumed that the three above sources were completely unpolarized at the frequency in question. Any errors in this assumption, as well as in procedural errors, were absorbed in the method for correcting for instrumental polarization. The method used for the 6 cm observations was somewhat

different, as will be described.

The proper determination of k requires an accurate knowledge of the baseline. The baseline parameters were determined from observations of several known calibrating sources and are accurate to better than 0.005λ. Accurate pointing was established by the method of Greisen (1972), except that correction charts were established as a function of declination only. Almost all sources were observed within one hour of transit; the antennas were individually pointed on those that were not. Pointing was checked periodically and found to be good to within one arc minute on calm days.

There were five separate observation periods with the parameters tabulated in Table 2-2.

TABLE 2-2

EQUIPMENT PARAMETERS FOR THE OBSERVING RUNS

Run	Date	Length (weeks)	Sources Observed	E-W Spacing	Frequency (MHz)	T_{sys} (°k)
1	SEP 71	1	40	100'	1395	75
2	DEC 71	3	170	100'	1665,55,40	80
3	MAR-APR 72	3	186	200'	1401	80
4	MAY 72	1	60	200'	1640	80
5	AUG 72	3	150	100'	5000	165

The various observation frequencies for run 2 were not an attempt to get information at more than one frequency for each source, but resulted from efforts to avoid several severe interference difficulties.

C. The Linear Polarization Observations and Reductions

The observations consisted of a voltage sample of the one minute fringes recorded on tape every five seconds. Using the accurate value for the baseline, the position of the source and the delay and phase of the 1 MHz phase shifter, which were also recorded on the tape, the period and phase expected were calculated. A sine wave of this period was then fitted to the observation points and an amplitude and phase difference were obtained as well as the r.m.s. errors for these values. For a parallel-horn record the phase obtained is just $\psi(t)$, the instrumental phase, as long as the position of the source is accurately known.

Similar phases and amplitudes, and their uncertainties, were obtained for at least one each of the code 2, 4, 6 and 8 records, as well as for the parallel-horn records flanking these. The instrumental phase and gain drifts were removed in an iterative procedure devised by G.L. Berge. On the first pass the source was assumed to be totally unpolarized, making the responses of all the parallel horn records equal to (k/2)I. The amplitude and phase calibration for the intervening crossed-horn record was then linearly interpolated between the two parallel-feed records. For codes 2 and 6, U/I could then be obtained from the real component of the observed fringes; and V/I, from the imaginary component. Similarly, Q/I can be taken from the code 4 and 8 records; and V/I, again, from the imaginary component. If A_o and ϕ_o denote the instrumental gain and phase, and A and ϕ, the observed ampli-

tude and phase for the crossed-feed record, then the following equations may be written:

$$\text{Code 2:} \qquad u = \frac{A}{A_o} \cos(\phi-\phi_o)$$

$$v = -\frac{A}{A_o} \sin(\phi-\phi_o)$$

$$\text{Code 4:} \qquad q = -\frac{A}{A_o} \cos(\phi-\phi_o)$$

$$v = -\frac{A}{A_o} \sin(\phi-\phi_o)$$

$$\text{Code 6:} \qquad u = -\frac{A}{A_o} \cos(\phi-\phi_o)$$

$$v = -\frac{A}{A_o} \sin(\phi-\phi_o)$$

$$\text{Code 8:} \qquad q = \frac{A}{A_o} \cos(\phi-\phi_o)$$

$$v = -\frac{A}{A_o} \sin(\phi-\phi_o) \qquad (2\text{-}6)$$

where $u = U/I$, $q = Q/I$ and $v = V/I$ are the fractional Stokes parameters.

All the values for q, u and v were averaged and errors assigned on the basis of the r.m.s. errors in A and ϕ. For the second iteration, adjustments were made to the code 1, 3, 5 and 7 fluxes since q and u were no longer zero. Now A_o was replaced by $A_o/(1+q)$ (for code 1), and the entire procedure was repeated. Since no observed polarizations were greater than 20%, this procedure converged very rapidly; usually after no more than two or three repetitions the resultant values were stable within 0.001%.

This procedure provided polarizations which were in no way independent of the instrumental polarization. Observations of completely unpo-

larized radio waves at the same time and from the same place as the source observations would have provided the ideal corrections. The resultant Stokes parameters, all but I being due to instrumental polarization, could then be subtracted from the parameters observed for the source to obtain the corrected values. This, of course, was impossible, and the alternative of making observations on a few calibrating sources defined to have zero polarization (Table 2-3 gives upper limits on the degree of polarization for these sources) was adopted. Correction curves were then plotted as a function of source declination. Depen-

TABLE 2-3

REPRESENTATIVE UPPER LIMITS FOR DEGREE OF POLARIZATION OF CALIBRATING SOURCES

Source	Maximum p (%)	Wavelength (cm)	Reference
CAS A	0.1	6	Sastry, Pauliny-Toth and Kellermann (1967)
CYG A	0.2	21	Morris and Radhakrishnan (1963)
ORI A	0.1	6	Sastry, Pauliny-Toth and Kellermann (1967)
HYD A	0.1 0.2	21 18	Gardner, Morris and Whiteoak (1969a)
3C123	0.4	11	Morris and Berge (1964b)
3C147	0.3	21	Morris and Berge (1964a)

dence of these correction curves on hour angle was considered irrelevant since sources were observed within one hour of transit, a very small range. Additionally, each of the various codes for each source and calibrator was observed at nearly the same hour angle so that the effective range of hour angle for each curve was less than 0.5 hour. Several calibrators were observed at ±1.5 hours, and no departure from the established curve was seen.

The sources used were Orion A, Cygnus A, Cassiopeia A, Hydra A and 3C123. In addition, 3C147 was used as a check on the procedure--that is, it was processed as an unknown source and later found to have zero polarization, as expected. Correction curves for the linear and circular components of the code 2, 4, 6 and 8 responses were then plotted as a function of source declination and used for the instrumental polarization correction. This procedure was satisfactory at 21 and 18 cm, but broke down for 6 cm because all the calibrators were either resolved or were no longer believed to be unpolarized.

The second calibration scheme was to assume that, since the source sample was entirely random and should therefore have randomly distributed position angles, the average values of q, u and v for all the sources should be zero within statistical limits. That is, if all the real components (u) of the code two observations were averaged together for all sources, the resultant value of u should be zero. If not, the non-zero value must be entirely due to the instrumental polarization. For each of the four codes, both the sine and cosine components of all sources were convolved with a Gaussian with a standard deviation of 40° in declination

to yield a calibration curve similar to the one based upon the calibrating sources. This width was chosen so that the smoothed curve would have about the same degree of freedom as the calibrator curve. A smaller width would make the curve too inaccurate. A larger one would make it too insensitive to declination. All q's and u's greater than 5% were discarded before averaging since their numbers were small and their effect upon the average, large. Plans were made to check the eliminations after the calibrations were performed, but the calibration curves, in most cases, barely departed from zero and any additional corrections were inconsequential. This left approximately 150 sources for observing runs 2 and 3. The distribution of the linear Stokes parameters for these sources were roughly gaussian (truncated at ±5°, of course) with a standard deviation of about 3%. When the sources were convolved with the 40° gaussian, the middle declination range had a weight (effective number of sources) of about 100. This tapered to half that at the extremes of the declination range. The uncertainty for this curve would then be $3\%/\sqrt{100} = 0.3\%$ at the middle and tapered to 0.43% at the ends. The values for the circular curves were lower, about 0.14% and 0.2%, respectively, since the v values had a much narrower distribution. These are the uncertainties in the instrumental polarization correction procedure for the averaging method.

Figure 2-2 illustrates both sets of calibration curves for all eight values for observation run number two, a three-week run conducted at 18 cm. The eight vertical scales are in percent and are the cosine (linear) or sine (circular) components of either the calibrators or the

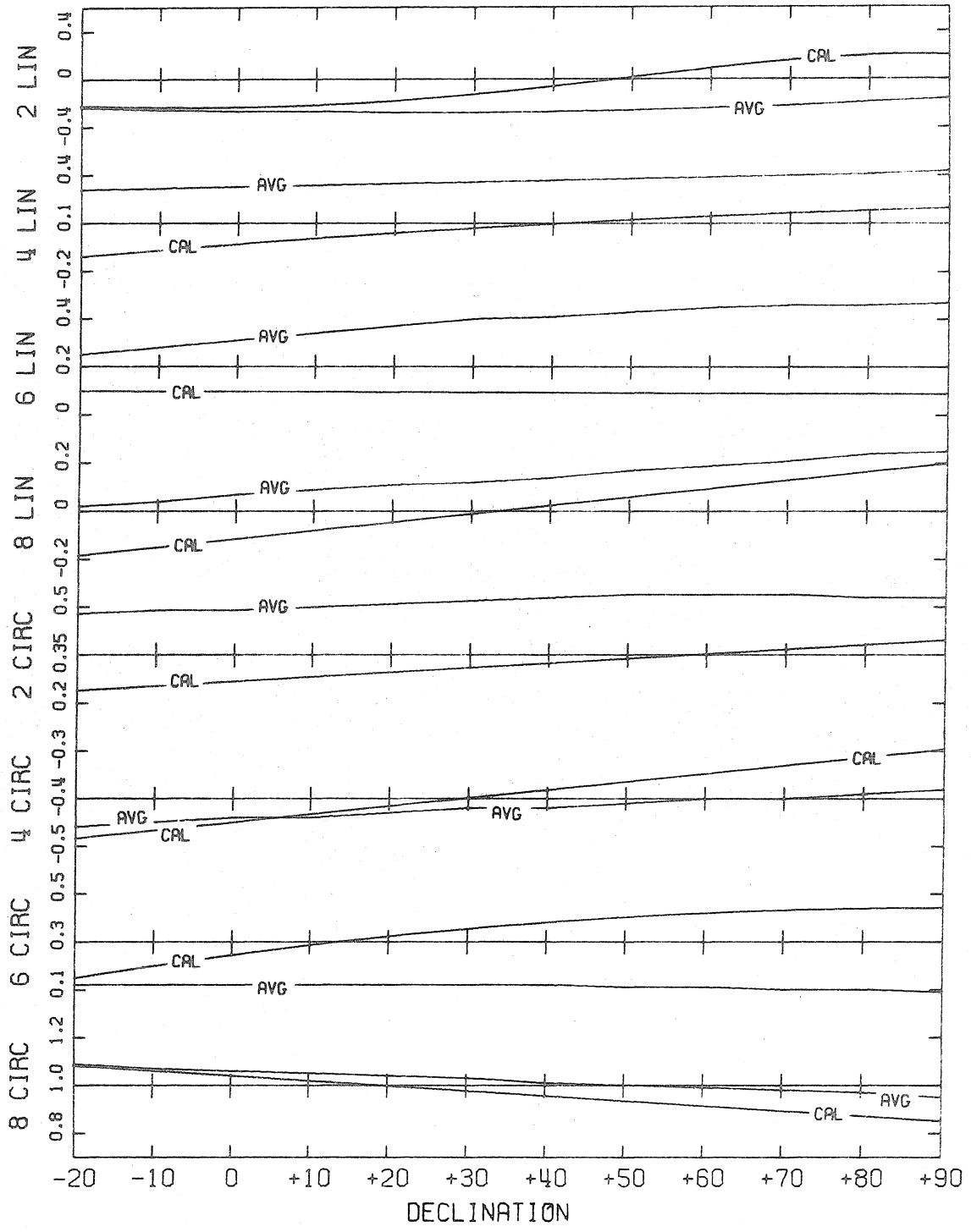

Fig. 2-2.--Instrumental polarization correction curves for run number two at 18 cm. Both the curves obtained from calibrating sources and from averaging all sources as described in the text are presented. All vertical scales are in percent.

average of all sources. Note the possible sign differences between these values and q, u and v. In every case the averaged curve coincides with the calibrator curve within the established errors. A similar situation holds for the other three sets of observations at 21 and 18 cm, although runs one and four are not nearly so significant since the number of observed sources was so small. The excellent agreement between the two calibration methods at 18 and 21 cm supports the use of the averaging method for the 6 cm observations, where no really good unpolarized calibrators exist. A final check was the observation of a few sources with previously observed 6 cm polarizations; these all agreed within the uncertainty limits.

The calibration procedure introduced additional errors into the derived values of the Stokes parameters due to uncertainty in the actual correction curves. The accuracy of the curves obtained from calibrators was felt to be ±0.09% due mostly to backlash and repeatability limits in the feed rotator system, as will be discussed later. Additional error could be introduced by any of the calibrators' not having exactly zero polarization. Since reliable work by others indicated a degree of polarization of less than 0.1%, this is considered unlikely. Polarizations of the order of 0.1% would affect the calibration by a similarly small amount.

This correction procedure corrects both for the instrumental polarization inherent to the structure of the feed, dish, and supporting booms, and for that caused by inaccuracies in determining the exact crossed-horn position angles. Once the angles were determined as a

function of declination, they were used for all observations and for the calibrating sources, so that setting errors would presumably be constant and therefore part of the instrumental correction. No long-term variation of the null angles was observed when they were measured several times throughout the run; the only short term variations were those due to setting errors and to backlash, amounting to less than 0.05°. It was not possible to separate the structural instrument polarization from this feed-setting error, nor was there any need to.

The calibration uncertainty for the 6 cm observations, based on the average of 150 sources as described for the smoothed 18 and 21 cm calibrations, was somewhat larger, being 0.4% near the center of the declination range and increasing to 0.55% at the ends. This increased uncertainty was due to the larger average polarizations for the sources at 5000 MHz. The calibration uncertainty for both 18 and 21 cm was 0.09% throughout the declination range based on the calibrating sources.

Once the calibration curves had been established, each source was run through the entire iterative procedure again, this time correcting each value of q, u, and v as generated. The additional errors from the calibration process were not entirely random. There was a random component due to the imperfect repeatability of the horn rotators, but non-random errors arose from the actual inaccuracy of the correction curves. Since there was no way to separate the random from the non-random errors, the entire error was treated as systematic and added in quadrature to the uncertainty for q, u or v for the average of all records of a given crossed-horn position. That is, if two separate

crossed-horn records of type two were taken for a source, the calibration error would be added in quadrature to the net error after averaging the two values of q and not to the individual errors before averaging.

Once this procedure had been completed, the information for each source consisted of the best values for q, u and v and their uncertainties. The accuracy of both the instrumental polarization correction procedure and the calculation of the uncertainty could be checked since observations of a relatively large number of sources were available. Since q and u had two independent determinations, the code 4 and 8 or code 2 and 6 crossed-feed observations respectively, the distributions of the residuals could be compared with the gaussian distribution expected for the Stokes parameters. Figure 2-3 shows this distribution for the values of q and u for the 6 cm observations. The lower and broader curve in each case is a gaussian with $\sigma = 1$. The more sharply peaked curve represents the actual distribution of the measurements in terms of the standard error. If the sample had been infinite and all calibration and error analysis procedures exact, this curve also would have been a gaussian with a standard deviation of one. The fact that the actual distribution curves are slightly more sharply peaked and have smaller standard deviations, 0.889 and 0.812 respectively, indicates that the error analysis has been somewhat pessimistic or that the calibration curves were slightly more accurate than expected. The same behavior was observed for all the other data taken and increases confidence in the entire procedure.

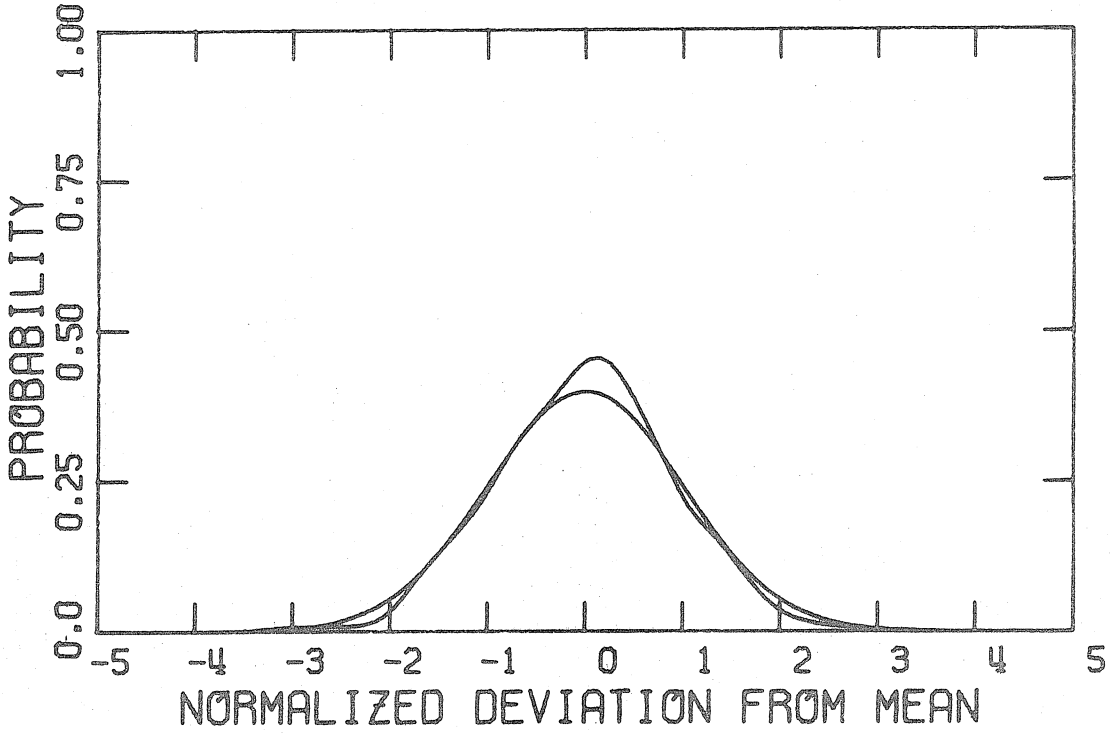

Fig. 2-3(a).--Normalized distribution of q measurements at 6 cm.

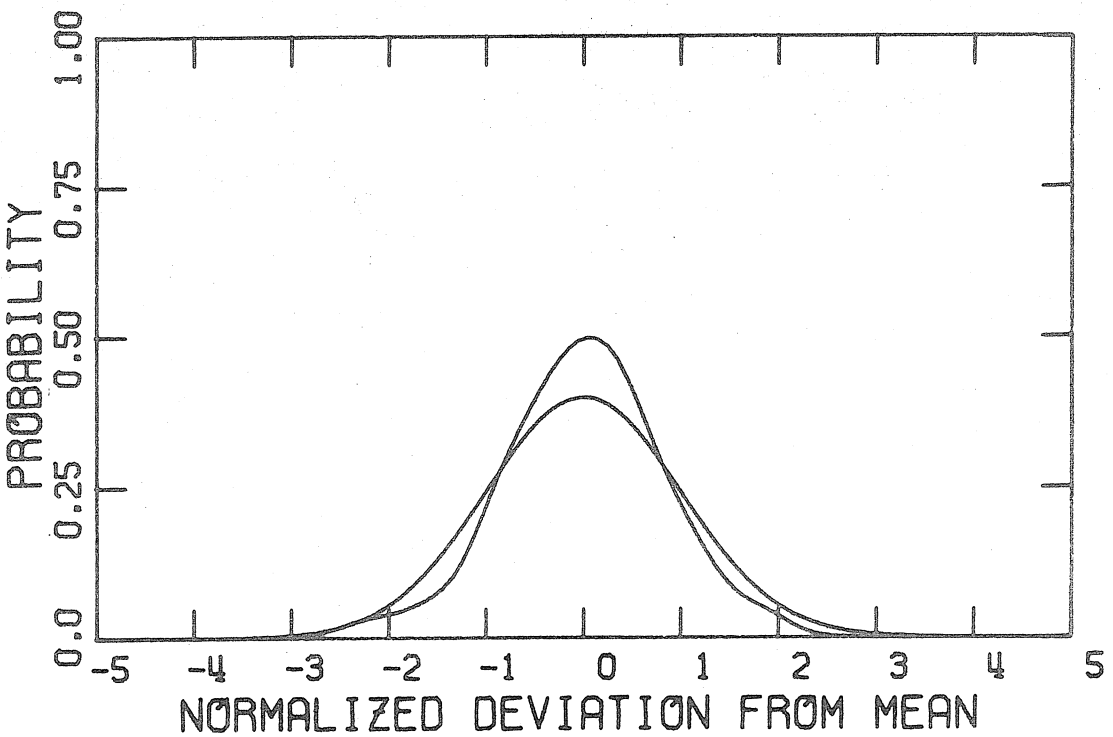

Fig. 2-3(b).--Normalized distribution of u measurements at 6 cm. The broader curve in each case is a gaussian with $\sigma = 1$.

If the individual measurements of q or u deviated by more than the computed uncertainty--i.e., if they were to lie beyond ±1 in Figure 2-3--the uncertainties were increased by this "excess error" factor. The values of q and u were converted into a degree of linear polarization and position angle and their uncertainties:

$$p = \sqrt{q^2 + u^2} \tag{2-7}$$

$$\psi = \frac{1}{2} \tan^{-1} \left(\frac{u}{q}\right) \tag{2-8}$$

$$\sigma_p = \left[\left(\frac{\partial p}{\partial u}\right)^2 \sigma_u^2 + \left(\frac{\partial p}{\partial q}\right)^2 \sigma_q^2\right]^{1/2} = \left(\frac{u^2 \sigma_u^2}{p^2} + \frac{q^2 \sigma^2}{p^2 q} \right)^{1/2} \tag{2-9}$$

$$\sigma_\psi = \left[\left(\frac{\partial \psi}{\partial u}\right)^2 \sigma_u^2 + \left(\frac{\partial \psi}{\partial q}\right)^2 \sigma_q^2\right]^{1/2} = \frac{1}{2p} \left(\frac{q^2 \sigma_u^2}{p^2} + \frac{u^2 \sigma_q^2}{p^2} \right)^{1/2} \text{rad.} \tag{2-10}$$

The probability distributions for p and ψ are gaussian only in the limit $\sigma_p << p$. The distribution for P is actually Rayleigh for $p << \sigma_p$, and that for ψ is considerably more complicated, when σ_q is taken equal to σ_u, as is usually approximately correct. Berge (1965), in the appendix to his doctoral thesis, develops the mathematical equivalent of this problem, with the restriction that $\sigma_q = \sigma_u \equiv \sigma$. The original development concerns the derivation of an amplitude and phase from a sine and cosine value. In the language of the present paper, he finds that the expectation value for p_o, the actual degree of polarization, is given by:

$$\langle p_o \rangle = \sigma \sqrt{2/\pi} \, [{}_1F_1(\tfrac{1}{2}, 1; -p^2/2\sigma^2)]^{-1} \tag{2-11}$$

where p is the measured value. When σ is of the same order as, or

greater than, p, the measured value will overestimate the actual value. Similarly, σ_p itself will be overestimated and the error distribution will be considerably skewed. Figure 2-4 illustrates the distribution for various values of p_o/σ. This distribution is given by

$$P(p) = \frac{p}{\sigma^2} I_o(pp_o/\sigma^2) \exp [-(p^2 + p_o^2)/2\sigma^2] \qquad (2\text{-}12)$$

where $I_o(x)$ is the Bessel function of zeroth order and imaginary argument. When the actual polarization goes to zero, this distribution has the limiting form

$$P(p) \sim \frac{p}{\sigma^2} \exp (-p^2/2\sigma^2), \qquad (2\text{-}13)$$

which is the Rayleigh distribution illustrated as the first curve of Figure 2-4. Notice that if the actual polarization is zero, there is no chance of making a measurement with the correct value. For the limit $p_o >> \sigma$, the distribution becomes

$$P(p) \sim \frac{1}{\sqrt{2\pi}\,\sigma} \exp [-(p-p_o)^2/2\sigma^2] \, (p/p_o), \qquad (2\text{-}14)$$

which is a gaussian for $p \simeq p_o$. For σ as great as p/3, the departure from the gaussian is less than 30% and mostly much less than that for p in the range of $p_o \pm \sigma$.

The case for the angular distribution is much the same, although the integrations required are much less tractable. Figure 2-5 illustrates the angular probability distributions. When the polarization is zero, the distribution of ψ is clearly uniform from 0° to 180°. For $p_o >> \sigma$, the distribution is gaussian for ψ within a few standard devi-

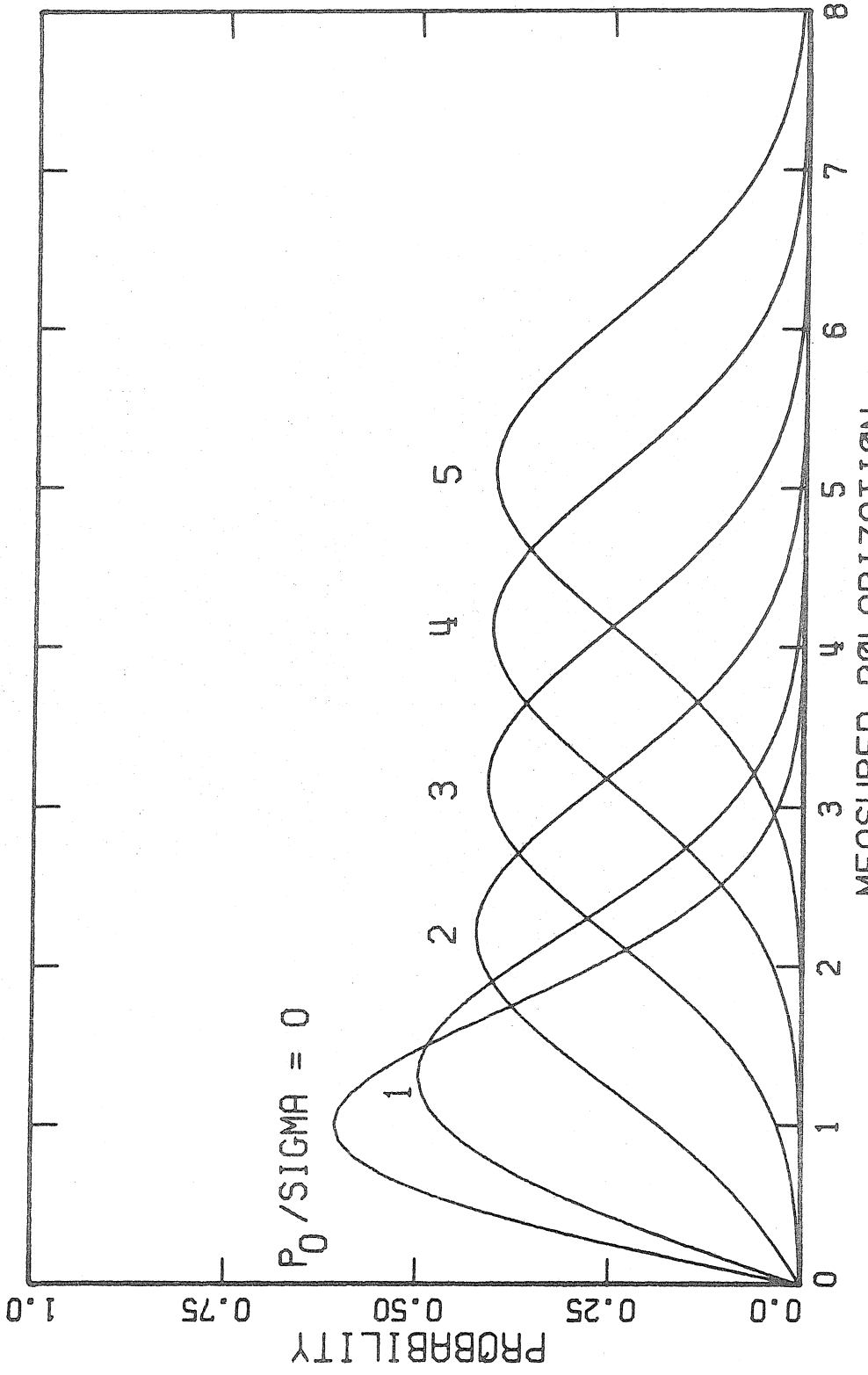

Fig. 2-4.--The curves give the probability of observing any particular value of p/σ for various values of p_o/σ, where p_o is the actual degree of linear polarization.

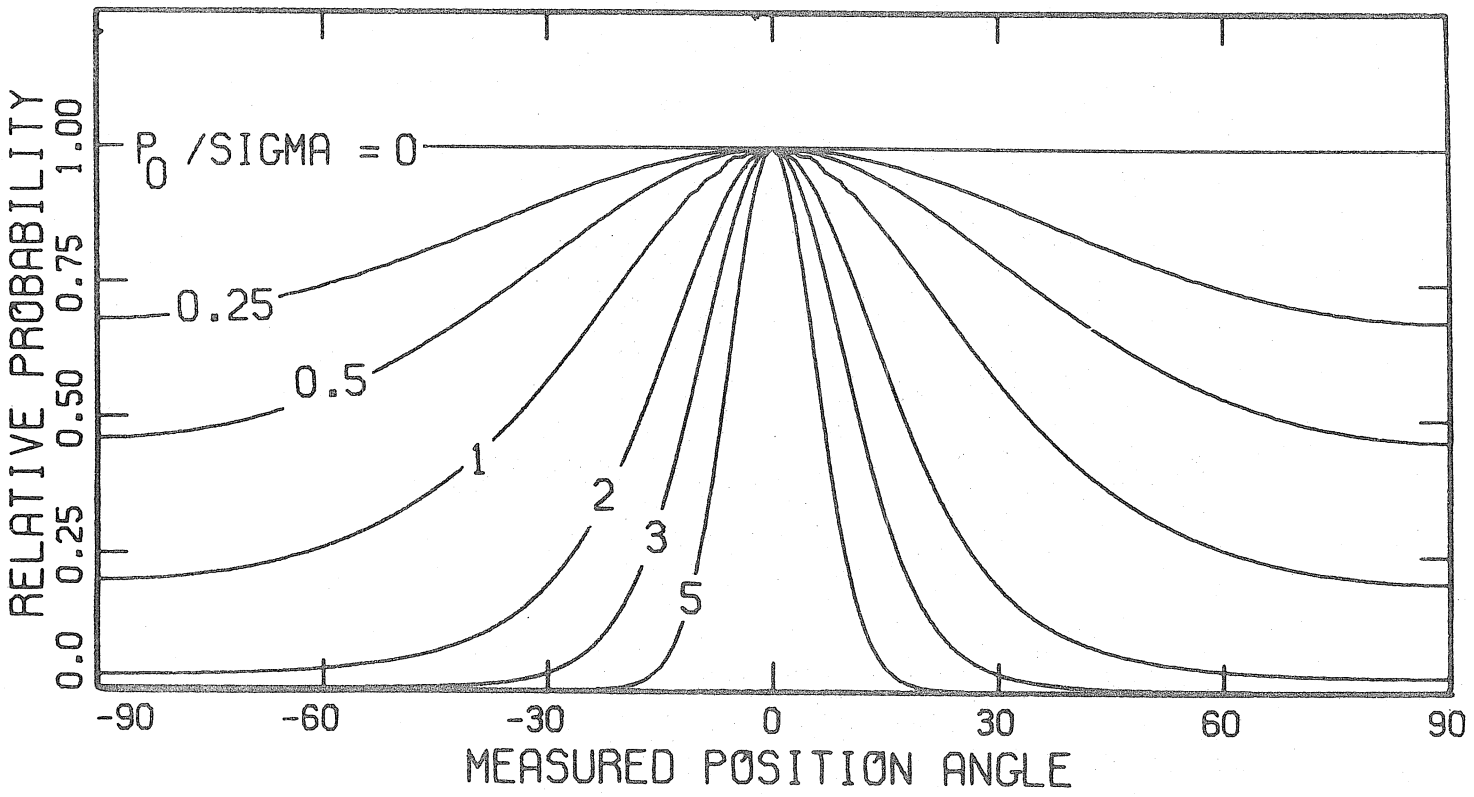

Fig. 2-5.--The curves give the probability of observing any particular value of $(\psi-\psi_o)$ for various values of p_o/σ, where p_o is the actual degree of linear polarization and ψ_o is the actual position angle.

ations of ψ_o. This can be seen to be true because the lines of constant ψ are nearly parallel at the maximum of the circular gaussian distribution, and therefore one dimension of the q-u distribution is simply integrated out--as long as $(\psi-\psi_o)$ is of the same order as σ/p. For intermediate cases the distribution is more flattened than a gaussian, and the wings do not taper off so rapidly to the cutoffs at $(\psi_o \pm 90°)$. When $p/\sigma = 3$, equation 2-10 gives $\sigma_\psi = 10°$. In this case numerical integration shows less than 10% departure from a gaussian within two standard deviations of ψ_o. Even for $\sigma_\psi = 20°$ the departure from gaussian is still less than 20%.

The additional effect of allowing differing values for σ_q and σ_u is negligible as long as the σ of the above discussion is taken as the maximum of the two for purposes of deciding which limits hold. The significance of all this as far as the data presented here are concerned can be summarized briefly. First, whenever $p \lesssim \sigma$, p overestimates the actual polarization. For $p = \sigma$, the correction factor is only a few percent. Since polarizations of such doubtful quality are generally regarded only as upper limits in any case, no corrections have been applied. Second, the ψ distributions are quite gaussian for $\sigma_\psi < 20°$, except for the elevated wings, with standard deviations well-represented by equation 2-10. For larger σ_ψ the distribution becomes markedly non-gaussian with a maximum standard deviation of 51.96° for $p = 0$. To adjust for the changing distribution, σ_ψ was replaced with

$$\sigma'_\psi = \{ 1/[(51.96)^{-2} + (\sigma_\psi)^{-2}] \}^{1/2} \quad (°) \qquad (2\text{-}15)$$

This artifice causes no significant change for $\sigma_\psi < 20°$ and sets the maximum at 51.96°. Since, as is pointed out in the next chapter, polarization measurements for which $\sigma_\psi > 20°$ are essentially worthless for determining rotation measures, the departure from gaussian and adjustment of the standard deviation are inconsequential. For each observational paper there is a different technique for determining and reporting σ_ψ, which is regrettable since the technique is often not described. The important thing to remember here is that a σ_ψ of 52° indicates that there is no knowledge about the position angle, particularly in view of the fact that the probability distributions are actually periodic in ψ if there is no knowledge of how many rotations have occured from some reference value.

Once the polarizations had been converted to a degree and position angle, the correction for misalignment between the indicated angles for the feed horns and the actual orientations could most easily be made. With the west antenna pointed at the southern horizon, a level was used for the comparison. When the level showed the feed horn to be located at 0° position angle, the readout indicated 0.00°±0.10 for the 21 cm package, 1.46°±0.10 for the 18 cm and 1.87°±0.10 for the 6 cm receiver package. These values did not change with subsequent removals and remountings.

Although the physical orientation of the feed horns was known to about 0.1°, the actual position angle of the polarization of the antenna was not quite as well known. The position angles for 3C348 at 18 and 21 cm agreed within 2° with the data of Gardner, Morris and Whiteoak (1969a),

but this gave no information about the absolute calibration of the position angles. The derived cross-feed position angles were always within 0.5° of 90° when the differences in the physical orientations of the feed horns on the two antennas were accounted for. This, combined with the four-fold symmetry of the antenna focus support system, indicated that a systematic error in the position angle of not more than 1° was reasonable. Therefore an additional uncertainty of 1° was added in quadrature to the value calculated for the position angle for all sources.

Ionospheric Faraday Rotation

Since radiation from all extraterrestrial radio sources must pass through the earth's ionosphere where both the electron density and magnetic field are non-zero, there must be some amount of Faraday rotation contributed by this region. Specifically, the electron density reaches a peak value of the order of 10^6 electrons/cm^3 between 200 and 500 km above the surface of the earth. The total line-of-sight integral of the electron density at the zenith ("total electron content") typically ranges from 0.5×10^{13} electrons/cm^2 at night to 5×10^{13} in the daytime with wide day-to-day variations. The earth's magnetic field in the region of the maximum concentration of electrons is approximately 0.35 gauss for middle latitudes. Assuming a source directly overhead and a magnetic field perpendicular to the surface of the earth, we obtain from equation 1-12 a value of about 4 rad/m^2 for the typical maximum daytime ionospheric Faraday rotation. This amounts to 10° at 21 cm, and can

clearly be of major importance when data taken at different times and from different locations are combined. Therefore correction for ionospheric Faraday rotation was necessary.

Most methods used to determine the total electron content and the distribution of electrons with height are either insensitive beyond the first maximum in electron density, or so complex that they are not easily and regularly carried out. With the introduction of earth-synchronous satellites a method exists for measuring the ionospheric Faraday rotation directly. A satellite sends linearly polarized radiation to earth where a ground station continuously monitors the position angle and hence the Faraday rotation.

The data used in the present work are those obtained by the Radioscience Laboratory of the Stanford Electronics Laboratories from the stationary satellite ATS-1. The observed Faraday rotation angle, Ω, was converted by the Stanford Laboratory to the vertical electron content, I, by

$$I = \frac{4.24 \times 10^{-11} f^2 \Omega}{B_L \sec \chi} \text{ electrons/cm}^2 \qquad (2\text{-}16)$$

where B_L is the longitudinal component of the earth's magnetic flux-density in webers/m^2, χ is the zenith angle of the ray-path, and f is the frequency in Hz. Since most of the electrons are located near 400 km above the earth, $B_L \sec \chi$ was computed at this height on the ray-path. This quantity does not vary quickly with height near the zenith, so that the approximation of assuming that all electrons are at this height is a good one. The data as provided by Stanford consist of daily plots or tables of zenith total electron content at the "ionospheric point", i.e.,

where the ground station-satellite line-of-sight reaches 400 km above the surface. For Stanford to ATS-1, this point is located at 34.2° N, 125.5° W. The Owens Valley Radio Observatory is located at 37.2° N, 118.3° W. The latitude difference of 3° can be ignored since the change in electron density profiles and therefore the total electron content with latitude is significant only near the magnetic equator and the magnetic poles (Davies, 1966). Only 2 or 3% difference can be expected between 30° and 40° N latitude. The quoted uncertainty in the Stanford data is 10% or 5×10^{12} electrons/cm^2, whichever is the greater, and therefore completely overshadows any error due to the difference in latitude.

Since the diurnal variation of the total electron content is primarily caused by the transit of the sun across the sky, it is expected that whatever content was observed at 125.5° W would have been observed 29 minutes earlier at 118.3° W. Differences could only be due to changes in the solar UV and X-ray flux, the solar wind, or a solar proton event (Ratcliffe, 1972). While significant changes can occur on a time scale shorter than 29 minutes, such changes are rare. Moreover, the typical observation of the present work extends over a period of two hours, and the value of the total electron content is obtained by averaging the Stanford data over that period. The assumption that the observed total electron content derived from the Stanford--ATS-1 line-of-sight represents the total electron content at the Owens Valley Observatory 29 minutes earlier would seem to be a highly plausible one.

The second part of the data required for the determination of the

Faraday rotation due to the earth's ionosphere is a knowledge of the geomagnetic field for the region in question. This was obtained from a computer program using a multipole expansion developed in 1964 for the National Aeronautics and Space Agency by R.H. Eckhouse, Jr., of the Electrical Engineering Research Laboratory of the University of Illinois. This program was provided by B.D. Mulhall of JPL. The field model produced by the program was compared with standard tables and agreed within 1%. Secular variation of the field since 1962, the year for which the coefficients were computed, is negligible. In addition, the changes in the earth's magnetic field due to the solar wind and ionospheric currents are also negligible, since they are of the order of 10^{-4} gauss or less, and the geomagnetic field at 400 km above the surface is approximately 0.35 gauss.

Corrections for the ionospheric Faraday rotation were computed and applied in the following manner. The source position, date, and average time of the observation, T_o, were used to compute the zenith angle, Z, and azimuth of the line-of-sight. The ionospheric point, P, was then calculated as the intersection of this line and the 400 km height plane. The longitude difference between this point and the observatory was converted into time, Δt, in minutes. This quantity is positive for a source west of the observatory. The zenith total electron content was then taken from the Stanford data for the time $(T_o + 29^m - \Delta t)$. The Stanford data had previously been smoothed in time by a gaussian with a standard deviation of 30 minutes. The magnetic field was calculated at the point P and the total Faraday rotation due to the ionosphere was calculated

according to

$$\psi_{ionos} = 2.62 \times 10^{-13}\ \hat{r}\cdot\underline{B}\ I(T_o+29^m-\Delta t)\ \lambda^2\ \sec Z\ [\text{rad}] \quad (2\text{-}17)$$

where $\hat{r}$ is the unit vector in the direction of the line-of-sight, $\underline{B}$ is the magnetic field in gauss, I is in electrons/cm^2, and λ is the observing wavelength in m. The correction to the observed position angle of the polarized radiation was then taken as the negative of this quantity and was added to the observed position angle to obtain the true position angle. This procedure was applied once, for the midpoint of the 2 hour observation, and not for each 20 minute code 2, 4, 6 or 8 record independently. The uncertainty in the total electron content increased the uncertainty in the position angle by either 10% of ψ_{ionos} or ψ'_{ionos}, which was computed from equation 2-17 by taking I equal to 5×10^{12} electrons/cm^2, whichever was the greater. This additional uncertainty was added in quadrature to the previous value.

Some observations at 21 and 18 cm had been repeated in different months and therefore at different times of day. These would have constituted an excellent check on the ionospheric correction method, except that the observational uncertainties were usually on the same order as the ionospheric correction for the sources repeated. Moreover, very few of the measurements were repeated at exactly the same frequency so that Faraday rotation might increase the spread. Nevertheless, the ionospheric correction usually did improve the correspondence of the two observations. For the 13 observations repeated at 21 cm the r.m.s deviation before the correction, in terms of the individual uncertainties,

was 1.14 σ. After the ionospheric rotation was removed, the r.m.s deviation dropped to 0.98 σ. For 13 sources with accurately determined uncertainties, the value should have been 1.00 ± 0.28 if no systematic effects were present. Therefore, although the test is not conclusive due to the large uncertainties in the position angle measurements for the sources repeated, the ionospheric correction procedure does reduce the systematic effects.

Additional sources of error

Backlash and repeatability of feed rotators.--After the observations were nearly complete backlash was discovered in the gear train of the feed rotators. For the west antenna, the backlash was 0.10° ± 0.03°; for the east, 0.05° ± 0.03°. The repeatability for each was 0.02°. Scatter in the observations of the strong, unpolarized calibrators had been noticed, and the individual points seemed to cluster at either end of the range of scatter. This and the fact that the total range of the scatter of the calibrators was about 0.09%, corresponding to a 0.06% angle error, for the linear terms indicate that the scatter was caused by this backlash. Different conditions of preloading surely exist for different hour angles and declinations and with different receiver package and cable combinations. Therefore, correcting the problem by always rotating the feeds in the same direction to the desired number would probably be ineffectual. In any case no such measures were carried out for the program presented here. This is the source of the 0.09% calibration uncertainty, and would have no other effect on the observations.

Corrective measures will be needed if more accurate observations are to be undertaken.

Pointing errors, feed ellipticity, and cross-polarization lobes.--In addition to the primary beam of the parabolic antenna, which preserves the sense of polarization of incoming waves, there exist cross-polarized side-lobes which effectively rotate the plane of polarization by 90°. As reported by Silver (1965), the worst of these lobes lie at 45°, 135°, 225° and 315° to the feed orientation and have maxima at only about λ/D radians from the axis of symmetry where D is the diameter of the dish. These maxima lie at 0.5°, 0.3°, and 0.1° off-axis for 21, 18 and 6 cm, respectively. Their peaks are at least 16 db down from the main beam. Ideally there is no cross-polarization at all on the E and H axes of symmetry.

If an unpolarized source were inadvertently placed off-axis in the direction of one of the cross-polarized lobes, the cross-feed records would no longer indicate zero polarization. If the source were on the maximum of the cross-polarized lobe, the signal from antenna's primary beam would correlate with the cross-polarized signal of the other even though the feeds were crossed. Polarizations as high as 100% could be recorded in this way, although the fact that the total flux was so low would surely make the investigator suspicious. Even at points midway between the primary beam and the crossed-polarized side-lobe (13' off-axis for the 90' antennas at 21 cm) a polarization of 15% could be indicated. However, these side-lobes have nulls at the center of the main

lobe and along the E and H symmetry planes, so that their effects close in are minimal. To estimate the importance of the cross-polarization lobes for the present work, observations of a source were made with both antennas offset by 10' in the direction of one of the cross-polarized side-lobes at 21 cm. The degree of polarization increased only 1%. Pointing errors for only one antenna gave slightly less severe results. Recalling that all pointing was accurate within 1', the effects are expected to be much less than 0.1% even at 6 cm. No attempt was made at a detailed measurement of the cross-polarization pattern, but this information would be useful, especially so for those making polarization synthesis maps of extended sources.

Another effect is mixed in with this. If the illumination pattern of the feed is elliptical rather than exactly circular, the flux level received from an off-axis source changes with the feed position angle. For single-dish polarimetry, this effect is indistinguishable from a genuine polarization. The elliptical feed, and hence elliptical beam, affects interferometric polarimetry only in the second order; there is no cross-polarization so there is no first order effect in the crossed-feed records for linear polarization. Equation 2-2 does show a term in the first order in I and θ, the ellipticity, but this is imaginary and affects only V.

Wind.--Excessive wind can change the pointing of an antenna and cause errors in the polarization as discussed above. Wind fluctuations within a record can cause variations in the signal and increase the r.m.s

noise, particularly at 6 cm. Finally, the wind can be sufficient to flex the antenna and alter its figure and therefore the instrumental polarization. More than twenty sources were observed in various winds and, later, in the calm. These observations were taken at several frequencies. In not one case was the degree or position angle of the measured polarization significantly altered by winds as high as 30 mph. For example, 3C249.1 was observed on August 14, 1972 at 5000 MHz with winds gusting to 30 mph. The measured polarization was 4.3% ± 2.0% at 12° ± 15°. On August 26, when the wind was less than 5 mph, the values were 3.8% ± 1.7% and 179° ± 12°. The noise levels were increased by the wind, but the polarization was essentially unchanged. Nonetheless other observers have reported wind effects on the Owens Valley Interferometer, particularly for somewhat extended sources. Therefore the table of polarization observations contains a note on the wind for the few observations taken on a windy day--wind greater than 15 mph--for which no confirmation could be had on a calm day.

Gain and phase drifts.--The reference gain and phase for a crossed-feed observation are obtained by linear interpolation from the immediately preceding and following parallel-horn records. These records are usually not separated by more than 22 minutes; their r.m.s phase uncertainty is always less than 0.4°, and their amplitude uncertainty is usually less than 2%. If, however, the instrumental gain or phase show significant departure from linearity on a short time scale, the observed relative phase or amplitude of the crossed-feed record could have uncer-

tainties in excess of that calculated on the basis of r.m.s scatter alone. Assume that r.m.s. uncertainty of the observed phase is zero, and that the uncertainty due to non-linearity of the instrumental phase-time curve is ε. This has the effect of mixing the real and imaginary parts of the response. In particular, if $v = 0$ for the source, v will now appear to be $q \sin \varepsilon$ for a code 4 observation. For $q = 10\%$ and $\varepsilon = 10^\circ$, v will appear to be 1.7%, which is tremendous compared with the expected calibration error of 0.1%. Clearly short term phase stability is of the utmost importance in trying to measure the circular polarization of sources with high linear polarization, or the linear polarization of sources with high circular polarization--none of which exist, as far as is known. The linear components are not so severely affected when $v = 0$, for now q would seem to be $q \cos \varepsilon$, or about $0.98q$ in the above example.

To measure the short term phase stability a few long series of short observations of a strong calibrator were made. The departure of the phase from a linear time dependence on a scale of 10 to 20 minutes is 0.001 to 0.002 lobes--0.36° to 0.72°--on the average, but never more than 0.004 lobes. This is sufficient to make the circular polarization determinations of moderately to highly polarized sources very questionable, but to have no significant effect upon the linear polarization. The expected large scatter of the individual determinations of v for strongly polarized sources has been observed, but was originally attributed to the inability of the feed-antenna system to completely separate the modes of polarization. The phase instability is the more likely explanation.

This will be mentioned again in the comments on the circular polarization table.

The amplitude or gain stability was found to be better than 5% in 20 minutes. This would have no significant effect on the polarization determinations and was ignored. Again, this demonstrates the power of the crossed-feed interference polarimeter and its null technique. To ignore a 5% gain change in single-dish polarimetry would mean disaster.

Cross-talk, or cross-polarization in the feed.--No feed can completely isolate one mode of polarization from the other, but separations of 30 to 40 db are typical. The minimum responses obtained at the optimum crossed-horn orientation for the strong, 'unpolarized' calibrators were less than 0.1% of the parallel-horn value, indicating an isolation of at least 30 db for the entire system for an on-axis source. The values at the 45-135 and 135-225 positions were consistently higher than those at the 0-90 and 90-180 positions. This most likely was related to the four focus-support booms at 0, 90, 180, and 270°, but was insignificant as the worst case still indicated an isolation of 30 db.

Spillover.--Ground radiation is highly polarized and, in single-dish systems, can contribute a polarized flux of several flux units. Moreover, this is a function of the precipitation, humidity, wind and orientation of the antenna, and therefore poses very difficult problems when attempts are made to separate out the few hundredths of a flux unit of polarized signal from the source. For an interferometer the ground "source" is of such large extent as to be totally resolved. Any residual fringes are

apt to be at a rate very different from those of the source. Spillover will, of course, contribute to the system temperature, mostly at large zenith angles. The zenith angle for these observations rarely exceeded 50° so that spillover was not significant in any respect.

Galactic background emission.--At the lower frequencies the galactic background contributes a substantial polarized flux density, particularly near the galactic plane. Since the scale size of this emission is generally greater than 2 or 3 degrees of arc (Berkhuijsen, 1971), one would expect it to be totally resolved at the spacings and baselines used. A few observations were made of areas which were devoid of known sources, and no detectable polarized emission greater than 0.01 fu was seen. This was at or below the noise level of most individual observations and was therefore ignored.

Resolution effects.--Morris, Radhakrishnan and Seielstad (1964) have given the response of the interferometer to an extended distribution of polarized emission (equation 2-2 of the present work), and this can be used for a detailed examination of what happens when a source becomes resolved. Since only two sources at 6 cm show resolution effects, a general understanding will suffice. If all four Stokes parameters were distributed across the source in exactly the same way then the partial resolution of the source would have no effect upon the polarization determination. High resolution polarization maps show that such sources probably do not exist, and that the actual distributions of Q and U are very complex and quite different from each other and that of I. The q,

u and v obtained from a partially resolved source will probably bear little relation to those obtained for the integrated radiation. The 5000 MHz observations of the two sources listed as being partially resolved should be treated with some skepticism; the rotation measures derived for these sources are uncertain anyway, so that no further degradation of their quality is necessary.

Confusion.--Two types of confusion are relevant here. One consists of having a strong source, polarized or not, either near the primary beam or on some sidelobe; the other, of one or more small, polarized, perhaps unknown sources in the main beam in addition to the source being observed. The first is important for a few sources, such as 3C011.1, which are known to be confused at the spacings used, and for many other sources observed in the daytime when the sun was inconveniently located. Usually the fringe rate for the sun was sufficiently different from the 1/60 Hz of the source that the two could be separated with no more effect than an increase in noise. When such was not the case, the observation was discarded and hopefully repeated at a more appropriate time. Little could be done to correct those sources known to be confused as it was almost impossible to determine the direction of the effect. Such sources have been included with a note to that effect and must be considered with some caution.

The sort of confusion consisting of small, unknown sources proved to be insignificant at 21 cm and therefore, presumably, at the higher frequencies. Several blank regions were observed and found to have less

than 0.01 fu of polarized emission, as mentioned in the section on the galactic background. This limit was at or below the noise level of most of the observations and was therefore ignored.

The Linear Polarizations

Table 2-4 presents all the polarization observations made in the course of this research. The first two columns of the table give the 3CR source name and an alternate. The alternate list is not complete and contains only names which have been useful in preparing this paper. In the event a source is not a 3CR source, the decimal point is omitted. Alternate names of the form 0003-00 are all Parkes sources; other names are self-explanatory.

The third column gives the observing frequency in MHz, and column four contains the observed flux. The reader is again cautioned that no attempt was made to perform absolute flux calibrations during these observations and that these flux densities are approximate and are included only for comparisons with the polarization and errors. Errors of 10 to 20% in these fluxes are not uncommon.

The fifth and sixth columns give the percentage of linear polarization of the source and the uncertainty for this measurement, respectively. The seventh and eighth columns give the position angle of the polarized radiation, measured from north to east, and its uncertainty. All sources of error have been included, and all corrections have been performed.

The ionospheric correction applied to the observed polarization is

supplied by the ninth column. This correction is in degrees, and has already been added to the observed position angle to obtain the values tabulated in column seven.

The next two columns give the date and Pacific Standard Time of the observation in hours. If observations on more than one day have been averaged together, the date and time given is that for the observation contributing the largest share. In such cases the ionospheric corrections are calculated separately for each day, and the tabulated value is the mean of these corrections.

The somewhat cryptic symbols in the final column consist of one or more of the following:

C, or CONF	This source may be confused, as explained in the section on confusion, page 59.
W	Often followed by an integer. This observation was taken on a day when the wind was greater than 15 mph, and could not be confirmed by an observation on a calm day. The effects of the wind are discussed on pages 54-55.
Q1.4, U1.8 or QU2	This indicates the 'excess error' in Q, U or both. This is more completely developed on page 41. Any necessary corrections have already been applied to the other figures tabulated.
3.3'	Indicates the E-W dimension of the source for the two 6 cm observations for which the source is partially resolved. The polarization parameters for these observations are suspect. See page 58.

The final digit in the Notes column indicates the session during which the observations were made. The numbers 1 through 5 refer to Table 2-2 of page 30 which provides all the equipment parameters.

TABLE 2-4

LINEAR POLARIZATION OBSERVATIONS

SOURCE	ALTERNATE NAME	FREQ MHZ	FLUX FU	P(%)	+/-	POSITION ANGLE	+/-	IONOS CORR.	OBS. DATE	AVG PST	NOTES
3C002.0	0003-00	1640	3.7	0.7	0.2	146.3	8.3	-1.4	12/28/71	17.28	2
3C006.1	NRAO14	5000	0.91	0.6	1.6	149.	41.	-0.2	8/17/72	1.98	5
		1640	3.5	0.5	0.2	5.	13.	-0.8	12/24/71	17.89	2
		1395	3.4	1.0	0.4	63.	12.	-1.0	9/22/71	0.11	Q1.7 1
3C011.1	NRAO25	1640	2.8	0.7	0.5	132.	19.	-0.7	12/26/71	17.89	QU2C 2
		1640	2.2	3.4	0.7	118.7	7.7	-3.7	5/13/72	8.56	Q1.7C4
		1395	3.1	4.7	0.7	62.6	3.9	-1.0	9/23/71	0.19	QU2C 1
3C013.0	4C+39.01	5000	0.42	2.6	2.3	118.	25.	-0.2	8/13/72	2.09	Q1.4 5
		1640	1.7	1.1	0.5	92.	12.	-1.7	12/29/71	17.54	2
		1401	1.9	1.0	0.4	33.	13.	-6.5	4/ 2/72	11.83	3
3C014.0	0033+18	1665	1.8	1.6	0.4	102.8	7.9	-0.8	12/18/71	18.46	2
		1401	2.1	0.2	0.7	159.	47.	-8.6	4/ 4/72	11.18	QU2 3
3C014.1	4C+58.02	5000	0.60	1.2	2.4	136.	35.	-0.2	8/18/72	2.24	5
		1640	2.1	2.0	0.5	59.6	6.9	-3.3	5/14/72	8.42	4
		1401	2.4	2.6	0.3	79.7	4.0	-9.7	4/ 8/72	10.80	3
3C016.0	0035+13	1665	1.8	5.9	0.5	103.3	2.2	-0.9	12/19/71	18.47	2
		1401	1.9	6.4	0.7	159.7	2.5	-10.0	4/ 9/72	10.62	3
3C017.0	0035-02	1640	4.5	0.9	0.3	172.0	6.8	-5.2	5/15/72	8.49	4
		1401	5.8	0.3	0.2	3.	19.	-12.8	4/11/72	10.51	3
3C019.0	4C+32.03	5000	1.15	4.2	1.1	120.0	7.5	-0.2	8/19/72	2.28	5
		1640	2.6	0.7	0.7	40.	24.	-3.4	5/16/72	8.63	QU2 4
		1401	3.2	0.5	0.3	150.	16.	-10.9	4/12/72	10.56	3
3C021.1	NRAO37	1401	0.7	2.3	1.8	21.	17.	-10.6	4/13/72	11.46	U2 3
3C022.0	4C+50.04	5000	0.62	5.7	1.6	9.2	9.4	-0.2	8/20/72	2.19	5
		1640	1.8	1.5	0.6	49.	11.	-4.6	5/17/72	9.32	4
		1401	2.2	4.0	0.3	170.9	2.7	-8.9	4/14/72	10.92	3
3C028.0	0053+26	5000	0.13	13.3	10.5	51.	17.	-0.2	8/10/72	2.79	5
		1665	1.5	1.4	0.5	51.	11.	-1.1	12/16/71	18.91	2
		1395	1.5	1.1	0.5	124.	15.	-1.3	9/21/71	0.90	1
3C031.0	4C+32.05	5000	1.6	3.5	0.8	20.0	6.6	-0.2	8/22/72	2.51	5
		1640	5.0	3.2	0.2	97.6	2.0	-1.0	12/25/71	18.58	U1.2 2
		1640	3.4	2.8	0.2	84.9	2.3	-6.2	5/20/72	8.59	4
		1395	4.8	1.9	0.4	48.2	3.0	-1.1	9/24/71	0.83	U2 1
3C033.1	4C+72.01	5000	0.67	6.6	2.1	130.4	9.1	-0.2	8/23/72	2.50	5
		1665	3.0	3.7	0.3	106.7	2.1	-0.6	12/20/71	19.02	2
		1401	2.7	3.0	0.3	89.0	4.4	-10.4	3/29/72	12.31	3
3C033.2	4C+57.04	5000	0.81	1.6	1.1	158.	19.	-0.2	8/16/72	3.09	5
		1640	1.4	0.7	0.7	165.	25.	-4.1	5/13/72	10.24	4
		1401	1.6	1.6	0.6	4.3	9.8	-7.4	4/15/72	11.05	3
3C034.0	4C+31.02	5000	0.38	9.1	3.4	170.	10.	-0.2	8/25/72	2.79	5
		1640	1.5	1.7	0.7	51.	11.	-4.0	5/14/72	10.01	4
		1401	1.9	0.4	0.5	3.	24.	-9.3	4/16/72	10.77	3
3C035.0	NRAO61	5000	0.27	7.9	3.8	31.	16.	-0.1	8/12/72	3.68	5
		1665	2.2	3.3	0.4	156.3	3.4	-0.5	12/14/71	19.52	2
		1401	1.6	2.6	0.5	68.2	5.0	-10.8	4/ 8/72	12.38	3

TABLE 2-4--Continued

SOURCE	ALTERNATE NAME	FREQ MHZ	FLUX FU	P(%)	+/-	POSITION ANGLE	+/-	IONOS CORR.	OBS. DATE	AVG PST	NOTES	
3C036.0	4C+45.03	5000	0.36	1.9	3.3	78.	35.	-0.1	6/11/72	3.68		5
		1640	1.0	1.8	1.4	124.	16.	-4.4	5/15/72	10.26		4
		1401	1.3	1.3	0.7	97.	13.	-7.0	4/ 4/72	12.78		3
3C041.0	4C+32.06	5000	1.36	5.4	1.0	9.4	5.3	-0.2	8/14/72	3.85		5
		1665	3.8	7.1	0.2	94.8	1.1	-0.9	12/17/71	19.47		2
		1401	3.2	7.4	0.5	41.4	1.7	-11.3	3/30/72	12.53		3
3C042.0	4C+28.04	5000	1.04	1.2	1.3	9.	27.	-0.2	8/10/72	4.00		5
		1640	2.7	3.1	0.3	103.0	2.9	-0.4	12/28/71	18.99		2
		1401	2.7	2.9	0.4	66.9	3.8	-10.6	4/ 9/72	12.23		3
3C043.0	0127+23	5000	1.11	3.1	1.1	166.	11.	-0.2	8/15/72	3.81		5
		1640	2.4	0.8	0.5	119.	23.	-3.8	5/12/72	9.84	Q1.5	4
		1401	2.8	1.5	0.4	172.3	6.4	-8.1	4/ 1/72	13.10	Q1.7	3
3C044.0	0128+06	5000	0.37	11.3	3.4	94.2	9.5	-0.2	8/17/72	3.99		5
		1640	1.1	8.0	0.1	102.8	3.8	-7.1	5/20/72	10.04	U1.5	4
3C046.0	4C+37.05	5000	0.23	16.2	4.4	148.8	8.1	-0.3	8/26/72	3.13		5
		1655	1.27	10.0	0.7	171.8	2.2	-0.5	12/21/71	19.65		2
		1401	1.2	8.2	0.6	109.5	2.6	-11.5	4/12/72	12.15		3
3C049.0	0138+13	1640	2.6	0.4	0.3	56.	22.	-0.5	12/27/71	18.94		2
3C052.0	4C+53.02	5000	1.7	1.3	0.8	143.	16.	-0.2	8/ 9/72	4.31		5
		1665	4.1	3.2	0.2	51.7	1.8	-0.4	12/15/71	20.10		2
		1401	3.8	1.9	0.2	177.6	2.7	-11.4	4/13/72	12.65		3
3C054.0	4C+43.06	5000	0.59	5.2	2.5	38.	11.	-0.2	8/13/72	4.38		5
		1640	1.8	4.1	0.5	111.1	3.2	-0.7	12/22/71	19.51		2
		1401	1.8	4.7	0.5	49.7	3.0	-9.4	4/14/72	12.56		3
3C055.0	4C+28.05	5000	0.57	0.9	2.2	160.0	9.4	-0.2	8/18/72	4.19		5
		1640	2.4	5.9	0.3	170.8	1.5	-0.7	12/23/71	19.47		2
		1401	2.2	5.7	1.1	102.8	5.6	-9.7	4/15/72	12.72		3
3C058.0	4C+64.02	1640	32.6	1.7	0.1	1.0	1.6	-0.4	12/24/71	19.35		2
		1401	18.4	1.2	0.1	119.4	1.8	-7.9	3/31/72	12.90		3
3C065.0	4C+39.07	5000	0.83	13.7	1.3	144.6	2.7	-0.2	8/20/72	4.00		5
		1665	3.2	2.9	0.3	21.9	2.7	-0.7	12/18/71	20.29		2
		1401	3.2	0.9	0.2	122.2	7.8	-6.4	4/ 2/72	13.67		3
3C066.0	NRAO102	5000	1.8	2.3	0.7	69.6	8.7	-0.2	8/19/72	4.22	6°	5
		1640	6.3	2.7	0.3	117.3	2.6	-0.3	12/26/71	19.78	U2.5	2
		1395	2.8	1.3	0.3	88.9	6.8	-1.3	9/22/71	2.23		1
3C067.0	4C+27.08	5000	1.04	2.8	0.9	54.2	8.3	-0.2	8/21/72	4.01		5
		1665	3.0	1.5	0.3	105.3	5.4	-0.9	12/19/71	20.34		2
3C068.1	4C+34.08	5000	0.82	5.7	1.2	79.4	6.7	-0.2	8/22/72	4.26		5
		1640	2.3	6.3	0.3	135.7	1.4	-1.4	12/29/71	19.96		2
		1395	2.5	5.5	0.4	96.8	2.0	-1.3	9/23/71	2.23		1
3C068.2	NRAO108	1640	0.7	4.5	3.2	9.	16.	-3.6	5/16/72	10.96		4
		1401	0.8	3.1	1.7	129.6	7.9	-9.6	4/ 9/72	13.84	Q1.4	3
3C069.0	4C+58.08	5000	0.84	4.5	1.5	68.6	9.7	-0.2	8/23/72	4.61		5
		1640	3.3	9.0	0.5	123.0	1.2	-0.3	12/25/71	20.35	U2	2
		1401	3.2	4.9	0.3	171.7	1.7	-10.8	4/11/72	12.76		3

TABLE 2-4--Continued

SOURCE	ALTERNATE NAME	FREQ MHZ	FLUX FU	P(%)	+/-	POSITION ANGLE	+/-	IONOS CORR.	OBS. DATE	AVG PST	NOTES	
3C071.0	0240-00	1665	5.3	0.2	0.2	54.	23.	-0.6	12/16/71	20.72		2
		1401	4.9	0.3	0.2	99.	13.	-11.1	3/30/72	14.23		3
3C075.0	0255+05	5000	1.33	1.4	1.3	96.	25.	-0.3	8/11/72	5.63		5
		1665	5.4	0.9	0.2	59.0	5.4	-0.9	12/20/71	21.10		2
		1401	4.1	0.2	0.2	133.	22.	-13.7	3/29/72	14.18		3
3C083.1	4C+41.06	5000	1.8	7.8	0.7	106.4	2.7	-0.2	8/10/72	5.93		5
		1665	6.4	3.5	0.2	147.2	1.3	-0.6	12/17/71	21.45		2
		1640	6.0	4.0	0.2	149.8	1.1	-0.5	12/27/71	20.63		2
		1640	4.1	2.8	0.3	155.0	2.8	-3.8	5/12/72	11.56		4
		1395	5.0	1.5	0.4	24.9	7.5	-1.1	9/24/71	2.92	QU2	1
3C089.0	0331-01	1640	2.4	0.5	0.2	132.	14.	-0.8	12/23/71	20.79		2
		1401	2.5	0.8	0.3	179.2	9.4	-8.4	3/31/72	14.61		3
3C091.0	4C+50.10	5000	1.40	3.8	0.7	25.1	5.4	-0.2	8/12/72	5.45		5
		1665	3.6	6.5	0.3	161.7	1.1	-0.4	12/14/71	22.20		2
		1640	2.7	6.2	0.3	140.0	1.5	-5.3	5/19/72	11.43		4
		1401	3.3	7.1	0.2	50.1	1.1	-5.5	4/ 4/72	14.41		3
3C093.0	0340+04	1640	2.7	2.9	0.3	150.0	2.8	-1.0	12/22/71	21.03		2
		1401	2.8	2.0	0.3	159.9	4.2	-14.4	4/12/72	13.97		3
3C093.1	4C+33.08	5000	0.79	1.1	1.2	87.	24.	-0.2	8/ 9/72	5.52		5
		1655	2.2	1.0	0.4	113.	12.	-0.7	12/21/71	21.53		2
		1401	2.1	0.3	0.4	175.	34.	-12.1	4/13/72	14.35		3
3C099.0	0358+00	1640	1.6	3.9	0.5	56.2	3.8	-0.5	12/26/71	21.54		2
		1401	1.6	1.5	0.5	29.1	9.6	-11.7	4/14/72	14.30		3
3C103.0	4C+42.11	5000	1.33	10.8	0.9	65.5	2.3	-0.2	8/13/72	5.54		5
		1665	4.9	2.9	0.2	171.8	1.6	-0.4	12/15/71	22.46		2
		1401	4.7	1.7	0.1	143.4	2.7	-5.4	4/ 2/72	15.37		3
3C107.0	0409-01	5000	0.35	4.2	2.8	93.	16.	-0.3	8/15/72	5.52		5
		1665	1.32	3.1	0.6	32.4	5.9	-0.6	12/19/71	22.31		2
		1401	1.5	2.3	0.5	15.0	6.5	-11.3	4/15/72	14.57		3
3C114.0	0417+17	5000	0.24	4.7	4.5	121.	24.	-0.3	8/18/72	6.03		5
		1665	0.98	6.1	0.8	118.3	3.9	-0.6	12/18/71	22.13		2
		1401	0.9	4.9	1.2	107.4	5.6	-11.6	4/11/72	14.62	U1.3	3
		1395	1.0	3.9	0.9	107.1	6.8	-1.5	9/22/71	4.19		1
3C119.0	4C+41.13	1665	8.9	0.3	0.1	115.	11.	-0.6	12/16/71	22.76		2
		1640	8.7	0.3	0.2	148.	20.	-0.3	12/24/71	21.99	Q2	2
		1401	8.3	0.1	0.1	82.	14.	-10.8	4/12/72	15.07		3
		1395	7.7	0.3	0.1	139.	13.	-1.2	9/23/71	4.48		1
3C124.0	0439+01	5000	0.21	0.5	5.8	12.	51.	-0.4	8/20/72	6.26		5
		1640	0.8	0.6	0.8	89.	29.	-8.7	5/20/72	12.47	CONF?	4
		1401	1.0	1.8	0.8	105.	11.	-9.3	4/ 3/72	15.51		3
3C125.0	4C+39.15	5000	0.54	0.3	1.5	47.	50.	-0.3	8/16/72	6.99		5
		1640	1.5	3.1	0.7	54.8	6.3	-6.7	5/13/72	13.15		4
		1401	1.9	5.9	0.9	50.7	3.3	-8.0	3/29/72	15.99	U2.4	3
3C130.0	NRAO196	5000	0.66	6.3	1.2	141.2	6.4	-0.2	8/19/72	5.77		5
		1640	2.6	1.3	0.4	9.6	8.0	-0.9	12/29/71	22.37		2
		1640	1.8	0.9	0.5	128.	19.	-6.7	5/15/72	13.34		4
		1401	2.4	1.7	0.3	124.2	4.8	-5.3	3/30/72	16.07		3

TABLE 2-4--Continued

SOURCE	ALTERNATE NAME	FREQ MHZ	FLUX FU	P(8)	+/-	POSITION ANGLE	+/-	IONOS CORR.	OBS. DATE	AVG PST	NOTES	
3C131.0	4C+31.18	5000	0.78	3.7	1.3	60.6	9.8	-0.3	8/11/72	7.04		5
		1640	2.6	1.2	0.3	61.0	7.4	-0.4	12/28/71	22.12		2
		1401	2.8	1.1	0.3	158.2	7.3	-8.8	4/ 8/72	15.65		3
3C132.0	4C+22.11	1640	3.1	4.0	0.2	124.7	1.6	-0.5	12/27/71	22.35		2
		1401	3.4	3.2	0.2	94.6	2.0	-5.5	4/ 4/72	16.01		3
3C137.0	4C+50.16	5000	0.58	8.9	1.6	34.4	5.7	-0.3	8/14/72	7.02		5
		1665	1.9	4.7	0.4	30.1	2.6	-0.5	12/20/71	23.04		2
		1401	1.8	4.4	0.4	22.7	2.4	-7.6	4/ 9/72	15.74		3
		1395	1.9	3.3	0.5	34.5	4.3	-0.9	9/24/71	4.95		1
3C139.2	4C+28.15	5000	0.31	8.4	3.0	152.	11.	-0.3	8/15/72	7.49		5
		1640	1.7	2.7	0.5	109.7	5.3	-0.6	12/21/71	23.41	Q1.5	2
		1401	1.6	4.4	0.5	142.1	2.9	-4.4	3/31/72	16.43		3
3C141.0	4C+32.18	5000	0.63	6.1	1.6	39.7	6.7	-0.4	8/12/72	7.30		5
		1665	2.2	6.4	0.4	35.1	1.6	-0.4	12/17/71	23.40		2
		1401	2.3	4.1	0.3	37.3	2.4	-7.3	4/ 7/72	16.00		3
3C147.0	NRAO221	5000	8.1	0.7	0.4	144.9	7.8	-0.4	8/24/72	7.59		5
		1640	22.3	0.2	0.1	144.	11.	-0.5	12/22/71	23.31		2
		1401	19.1	0.1	0.1	1.	15.	-4.4	4/ 2/72	16.49		3
3C152.0	0601+20	5000	0.34	1.5	2.6	121.	35.	-0.4	8/ 9/72	8.21		5
		1665	1.6	1.5	0.5	97.9	9.5	-0.5	12/18/71	23.97		2
		1401	1.6	1.4	0.3	143.1	6.6	-7.1	4/ 3/72	16.59		3
3C154.0	0610+26	1665	5.3	0.9	0.2	8.8	5.6	-0.4	12/16/71	0.65	Q1.6	2
		1640	4.1	1.1	0.2	33.2	6.1	-4.4	5/12/72	14.45		4
		1401	5.0	0.5	0.2	72.0	8.9	-9.5	4/12/72	16.53		3
		1395	5.1	0.2	0.2	47.	21.	-2.6	9/22/71	6.26		1
3C158.0	4C+14.17	5000	0.53	2.6	2.2	141.	21.	-0.4	8/13/72	8.69	W15	5
		1665	2.1	0.5	0.4	155.	21.	-0.5	12/20/71	0.14		2
		1640	1.6	0.6	1.0	176.	16.	-0.4	12/25/71	23.53		2
		1401	2.1	0.7	0.3	121.	19.	-4.7	4/ 1/72	17.54	Q1.5	3
3C165.0	0640+23	5000	0.69	9.4	1.7	93.8	5.5	-0.4	8/14/72	9.00	W25	5
		1665	2.6	1.9	0.3	174.8	4.7	-0.5	12/15/71	0.90		2
		1640	1.6	2.2	0.7	25.	12.	-6.9	5/19/72	14.37	Q1.4	4
		1401	1.7	4.2	0.4	49.2	3.0	-8.1	4/15/72	16.70		3
		1395	1.8	2.5	0.5	45.1	5.6	-2.9	9/23/71	6.42		1
3C166.0	0642+21	1640	2.7	1.0	0.3	59.0	8.7	-0.6	12/17/71	0.82		2
		1640	1.9	2.0	0.6	34.0	9.9	-8.0	5/15/72	14.82		4
		1401	2.3	1.0	0.3	111.9	7.8	-5.4	3/29/72	17.82		3
3C169.1	4C+45.12	5000	0.24	3.4	5.0	30.	33.	-0.4	8/15/72	8.32		5
		1640	1.15	6.2	1.0	79.9	3.4	-0.4	12/25/71	0.30	Q1.5	2
		1401	1.1	4.1	0.6	83.7	4.3	-2.9	3/30/72	18.10		3
3C173.0	4C+38.19	5000	0.45	3.6	2.5	91.	20.	-0.3	8/11/72	9.38		5
		1665	1.7	2.3	0.5	153.7	6.0	-0.6	12/21/71	0.81		2
		1401	1.4	1.9	0.5	156.4	7.5	-2.8	3/31/72	18.29		3
3C173.1	4C+74.12	5000	0.70	5.1	2.1	43.	11.	-0.3	8/16/72	9.29		5
		1640	2.6	6.8	0.3	176.0	1.3	-0.3	12/27/71	0.43		2
		1401	2.7	5.0	0.3	151.7	1.7	-4.1	4/ 4/72	17.70		3
3C175.1	0711+14	1665	2.0	1.6	0.5	121.0	8.0	-0.6	12/13/71	1.27	U1.4	2
		1401	1.8	2.0	0.4	21.2	6.0	-6.2	4/ 7/72	17.62		3

TABLE 2-4--Continued

SOURCE	ALTERNATE NAME	FREQ MHZ	FLUX FU	P(6)	+/-	POSITION ANGLE	+/-	IONOS CORR.	OBS. DATE	AVG PST	NOTES	
3C177.0	0721+15	5000	0.16	20.6	8.6	29.6	9.8	-0.4	8/17/72	8.54		5
		1640	1.20	14.7	0.7	139.1	1.4	-0.8	12/23/71	1.06		2
		1401	1.1	13.8	0.6	7.0	1.3	-3.2	4/ 2/72	18.59		3
3C180.0	0724-01	1640	2.8	2.1	0.3	46.4	4.3	-0.7	12/24/71	0.96		2
		1401	2.6	1.5	0.3	87.3	5.5	-8.1	4/ 8/72	17.77		3
3C181.0	0725+14	5000	0.56	2.3	3.2	95.	24.	-0.5	8/18/72	9.43	Q1.5	5
		1640	2.4	2.2	0.4	162.5	7.1	-0.4	12/26/71	1.20	U1.7	2
		1401	2.3	2.1	0.3	25.0	4.4	-6.8	4/ 9/72	17.85		3
3C184.0	4C+70.06	5000	0.54	6.3	3.4	164.	12.	-0.4	8/12/72	9.90	Q1.5	5
		1655	2.1	4.3	0.3	19.0	1.9	-0.9	12/30/71	0.80		2
		1401	2.6	1.9	0.3	8.2	3.7	-2.9	4/ 3/72	18.82		3
3C184.1	NRAO271	5000	0.76	2.3	1.7	58.	19.	-0.4	8/20/72	9.53		5
		1640	2.5	2.6	0.4	40.8	4.6	-3.0	5/12/72	15.69		4
		1401	3.0	3.2	0.3	25.1	2.4	-4.6	4/10/72	17.99		3
3C186.0	4C+38.21	5000	0.25	3.0	5.0	127.	35.	-0.6	8/21/72	9.21		5
		1665	1.14	1.3	0.8	85.	16.	-0.4	12/19/71	1.65		2
		1640	1.1	2.7	0.7	72.7	7.3	-5.5	5/20/72	15.84		4
		1401	1.3	1.1	0.7	162.	17.	-6.0	4/11/72	17.88	Q1.4	3
3C187.0	0742+02	5000	0.36	10.4	3.6	54.5	7.7	-0.6	8/22/72	9.36		5
		1665	1.48	4.3	0.5	93.8	4.1	-0.6	12/20/71	1.83	U1.3	2
		1395	1.5	2.0	0.6	125.2	9.1	-4.2	9/21/71	7.56		1
3C190.0	0758+14	1640	2.4	0.6	0.3	148.	14.	-0.3	12/28/71	1.03		2
		1401	2.5	0.2	0.3	101.	30.	-2.7	4/ 1/72	19.20		3
3C191.0	0802+10	1640	1.5	0.8	1.0	71.	25.	-6.6	5/13/72	16.04	Q1.5	4
		1401	1.9	0.8	0.4	139.	13.	-7.3	4/12/72	18.17		3
3C194.0	4C+42.25	5000	0.66	6.6	1.9	67.3	8.1	-0.4	8/ 9/72	10.63		5
		1640	1.6	3.0	0.6	25.4	5.7	-3.7	5/14/72	16.15		4
		1401	2.1	1.0	0.7	50.	11.	-5.2	4/13/72	18.19	U2	3
3C196.0	NRAO285	1640	10.7	0.4	0.1	104.2	8.6	-5.6	5/15/72	16.35		4
		1401	14.1	0.1	0.1	148.	14.	-3.1	4/ 4/72	19.29		3
3C196.1	0812-02	1640	1.5	0.7	0.7	52.	24.	-4.1	5/16/72	15.99		4
		1401	1.9	0.3	0.4	18.	33.	-6.8	4/14/72	18.30		3
3C197.1	4C+47.28	5000	0.65	4.5	2.0	163.	13.	-0.5	8/23/72	9.70		5
		1640	1.9	2.1	0.4	159.5	5.9	-0.4	12/25/71	1.94		2
		1395	1.6	4.4	0.6	154.3	3.6	-3.3	9/22/71	8.21		1
3C198.0	0819+06	5000	0.28	14.1	4.4	105.8	9.2	-0.6	8/24/72	9.61		5
		1640	1.3	4.1	0.6	145.2	4.2	-6.8	5/19/72	15.93		4
		1401	1.8	4.0	0.4	165.0	3.0	-4.3	4/ 7/72	19.26		3
3C200.0	4C+29.29	5000	0.67	5.9	1.5	46.5	9.6	-0.6	8/25/72	9.86		5
		1665	1.9	5.3	0.7	60.1	2.9	-0.4	12/16/71	2.74	U2	2
		1401	2.0	3.8	0.4	73.2	2.7	-3.0	3/29/72	19.64		3
3C204.0	4C+65.09	5000	0.27	12.3	3.7	152.4	8.6	-0.5	8/26/72	10.22		5
		1665	1.17	1.9	0.8	85.	10.	-0.5	12/17/71	2.85		2
		1401	1.1	0.9	0.6	86.	21.	-1.2	3/30/72	19.89		3
3C205.0	4C+58.16	5000	0.50	6.0	2.6	74.	12.	-0.4	8/13/72	11.06	W15	5
		1640	2.4	7.7	0.3	42.8	1.4	-0.3	12/27/71	2.14		2
		1401	2.2	5.5	0.3	37.1	2.5	-1.2	3/31/72	19.98	Q1.5	3

TABLE 2-4--Continued

SOURCE	ALTERNATE NAME	FREQ MHZ	FLUX FU	P(A)	+/-	POSITION ANGLE	+/-	IONOS CORR.	OBS. DATE	AVG PST	NOTES	
3C208.0	0850+14	1665	2.5	0.2	0.5	79.	36.	-0.6	12/15/71	3.18		2
		1640	2.2	0.7	0.5	119.	18.	-0.5	12/29/71	2.07		2
		1395	2.4	1.0	0.4	132.	11.	-4.5	9/23/71	8.53	CONF?	1
3C208.1	0851+14	5000	0.77	4.1	1.7	106.	10.	-0.5	8/14/72	10.66	Q1.5	5
		1665	2.4	1.4	0.3	170.3	7.2	-0.7	12/18/71	2.21		2
		1401	1.6	1.6	0.4	4.5	8.1	-6.0	4/15/72	18.70	CONF?	3
3C210.0	4C+28.21	5000	0.42	6.5	2.7	89.	14.	-0.3	8/15/72	10.91		5
		1640	1.3	1.0	0.8	15.	20.	-3.2	5/12/72	17.56		4
		1401	1.6	0.8	0.4	46.	15.	-4.1	4/ 8/72	19.40		3
3C212.0	0855+14	1640	2.6	1.6	0.8	137.9	6.4	-0.8	12/23/71	2.94	U2.5	2
		1401	2.0	1.4	0.4	56.2	7.5	-6.5	4/16/72	18.74		3
3C213.1	4C+29.33	5000	0.70	3.9	1.8	152.	13.	-0.4	8/11/72	11.35		5
		1665	2.1	3.4	0.5	63.2	4.3	-0.6	12/21/71	2.71		2
		1401	1.9	2.4	0.3	77.7	3.8	-3.8	4/ 9/72	19.63		3
3C215.0	0903+16	5000	0.46	6.9	3.4	72.	14.	-0.4	8/16/72	11.28		5
		1640	1.6	1.4	0.5	135.	10.	-0.5	12/24/71	2.60		2
		1401	1.5	1.9	0.4	145.7	6.5	-1.7	4/ 2/72	20.26		3
3C216.0	4C+43.17	1640	3.1	0.5	0.3	39.	31.	-4.3	5/13/72	17.76	Q1.9	4
		1401	4.1	0.3	0.2	35.	14.	-3.6	4/12/72	19.86		3
3C217.0	4C+38.26	5000	0.38	5.7	3.6	10.	15.	-0.4	8/17/72	11.24		5
		1640	2.2	1.7	0.4	10.8	6.7	-0.4	12/26/71	2.88		2
		1401	2.1	2.2	0.4	30.4	4.5	-3.9	4/10/72	19.64		3
3C220.1	4C+79.06	5000	0.30	8.5	4.5	150.	15.	-0.4	8/18/72	11.48		5
		1640	2.0	0.6	0.4	22.	18.	-0.8	12/30/71	2.76	Q1.3	2
		1401	2.2	0.3	0.3	45.	27.	-2.6	4/13/72	19.81		3
3C220.2	4C+36.15	5000	0.46	2.8	3.2	140.	24.	-0.5	8/19/72	11.53		5
		1640	1.5	4.7	0.7	43.1	4.1	-4.4	5/15/72	18.20		4
		1401	1.8	2.5	0.4	60.3	4.6	-3.0	4/14/72	19.94		3
3C220.3	NRAO323	5000	0.32	5.8	4.4	18.	20.	-0.4	8/12/72	11.91	W20	5
		1640	2.2	0.3	0.0	121.	39.	-2.0	5/16/72	17.85	U1.5	4
		1401	2.9	0.3	0.3	178.	32.	-1.6	4/ 3/72	20.49	U2	3
3C222.0	0933+04	1640	0.7	1.5	0.9	142.	16.	-5.5	5/19/72	17.71		4
		1401	1.0	0.7	0.7	39.	27.	-1.7	4/ 1/72	20.89		3
3C223.0	NRAO328	5000	0.91	7.7	1.3	82.9	5.5	-0.6	8/20/72	11.47		5
		1665	3.6	7.9	0.4	107.2	1.3	-0.6	12/20/71	3.57		2
		1401	3.4	7.3	0.2	119.8	1.1	-3.2	4/15/72	20.34		3
3C223.1	NRAO329	5000	0.74	0.6	1.7	72.	43.	-0.6	8/21/72	11.13		5
		1640	1.6	3.2	0.6	51.1	5.4	-2.3	5/12/72	19.22		4
		1401	2.0	3.2	0.4	53.7	3.3	-2.2	4/ 4/72	20.85		3
3C225.0	0939+14	5000	0.92	4.9	2.6	106.	12.	-0.5	8/22/72	11.43	Q2	5
		1640	4.0	1.6	0.2	56.0	3.6	-0.4	12/29/71	3.31		2
		1401	4.2	1.1	0.2	47.6	4.6	-4.1	4/16/72	20.34		3
3C226.0	0941+10	1640	2.2	5.3	0.5	90.2	1.9	-0.4	12/28/71	3.13	Q1.5	2
		1395	2.1	4.0	0.5	96.4	3.5	-5.3	9/21/71	9.50		1
3C231.0	M82	1640	8.5	0.4	0.2	155.	14.	-0.3	12/25/71	3.57	U2	2
		1401	7.7	0.3	0.1	62.	11.	-2.3	4/11/72	20.72		3

TABLE 2-4--Continued

SOURCE	ALTERNATE NAME	FREQ MHZ	FLUX FU	P(6)	+/-	POSITION ANGLE	+/-	IONOS CORR.	OBS. DATE	AVG PST	NOTES	
3C234.0	NRAO343	5000	1.20	1.0	1.3	4.	26.	-0.4	8/ 9/72	12.61		5
		1640	4.0	1.2	0.3	71.0	5.8	-3.7	5/13/72	19.38		4
		1401	5.2	1.5	0.2	115.3	3.7	-2.3	3/29/72	21.33	U2	3
3C236.0	NRAO344	5000	1.37	2.7	1.0	101.6	9.8	-0.6	8/23/72	11.70		5
		1640	3.0	3.2	0.3	132.5	2.6	-0.4	12/27/71	3.84		2
		1401	3.3	1.0	0.2	7.0	6.1	-2.0	4/ 8/72	21.02		3
3C239.0	4C+46.20	5000	0.31	3.6	4.0	128.	27.	-0.5	8/24/72	11.60		5
		1640	1.39	1.7	0.6	125.1	9.0	-0.4	12/24/71	4.22		2
		1640	1.2	1.1	0.6	146.	14.	-3.1	5/20/72	18.40		4
		1401	1.5	1.1	0.5	161.	12.	-2.0	4/ 7/72	20.91		3
3C241.0	1019+22	1640	1.38	0.3	0.6	127.	36.	-0.7	12/22/71	4.00		2
		1395	1.8	0.3	0.6	142.	34.	-4.6	9/22/71	10.09		1
3C244.1	4C+58.21	5000	0.60	5.9	1.4	147.1	7.5	-0.4	8/13/72	12.55		5
		1665	4.0	3.9	0.3	107.1	2.0	-0.5	12/17/71	4.58		2
		1401	3.9	3.2	0.1	110.7	1.2	-0.8	3/30/72	21.63		3
3C247.0	4C+43.20	5000	0.68	7.2	1.8	179.5	7.9	-0.4	8/11/72	13.33	3.3'	5
		1665	2.4	5.0	0.4	52.8	2.1	-0.5	12/15/71	5.13		2
		1395	2.9	3.2	0.5	60.9	4.7	-4.5	9/23/71	10.61	Q2	1
3C249.1	4C+77.02	5000	0.57	3.8	1.7	179.	12.	-0.4	8/14/72	12.84		5
		1640	2.3	2.8	0.4	141.3	3.7	-0.5	12/21/71	4.85		2
		1401	2.3	1.5	0.3	115.0	5.6	-1.1	4/ 2/72	21.99		3
3C250.0	1106+25	5000	0.20	6.3	6.4	44.	23.	-0.3	8/15/72	13.17	W20	5
		1640	1.11	3.9	0.7	111.0	5.4	-0.5	12/26/71	4.53		2
		1401	1.0	2.0	0.7	95.0	9.8	-2.6	4/ 9/72	21.52		3
3C252.0	4C+35.25	5000	0.25	12.5	4.5	104.	12.	-0.4	8/16/72	13.32		5
		1640	1.30	1.0	0.6	81.	16.	-0.8	12/23/71	4.80		2
		1401	1.3	1.2	0.5	64.	13.	-3.1	4/10/72	21.51		3
3C255.0	1116-02	5000	0.07	20.9	16.3	34.	19.	-0.6	8/17/72	13.59	W20	5
		1665	1.47	1.1	0.5	34.	12.	-0.5	12/16/71	5.45		2
		1401	1.7	0.3	0.4	70.	31.	-2.4	4/ 3/72	22.26		3
3C256.0	1118+23	5000	0.30	6.0	3.2	57.	14.	-0.6	8/18/72	12.94		5
		1640	1.29	1.0	0.6	77.	16.	-0.4	12/28/71	4.75		2
		1401	1.4	0.7	0.5	148.	18.	-2.2	4/ 4/72	22.40		3
3C257.0	1120+05	5000	0.43	6.3	3.0	167.	13.	-0.5	8/19/72	13.52		5
		1640	1.4	4.6	0.7	27.9	4.8	-3.2	5/14/72	19.46		4
		1401	1.6	3.5	0.4	6.8	4.0	-2.9	4/13/72	21.56		3
3C258.0	1122+19	1640	0.8	0.2	1.2	79.	50.	-3.2	5/15/72	20.10		4
		1401	0.9	1.6	0.8	8.	14.	-1.5	4/ 1/72	22.59		3
3C263.0	4C+56.13	5000	0.84	2.5	1.4	38.	18.	-0.4	8/12/72	13.89	W25	5
		1665	3.1	2.1	0.3	44.4	4.2	-0.5	12/20/71	5.46		2
		1640	2.9	2.1	0.4	34.9	4.9	-0.8	12/30/71	4.21		2
		1401	3.1	1.4	0.2	80.7	4.7	-2.4	4/12/72	21.75		3
3C263.1	1140+22	1640	2.7	2.6	0.3	123.6	3.7	-0.4	12/25/71	5.24		2
		1401	3.1	1.0	0.2	140.5	7.5	-2.6	4/14/72	21.51		3
		1395	3.1	1.6	0.4	128.6	7.0	-6.1	9/20/71	11.56		1
3C264.0	1142+19	1640	5.2	0.6	0.2	123.7	8.2	-0.4	12/29/71	5.00		2
		1401	5.0	0.5	0.2	160.3	8.3	-2.9	4/15/72	21.99		3
		1395	4.5	0.7	0.9	167.	26.	-6.2	9/21/71	11.53		1

TABLE 2-4--Continued

SOURCE	ALTERNATE NAME	FREQ MHZ	FLUX FU	P(%)	+/-	POSITION ANGLE	+/-	IONOS CORR.	OBS. DATE	AVG PST	NOTES
3C265.0	4C+31.37	5000	0.54	3.3	2.2	52.	17.	-0.6	8/20/72	13.59	5
		1640	2.1	5.5	0.3	33.8	1.4	-3.7	5/19/72	19.86	4
		1401	2.7	5.2	0.3	35.6	1.2	-2.1	3/29/72	23.09	3
3C266.0	4C+50.33	5000	0.31	10.5	3.5	90.7	8.6	-0.5	8/21/72	13.48	5
		1640	1.34	0.9	0.6	140.	19.	-0.3	12/27/71	5.53	2
		1401	1.4	1.4	0.5	9.	10.	-2.2	4/11/72	22.32	3
3C268.1	4C+73.11	1640	5.6	0.9	0.2	175.8	6.4	-1.6	5/12/72	20.92	4
		1401	6.4	1.0	0.1	158.8	3.7	-1.5	4/ 8/72	22.71	3
3C268.2	4C+31.39	5000	0.39	7.4	2.7	89.	11.	-0.5	8/22/72	13.82	5
		1640	1.07	4.3	0.6	118.0	4.4	-0.7	12/22/71	6.00	2
		1401	1.2	4.8	1.0	129.4	3.5	-1.9	4/ 7/72	22.59	U1.7 3
3C268.3	4C+64.14	5000	1.12	1.1	1.2	93.	26.	-0.6	8/23/72	13.65	5
		1640	3.6	0.3	0.2	61.	16.	-0.7	12/30/71	5.50	2
		1401	3.6	0.2	0.2	19.	24.	-0.9	3/31/72	23.35	3
3C268.4	4C+43.23	5000	0.58	11.3	2.3	45.2	5.6	-0.3	8/ 9/72	14.70	5
		1640	1.9	9.2	0.5	35.2	1.4	-0.4	12/24/71	5.79	2
		1401	1.9	8.0	0.4	38.6	1.3	-0.9	3/30/72	23.31	3
3C270.1	4C+33.29	5000	0.89	11.3	1.5	92.3	4.0	-0.3	8/10/72	14.51	5
		1665	2.8	7.7	0.3	91.5	1.1	-0.9	12/17/71	6.34	2
		1401	2.6	5.6	0.3	97.7	1.4	-2.3	4/16/72	22.26	3
		1395	2.7	5.9	0.5	90.4	2.4	-5.0	9/22/71	12.05	1
3C272.0	4C+42.35	5000	0.39	11.9	2.9	112.5	6.8	-0.6	8/24/72	14.07	5
		1640	1.44	5.7	0.6	109.8	2.9	-0.5	12/26/71	6.13	2
		1401	1.3	4.9	0.5	105.5	3.1	-1.3	4/ 2/72	23.64	3
3C274.0	VIR A	1640		0.3	0.1	46.0	6.4	-3.1	5/20/72	20.45	4
		1401		0.1	0.1	173.9	8.8	-2.5	4/14/72	22.68	3
3C275.0	1239-04	1640	3.5	1.3	0.2	62.1	5.2	-1.4	12/21/71	6.71	2
		1395	3.3	5.8	1.2	44.2	3.8	-6.3	9/23/71	12.55	U3 1
3C277.0	4C+50.35	5000	0.25	4.6	5.1	55.	33.	-0.5	8/11/72	15.32	U1.4 5
		1665	1.10	4.3	0.8	7.6	5.6	-1.3	12/13/71	6.84	2
		1401	1.0	4.4	0.7	1.2	4.4	-2.0	4/ 4/72	23.99	3
3C277.1	4C+56.40	5000	0.60	5.2	2.5	159.	28.	-0.4	8/13/72	15.04	U1.4W5
		1640	2.5	0.4	0.4	73.	25.	-0.8	12/23/71	6.41	2
		1640	2.0	0.3	0.5	164.	35.	-1.5	5/14/72	21.07	4
		1401	2.4	1.0	0.3	0.2	8.4	-2.3	4/10/72	23.17	3
3C277.2	1251+15	5000	0.49	8.2	2.9	93.8	8.3	-0.7	8/25/72	14.39	5
		1640	1.5	4.0	0.5	148.9	3.8	-2.0	5/13/72	21.39	4
		1401	1.9	4.2	0.4	153.3	2.6	-2.1	4/ 3/72	23.92	3
3C277.3	COM A	5000	1.10	5.3	1.1	4.5	5.4	-0.5	8/14/72	14.30	5
		1640	2.8	2.0	0.3	0.7	4.2	-0.6	12/28/71	6.38	2
		1401	3.1	1.6	0.2	17.9	4.1	-2.2	4/ 9/72	23.28	3
3C280.0	4C+47.36	1640	5.1	1.9	0.2	11.1	2.8	-0.8	12/25/71	6.87	2
		1401	5.0	1.9	0.2	3.1	2.3	-2.1	4/13/72	23.24	3
3C280.1	4C+40.32	5000	0.33	7.3	2.5	24.5	9.8	-0.3	8/15/72	15.12	5
		1665	1.30	1.9	0.7	162.7	9.3	-1.2	12/19/71	6.98	2
		1640	1.1	2.8	1.1	174.6	9.5	-2.2	5/15/72	21.43	4
		1401	1.3	2.2	0.5	159.0	7.1	-1.4	4/ 2/72	0.29	3

TABLE 2-4--Continued

SOURCE	ALTERNATE NAME	FREQ MHZ	FLUX FU	P(%)	+/-	POSITION ANGLE	+/-	IONOS CORR.	OBS. DATE	AVG PST	NOTES
3C284.0	NRAO421	5000	0.36	12.5	3.8	26.0	8.4	-0.7	8/ 8/72	15.82	5
		1665	1.9	8.1	0.6	6.2	1.4	-1.3	12/16/71	7.19	2
		1401	1.8	7.5	0.4	6.0	1.6	-2.5	4/12/72	23.37	3
3C285.0	NRAO422	5000	0.52	7.8	2.3	82.9	8.3	-0.3	8/16/72	15.45	5
		1665	2.1	5.6	0.4	44.7	2.0	-1.5	12/15/71	7.50	2
		1401	1.9	6.1	0.4	38.3	3.2	-2.1	4/11/72	23.92	U1.7 3
3C288.0	4C+39.39	5000	0.86	1.6	2.2	15.	28.	-0.4	8/12/72	15.91	U1.7W5
		1640	3.3	0.3	0.3	107.	22.	-1.2	12/24/71	7.34	2
		1401	3.4	0.6	0.2	37.	11.	-1.1	3/31/72	0.99	3
3C288.1	4C+60.18	5000	0.30	5.2	4.4	108.	21.	-0.4	8/17/72	15.92	5
		1640	1.25	1.4	0.7	141.	13.	-1.0	12/27/71	7.18	2
		1401	1.5	0.5	0.5	143.	25.	-1.7	3/30/72	0.83	3
3C289.0	4C+50.37	5000	0.62	5.3	1.4	87.0	7.3	-0.4	8/18/72	15.52	5
		1640	2.2	1.2	0.3	179.6	7.7	-1.0	12/29/71	6.80	2
		1401	2.3	0.2	0.3	91.	41.	-2.0	4/14/72	24.00	3
		1395	2.2	0.2	0.5	113.	39.	-5.5	9/21/71	13.53	1
3C293.0	NRAO433	5000	1.49	1.0	0.7	78.	22.	-0.4	8/19/72	15.78	5
		1665	4.9	1.7	0.2	65.2	3.5	-1.7	12/20/71	7.66	2
		1401	4.5	1.5	0.2	58.8	2.9	-1.1	4/ 1/72	1.06	3
3C293.1	1352+16	5000	0.16	17.2	9.8	128.	11.	-0.6	8/20/72	15.70	5
		1640	0.5	6.5	2.0	145.2	7.8	-1.4	5/12/72	22.72	4
		1401	0.8	4.8	1.0	149.1	5.5	-1.9	4/ 9/72	0.44	3
3C294.0	4C+34.38	5000	0.27	1.8	2.9	17.	34.	-0.3	8/10/72	16.45	5
		1640	1.38	2.1	0.5	84.2	5.3	-1.3	12/26/71	7.48	2
		1401	1.2	0.4	0.4	16.	29.	-1.5	4/ 3/72	0.45	3
3C295.0	4C+52.30	5000	6.2	0.2	0.4	93.	25.	-0.3	8/ 9/72	16.77	5
		1640	21.3	0.4	0.2	135.7	7.2	-1.9	12/22/71	7.80	U2 2
		1401	1.1	0.0	0.1	40.	47.	-2.4	4/11/72	0.76	3
3C298.0	1416+06	1640	4.7	0.2	0.2	24.	26.	-1.7	5/14/72	22.42	4
		1401	5.9	0.1	0.1	19.	32.	-2.8	4/16/72	0.23	3
		1395	5.8	1.0	0.2	112.7	7.2	-7.5	9/20/71	14.16	1
3C299.0	4C+41.27	5000	0.95	1.2	1.3	143.	28.	-0.4	8/21/72	16.04	5
		1640	2.4	0.3	0.4	36.	30.	-2.1	5/15/72	22.56	4
		1401	3.0	0.6	0.2	79.	11.	-1.7	4/ 4/72	1.57	3
3C300.0	1420+19	1640	3.7	1.6	0.3	85.7	4.9	-2.1	12/23/71	8.06	2
		1395	3.5	1.5	0.3	85.3	4.9	-4.7	9/22/71	14.10	1
3C300.1	1425-01	1665	2.6	1.1	0.4	60.4	9.6	-4.1	12/18/71	8.69	2
		1401	2.7	0.4	0.2	173.	17.	-2.3	3/29/72	1.80	3
3C303.0	4C+52.33	5000	0.96	4.7	0.9	44.7	6.0	-0.4	8/13/72	16.83	5
		1640	2.6	8.4	0.5	73.5	2.8	-2.6	12/21/71	8.51	U1.8 2
		1401	2.5	5.2	0.3	82.3	1.4	-1.2	4/ 2/72	1.97	3
3C303.1	NRAO453	1665	1.47	0.7	1.0	94.	28.	-1.9	12/19/71	8.69	2
		1401	2.4	0.3	0.3	91.	24.	-1.7	4/ 5/72	1.61	3
3C305.0	NRAO456	5000	0.96	4.1	1.0	69.3	7.2	-0.3	8/22/72	16.62	5
		1640	2.9	0.7	0.3	159.	13.	-1.6	12/28/71	8.07	2
		1401	2.8	0.1	0.3	104.	37.	-1.7	4/17/72	1.25	3
		1395	3.0	0.4	0.4	126.	22.	-3.9	9/23/71	14.52	1

TABLE 2-4--Continued

SOURCE	ALTERNATE NAME	FREQ MHZ	FLUX FU	P(6)	+/-	POSITION ANGLE	+/-	IONOS CORR.	OBS. DATE	AVG PST	NOTES	
3C305.1	4C+77.14	5000	0.37	4.1	3.4	107.	21.	-0.3	8/11/72	17.38		5
		1640	1.09	0.6	1.3	22.	40.	-1.6	12/25/71	8.51		2
		1401	2.3	0.3	0.3	141.	24.	-1.6	4/10/72	1.17		3
3C306.1	1452-04	1640	1.6	9.8	0.4	76.0	1.2	-3.0	5/19/72	22.69		4
		1401	2.0	8.3	0.4	72.5	1.2	-3.3	4/13/72	1.08		3
3C309.1	4C+71.15	1640	7.9	1.9	0.1	159.9	2.1	-2.5	12/29/71	8.47		2
		1401	8.2	0.8	0.1	33.3	3.3	-1.8	4/14/72	1.12		3
3C314.1	4C+70.16	5000	0.22	1.5	4.0	91.	42.	-0.3	8/14/72	17.26		5
		1665	1.37	1.1	0.6	130.	18.	-1.8	12/15/71	9.52		2
		1401	1.4	1.7	0.5	132.	10.	-2.0	4/12/72	1.52		3
3C317.0	1514+07	1640	4.1	0.1	0.2	73.	35.	-2.3	5/20/72	23.04		4
		1401	5.4	0.2	0.2	105.	25.	-2.1	3/30/72	2.54	Q2	3
3C318.0	1517+20	1640	2.1	0.3	0.4	110.	29.	-1.4	5/13/72	23.76		4
		1401	2.6	0.6	0.3	156.	12.	-1.2	3/31/72	2.70		3
3C319.0	4C+54.34	5000	0.69	5.2	1.3	90.2	6.7	-0.5	8/ 8/72	17.42		5
		1640	2.6	2.8	0.4	112.7	3.6	-1.9	12/24/71	8.95		2
		1401	2.5	2.5	0.3	106.6	3.0	-1.0	4/ 1/72	2.86		3
3C320.0	4C+35.36	5000	0.49	0.5	2.4	79.	49.	-0.3	8/16/72	17.55		5
		1640	1.5	0.7	0.7	126.	25.	-1.2	5/13/72	0.36		4
		1401	1.8	0.5	0.4	124.	21.	-1.7	4/ 9/72	2.25		3
3C322.0	4C+55.31	5000	0.42	1.9	2.5	109.	30.	-0.3	8/12/72	17.42		5
		1665	1.7	1.4	0.8	51.	23.	-2.5	12/20/71	9.51	Q1.9	2
		1401	1.8	0.9	0.4	0.	12.	-2.3	4/11/72	2.33		3
3C323.0	4C+60.21	5000	0.32	7.6	3.6	132.	12.	-0.4	8/20/72	17.80		5
		1640	1.25	1.7	1.1	11.	23.	-2.3	12/16/71	9.17		2
		1401	1.3	1.2	0.5	118.	11.	-1.2	4/ 3/72	2.92		3
3C324.0	1547+21	1640	2.4	2.8	0.5	36.6	5.2	-2.8	12/26/71	9.35		2
		1401	2.5	3.9	0.3	88.5	1.9	-2.5	4/16/72	1.96		3
		1395	2.5	4.0	0.4	89.8	2.6	-4.4	9/21/71	15.62		1
3C325.0	4C+62.25	5000	0.78	7.3	4.0	89.1	6.0	-0.4	8/17/72	18.02	Q2.0	5
		1640	2.9	3.2	0.3	67.2	2.7	-1.2	5/15/72	0.39		4
		1401	3.5	3.3	0.2	57.3	1.8	-1.4	4/ 4/72	3.10		3
3C327.1	1602+01	1640	3.3	0.9	0.3	107.9	9.1	-2.1	5/16/72	0.53		4
		1401	3.8	0.3	0.2	125.	14.	-1.7	3/29/72	3.58		3
3C332.0	4C+21.47	5000	0.90	9.1	1.0	120.4	3.1	-0.3	8/ 9/72	18.11		5
		1640	2.2	6.0	0.4	127.5	2.4	-3.5	12/30/71	9.16		2
		1401	2.5	3.2	0.3	126.4	2.4	-1.0	4/ 2/72	3.61		3
3C334.0	1618+17	1640	1.8	4.6	0.7	127.7	4.0	-2.9	12/27/71	10.24		2
		1401	1.9	3.3	0.3	150.6	2.9	-2.4	4/15/72	2.52		3
		1395	1.9	2.5	0.5	158.1	5.9	-3.6	9/22/71	16.06		1
3C337.0	4C+44.28	5000	0.81	2.0	1.4	76.	19.	-0.4	8/19/72	18.21		5
		1640	2.8	5.2	0.3	137.5	2.0	-2.5	12/25/71	10.33		2
		1401	3.0	4.3	0.3	166.0	1.7	-2.0	4/10/72	2.85		3
3C338.0	4C+39.45	5000	0.46	4.7	3.2	85.	25.	-0.3	8/18/72	18.47	QU2	5
		1665	3.1	0.9	0.4	119.	13.	-3.3	12/18/71	10.63		2
		1401	3.4	0.5	0.2	71.	13.	-1.6	4/ 5/72	3.22		3

TABLE 2-4--Continued

SOURCE	ALTERNATE NAME	FREQ MHZ	FLUX FU	P(%)	+/-	POSITION ANGLE	+/-	IONOS CORR.	OBS. DATE	AVG PST	NOTES	
3C340.0	4C+23.44	1665	2.5	4.9	0.3	40.1	2.1	-3.9	12/19/71	10.60		2
		1401	2.3	4.1	0.3	57.1	2.3	-2.5	4/13/72	2.69		3
3C341.0	4C+27.33	5000	0.54	21.9	1.5	147.2	1.9	-0.3	8/10/72	18.75		5
		1665	1.8	18.4	0.6	1.1	1.7	-7.8	12/17/71	10.43	U2	2
		1401	1.8	19.5	0.4	15.1	1.1	-2.1	4/17/72	2.87		3
		1395	1.7	19.5	0.5	16.5	1.1	-3.8	9/20/71	16.34		1
3C343.0	4C+62.26	1640	3.9	0.3	0.2	24.	17.	-1.8	5/20/72	0.81		4
		1401	4.9	0.5	0.1	74.7	7.0	-1.6	4/14/72	2.87		3
3C343.1	4C+62.27	5000	1.16	3.0	1.1	147.	11.	-0.4	8/23/72	18.33		5
		1640	4.8	0.3	0.2	47.	16.	-2.5	12/24/71	10.57		2
		1401	4.8	0.7	0.1	101.2	5.8	-1.9	4/12/72	3.25		3
3C346.0	1641+17	1640	3.0	2.1	0.2	110.3	3.1	-2.0	5/21/72	1.04		4
		1401	3.6	1.7	0.2	84.3	3.2	-1.6	3/30/72	4.18		3
3C348.0	HER A	1640	32.6	1.8	0.1	46.3	1.5	-2.9	12/28/71	10.30		2
		1395	42.0	1.4	0.1	44.6	2.3	-5.3	9/23/71	16.54		1
3C349.0	4C+47.45	5000	1.22	3.8	1.1	40.0	7.5	-0.3	8/11/72	19.37		5
		1640	3.1	4.3	0.3	62.1	2.0	-3.3	12/22/71	10.61		2
		1401	3.3	4.3	0.2	68.7	1.4	-1.0	3/31/72	4.41		3
3C351.0	4C+60.24	5000	1.21	2.1	0.9	172.	11.	-0.3	8/13/72	18.90		5
		1640	2.8	1.2	0.5	9.	17.	-3.3	12/29/71	10.36		2
		1401	3.2	0.3	0.2	40.	19.	-1.5	4/ 9/72	3.87		3
3C352.0	4C+46.34	5000	0.55	2.4	1.5	62.	17.	-0.3	8/15/72	19.10		5
		1640	2.0	2.7	0.5	78.3	5.5	-3.4	12/26/71	10.97		2
		1401	1.8	2.7	0.5	102.7	4.6	-1.0	4/ 1/72	4.53	Q1.5	3
3C356.0	4C+51.36	5000	0.39	8.2	2.6	135.2	8.9	-0.3	8/14/72	19.21		5
		1665	1.49	4.8	0.6	140.5	4.1	-2.8	12/15/71	11.64		2
		1401	1.5	3.8	0.5	152.1	3.4	-1.3	4/ 4/72	4.68		3
3C357.0	NRAO528	5000	0.92	3.5	1.0	34.2	8.3	-0.4	8/ 8/72	19.46		5
		1640	2.2	0.7	0.9	111.	27.	-3.5	12/20/71	11.20	U2.7	2
		1640	2.0	0.6	0.3	136.	15.	-1.4	5/13/72	1.88		4
		1401	2.4	1.8	0.3	61.4	4.6	-1.2	4/ 3/72	4.54		3
3C368.0	1802+11	5000	0.22	5.8	6.1	156.	26.	-0.3	8/12/72	20.34	M20	5
		1640	1.09	0.8	0.6	47.	25.	-4.3	12/16/71	12.21		2
		1401	1.1	2.3	0.5	15.1	6.5	-2.4	4/11/72	4.54		3
		1395	1.1	1.7	0.9	11.	14.	-3.1	9/23/71	17.88		1
3C371.0	4C+69.24	1665	2.3	3.6	0.4	19.1	3.4	-7.1	12/17/71	12.21		2
		1401	2.2	3.4	0.3	21.0	2.7	-1.0	4/ 2/72	5.25		3
3C379.1	4C+74.23	5000	0.61	4.3	1.4	115.1	9.4	-0.2	8/ 9/72	20.87		5
		1665	1.8	2.1	0.6	39.	12.	-3.0	12/18/71	12.51	Q1.4	2
		1401	1.8	2.8	0.3	27.6	3.2	-1.4	4/15/72	4.69		3
		1395	1.7	3.7	0.5	15.8	4.2	-2.1	9/22/71	18.07		1
3C381.0	NRAO568	5000	1.43	4.0	0.6	80.6	4.4	-0.2	8/10/72	20.91		5
		1655	3.3	4.0	0.6	112.9	3.8	-3.2	12/21/71	12.15	Q1.3	2
		1401	3.7	4.3	0.2	137.5	1.2	-2.0	4/16/72	4.72		3
		1395	3.6	4.5	1.0	138.9	2.2	-2.3	9/20/71	18.37	U4M201	
3C382.0	CTA 80	5000	2.0	1.9	0.5	53.8	7.7	-0.2	8/16/72	20.09		5
		1640	5.2	1.2	0.5	163.3	7.2	-4.6	12/22/71	12.44	Q2.5	2
		1401	5.2	1.2	0.1	55.1	3.4	-2.2	3/30/72	5.80		3

TABLE 2-4--Continued

SOURCE	ALTERNATE NAME	FREQ MHZ	FLUX FU	P(6)	+/-	POSITION ANGLE	+/-	IONOS CORR.	OBS. DATE	AVG PST	NOTES	
3C388.0	NRAO577	5000	1.7	1.7	0.5	165.7	8.3	-0.3	8/17/72	20.37		5
		1665	3.9	1.8	0.3	160.2	4.1	-4.4	12/19/71	12.42		2
		1401	5.6	0.2	0.1	82.	18.	-1.7	3/31/72	6.02		3
3C389.0	4C-03.70	5000	2.1	1.2	0.4	76.4	9.7	-0.4	8/19/72	20.30		5
		1640	11.0	2.9	0.2	167.5	2.3	-4.7	12/25/71	12.23		2
		1401	4.2	1.7	0.2	18.9	2.9	-3.4	4/ 9/72	5.56		3
3C390.0	1843+09	1640	5.1	1.3	0.2	79.5	4.7	-4.9	12/24/71	12.27		2
		1401	4.7	0.9	0.2	120.3	4.6	-2.3	4/12/72	5.02		3
3C390.3	NRAO582	5000	3.1	4.9	0.3	16.3	1.8	-0.2	8/18/72	20.66		5
		1640	8.4	7.4	0.2	8.5	1.1	-2.5	12/28/71	12.38		2
		1401	9.9	6.1	0.1	1.8	1.1	-1.2	4/13/72	4.92		3
3C391.0	1846-00	1640	16.4	0.7	0.2	118.6	9.2	-3.9	12/27/71	12.47		2
		1401	12.5	0.2	0.1	97.	11.	-2.5	4/17/72	4.86		3
		1395	13.4	0.2	0.1	47.	11.	-2.8	9/23/71	18.69		1
3C394.0	4C+12.67	5000	0.85	5.4	1.0	123.5	5.7	-0.2	8/11/72	21.37		5
		1665	2.7	3.0	0.6	78.4	3.3	-4.1	12/26/71	12.69		2
		1640	2.3	2.9	0.4	26.5	4.4	-1.6	5/15/72	3.70		4
		1401	2.6	1.5	0.2	45.7	3.8	-2.2	4/ 1/72	6.23		3
3C399.1	4C+30.35	5000	0.85	15.3	1.0	91.2	2.0	-0.3	8/13/72	21.38	W15	5
		1640	2.8	10.9	0.6	9.1	2.0	-3.8	12/20/71	13.24	U2.5	2
		1640	2.4	11.9	0.4	10.5	1.1	-1.5	5/14/72	3.50		4
		1401	2.7	11.1	0.2	55.8	1.1	-2.1	4/ 3/72	5.96		3
3C401.0	4C+60.29	5000	1.7	1.9	0.7	17.	11.	-0.3	8/ 8/72	22.31		5
		1665	4.5	0.4	0.2	142.	15.	-4.3	12/17/71	13.94		2
		1401	4.9	0.2	0.2	19.	26.	-2.7	4/ 2/72	6.92		3
3C409.0	2012+23	5000	3.5	2.1	0.4	93.3	4.1	-0.2	8/12/72	22.15		5
		1665	2.1	0.2	0.1	102.	17.	-3.0	12/19/71	14.32		2
		1401	3.2	0.3	0.1	132.3	6.2	-6.1	3/30/72	7.41		3
		1395	3.4	0.3	0.1	134.3	9.7	-2.0	9/21/71	19.99		1
3C415.2	4C+53.46	5000	0.25	9.5	2.9	134.4	8.2	-0.1	8/ 9/72	22.68		5
		1665	1.07	3.0	1.4	138.	15.	-2.8	12/18/71	14.64	Q2	2
		1640	0.96	4.9	1.0	168.3	5.2	-3.6	12/23/71	14.08		2
		1401	1.2	1.0	0.4	102.	12.	-3.3	4/ 3/72	7.31		3
		1395	1.1	1.6	0.8	140.	15.	-1.4	9/22/71	20.22		1
3C418.0	4C+51.42	5000	3.5	2.4	0.4	94.6	4.8	-0.2	8/10/72	23.03		5
		1640	4.8	2.4	0.3	172.6	2.6	-3.8	12/22/71	14.43		2
		1401	5.1	2.0	0.1	166.8	1.7	-5.3	4/11/72	7.04		3
		1395	4.9	2.2	0.2	161.9	2.4	-2.0	9/20/71	20.54		1
3C427.1	4C+76.13	5000	0.92	5.3	1.0	51.5	5.4	-0.2	8/11/72	22.95		5
		1640	3.7	0.7	0.4	169.	17.	-3.0	12/24/71	14.70		2
		1401	3.6	0.2	0.2	80.	41.	-3.7	4/ 1/72	7.97	U2	3
3C428.0	4C+49.36	5000	0.52	11.9	1.5	166.1	3.7	-0.2	8/17/72	23.29		5
		1665	1.9	3.3	0.5	100.2	4.1	-2.9	12/20/71	14.88		2
		1640	1.9	2.9	0.5	93.1	4.7	-3.1	12/26/71	14.48		2
		1640	1.7	4.4	0.5	87.3	3.7	-2.3	5/14/72	5.22		4
		1401	2.1	4.1	0.4	25.6	2.8	-4.9	3/31/72	8.55		3
3C432.0	2120+16	5000	0.39	3.2	1.9	13.	17.	-0.2	8/14/72	23.58		5
		1640	1.41	2.5	1.3	25.	12.	-2.7	12/27/71	14.54		2
		1640	1.2	1.7	0.7	129.	11.	-2.6	5/15/72	5.60		4
		1401	1.7	2.0	0.4	57.8	5.9	-5.0	4/ 2/72	8.55		3

TABLE 2-4--Continued

SOURCE	ALTERNATE NAME	FREQ MHZ	FLUX FU	P(%)	+/-	POSITION ANGLE	+/-	IONOS CORR.	OBS. DATE	AVG PST	NOTES	
3C435.0	2126+07	5000	0.59	3.9	2.6	154.	19.	-0.2	8/19/72	23.14	Q1.4	5
		1640	1.8	1.7	0.5	123.6	8.9	-2.5	12/28/71	14.72		2
		1640	1.6	1.7	0.4	129.1	6.0	-3.6	5/20/72	5.48		4
		1401	2.1	1.6	0.4	153.2	6.3	-5.7	4/ 4/72	8.34		3
3C436.0	NRAO665	5000	1.10	7.7	0.9	151.9	3.1	-0.3	8/ 8/72	23.72		5
		1665	3.2	6.1	0.3	71.7	1.4	-3.0	12/17/71	15.65		2
		1401	3.4	4.7	0.2	33.4	1.4	-7.7	3/29/72	8.90		3
3C438.0	4C+37.63	5000	1.42	1.1	0.9	91.	25.	-0.2	8/13/72	23.96		5
		1555	6.7	0.4	0.2	73.	13.	-3.0	12/21/71	15.57		2
		1640	5.4	0.4	0.2	82.	11.	-2.4	5/16/72	6.12		4
		1401	6.8	0.2	0.3	176.	32.	-8.5	3/30/72	9.09	QU2	3
3C441.0	4C+29.65	5000	0.73	9.7	1.2	149.1	3.4	-0.2	8/28/72	0.09		5
		1640	2.5	5.6	0.4	120.5	2.7	-3.0	12/23/71	15.73	Q1.4	2
		1401	2.5	4.4	0.2	32.3	1.8	-5.6	4/ 3/72	8.93		3
		1395	2.5	4.3	0.4	25.0	2.5	-1.8	9/21/71	22.01		1
3C446	2223-05	5000	4.3	3.9	0.3	171.9	2.3	-0.2	8/23/72	0.33		5
3C449.0	NRAO692	5000	1.11	7.1	0.8	68.6	3.3	-0.2	8/10/72	0.71		5
		1665	3.3	4.1	0.2	140.0	1.7	-2.8	12/16/71	16.71		2
		1640	3.4	3.7	0.3	131.5	2.0	-2.0	12/26/71	16.15		2
		1640	2.6	4.0	0.4	137.8	2.6	-3.1	5/14/72	6.79		4
		1401	3.1	1.8	0.2	23.0	3.8	-6.8	4/ 1/72	9.79		3
		1395	3.0	2.6	0.3	10.7	5.3	-1.3	9/22/71	22.19	U2	1
3C454.1	4C+71.20	5000	0.28	2.8	3.7	17.	30.	-0.1	8/11/72	0.70		5
		1665	1.41	0.7	0.8	124.	23.	-1.3	12/18/71	16.60		2
		1401	1.5	1.3	0.5	31.	10.	-7.4	4/ 8/72	9.16		3
		1395	1.6	1.2	0.6	171.	14.	-0.8	9/23/71	22.72		1
3C454.2	4C+64.24	5000	0.67	0.6	1.1	121.	39.	-0.2	8/12/72	0.70		5
		1665	2.3	0.8	0.5	110.	16.	-1.6	12/19/71	16.59		2
		1401	2.2	0.7	0.4	138.	25.	-5.3	4/ 2/72	10.22	Q2	3
		1395	2.3	0.3	0.4	67.	35.	-1.2	9/20/71	22.62		1
3C460.0	2318+23	5000	0.31	4.2	3.4	89.	26.	-0.2	8/16/72	1.37		5
		1665	1.49	1.0	0.5	122.	15.	-2.9	12/17/71	17.51		2
		1640	1.38	1.4	0.6	140.	12.	-1.8	12/25/71	16.75		2
		1401	1.5	2.2	0.6	114.	15.	-11.7	3/29/72	10.54	Q2.4	3
3C465.0	2335+26	1665	7.1	1.5	0.1	37.5	2.4	-1.0	12/15/71	17.96		2
		1640	5.1	1.8	0.2	19.1	3.0	-1.0	12/27/71	17.28		2
		1401	5.3	2.1	0.2	116.8	3.2	-11.1	3/30/72	10.79		3
3C468.1	4C+64.25	5000	1.00	1.5	1.1	153.	20.	-0.1	8/ 9/72	2.30		5
		1655	4.5	0.8	0.3	177.	12.	-0.9	12/21/71	17.80		2
		1401	4.6	0.3	0.2	177.	15.	-5.9	4/15/72	9.52		3
3C469.1	4C+79.23	5000	0.37	9.3	2.6	91.3	8.1	-0.2	8/15/72	1.33		5
		1640	1.5	3.8	0.6	99.3	4.1	-1.0	12/23/71	17.50		2
		1640	1.4	5.8	0.9	93.2	5.2	-3.7	5/17/72	7.61		4
		1401	1.7	4.3	0.7	105.4	3.9	-1.2	4/ 3/72	22.11	Q1.4	3
3C470.0	4C+43.59	5000	0.50	15.5	2.1	123.4	3.6	-0.2	8/14/72	1.36		5
		1640	1.7	10.0	0.5	93.6	1.4	-1.6	12/22/71	17.66		2
		1401	1.8	8.3	0.4	76.4	1.8	-8.8	3/31/72	11.40		3

D. Circular Polarization

Table 2-5 presents the circular polarization information obtained for each source. For almost all sources the observed circular polarization was less than three standard errors in magnitude. In these cases, the quoted figure is an upper limit and is three times the standard error. For the few cases which are quoted as a detection, the result is listed as $v \pm \sigma_v$. The figure in parentheses is the degree of linear polarization. There are 542 separate observations listed here. On the basis of probability alone, one or two could be expected to exceed three standard errors. There are seven such cases, but none of these are confirmed at other frequencies and 3C125.0, and especially 3C341.0, have large linear polarizations which may lead to errors in the circular polarization determination as discussed in the preceding section. Of the five remaining, 3C043.0, 3C280.1, 3C357.0, 3C388.0 and 3C449.0, a few may be genuine detections. The most likely candidate is 3C043.0 since the upper limits for the other frequencies do not contradict the possible detection.

The question marks shown in various entries indicate that the observed scatter of the various determinations of v for the source in question was considerably larger than might be expected on the basis of the calculated uncertainties. Such scatter might logically be caused by some medium-scale structure producing some resolution effects or by some confusing source; the circular polarization is considerably more sensitive to this than is the linear polarization. Likely prospects for this

TABLE 2-5

UPPER LIMITS FOR CIRCULAR POLARIZATION (%)

Source	21 cm	18 cm	6 cm	Source	21 cm	18 cm	6 cm
3C002.0	0.6	0.5		3C075.0	0.4	0.4	2.8
3C006.1	0.6	0.5	3.2	3C083.1	0.5	0.3/?	?
3C011.1	0.6	?		3C089.0	0.6	0.5	
3C013.0	0.9	1.0	4.4	3C091.0	0.5	0.5	1.5
3C014.0	0.9	0.9		3C093.0	0.6	0.6	
3C014.1	0.7	1.0	4.7	3C093.1	0.9	0.9	2.3
3C016.0	?	1.0		3C099.0	1.0	1.1	
3C017.0	0.4	0.5		3C103.0	0.3	0.4	1.8
3C019.0	0.6	0.7	2.3	3C107.0	1.1	1.3	5.9
3C021.1	2.3	0.5		3C114.0	1.8	1.8	7.0
3C022.0	0.8	1.2	3.6	3C119.0	0.3	0.3	
3C028.0	1.2	1.2	19.	3C124.0	1.5	0.6	15.
3C031.0	0.5	0.4	1.7	3C125.0	.95±.27(5.9)	1.4	3.2
3C033.1	0.8	0.6	4.5	3C130.0	0.6	1.3	2.7
3C033.2	1.2	1.5	2.4	3C131.0	0.6		2.7
3C034.0	1.4	1.4	7.1	3C132.0	0.5	0.5	
3C035.0	1.1	0.8	8.5	3C137.0	0.8	0.9	3.5
3C036.0	1.4	2.5	6.9	3C139.2	?	?	6.3
3C041.0	0.8	0.5	2.1	3C141.0	0.7	0.8	3.2
3C042.0	0.8	0.6	2.7	3C147.0	0.3	0.3	0.4
3C043.0	-.81±.20(1.5)	1.1	2.4	3C152.0	0.7	1.1	5.2
3C044.0		1.5	7.5	3C154.0	0.4	0.3	
3C046.0	1.4	1.6	10.	3C158.0	0.7	0.9	4.6
3C049.0		0.6		3C165.0	0.9	0.6	3.8
3C052.0	0.3	0.4	1.6	3C166.0	0.6	0.6	
3C054.0	1.0	1.0	4.7	3C169.1	1.2	1.5	11.
3C055.0	2.3	0.7	4.7	3C173.0	1.1	1.0	5.6
3C058.0	0.5	?		3C173.1	0.6	0.7	4.4
3C065.0	0.5	0.6	2.7	3C175.1	0.9	0.8	
3C066.0	0.7	0.3	?	3C177.0	1.3	1.5	16.
3C067.0	0.7	0.6	1.8	3C180.0	0.6	0.6	
3C068.1	0.8	0.7	2.7	3C181.0	0.7	0.8	4.5
3C068.2	2.0	5.6		3C184.0	0.5	0.6	5.1
3C069.0	0.5	0.6	3.2	3C184.1	0.6	0.9	3.5
3C071.0	0.3	0.4		3C186.0	1.2	1.6	11.

TABLE 2-5--Continued

Source	21 cm	18 cm	6 cm	Source	21 cm	18 cm	6 cm
3C187.0	1.4	1.0	6.4	3C250.0	1.5	1.5	13.
3C190.0	0.6	0.7		3C252.0	1.1	1.3	10.
3C191.0	0.8	1.5		3C255.0	0.9	1.0	30.
3C194.0	0.7	1.3	4.0	3C256.0	1.1	1.2	6.5
3C196.0	0.3	0.3		3C257.0	1.0	1.6	6.2
3C196.1	0.8	1.4		3C258.0	1.6	2.5	
3C197.1	1.2	0.9	5.3	3C263.0	0.5	0.7	6.2
3C198.0	0.8	1.2	9.5	3C263.1	0.6	0.7	
3C200.0	0.7	0.9	3.6	3C264.0	0.3	0.4	
3C204.0	1.4	1.6	7.9	3C265.0	0.5	0.6	4.6
3C205.0	0.7	0.7	5.5	3C266.0	1.1	1.3	7.1
3C208.0	0.9	0.8	2.6	3C268.1	0.3	0.4	
3C208.1	1.0	0.7		3C268.2	1.2	1.3	5.8
3C210.0	0.9	?	6.2	3C268.3	0.4	0.4	2.5
3C212.0	0.8	0.7		3C268.4	0.8	1.0	4.8
3C213.1	0.7	1.0	3.8	3C270.1	0.6	0.6	3.2
3C215.0	0.9	1.0	7.4	3C272.0	1.1	1.2	6.1
3C216.0	0.4	0.7		3C274.0	0.3	0.3	
3C217.0	0.7	0.8	4.9	3C275.0	?	0.5	
3C220.1	0.7	0.7	9.7	3C277.0	1.5	1.7	10.
3C220.2	0.8	1.5	6.1	3C277.1	0.6	0.8	4.7
3C220.3	0.6	1.1	9.2	3C277.2	0.8	1.1	5.5
3C222.0	1.6	1.9		3C277.3	0.5	0.6	2.2
3C223.0	0.5	0.8	3.0	3C280.0	0.3	0.4	
3C223.1	0.8	1.3	3.5	3C280.1	1.1 - 1.47±.45(2.8)		5.4
3C225.0	0.4	0.4	3.1	3C284.0	?	1.0	4.9
3C226.0	1.0	0.8		3C285.0	?	0.8	4.8
3C231.0	0.3	0.3		3C288.0	0.4	0.6	3.1
3C234.0	?	?	2.4	3C288.1	1.0	1.5	9.0
3C236.0	0.5	0.6	2.0	3C289.0	0.8	0.7	2.9
3C239.0	1.0	1.2	8.1	3C293.0	0.3	0.4	1.6
3C241.0	1.2	1.2		3C293.1	2.0	3.9	16.
3C244.1	0.3	0.5	3.2	3C294.0	0.9	0.9	6.2
3C247.0	0.7	0.8	4.0	3C295.0	0.3	0.3	0.5
3C249.1	0.3	0.8	3.6	3C298.0	0.3	0.5	

TABLE 2-5--Continued

Source	21 cm	18 cm	6 cm	Source	21 cm	18 cm	6 cm
3C299.0	0.5	0.8	2.8	3C371.0	0.7	0.9	
3C300.0	0.6	0.5		3C379.1	0.7	1.3	3.0
3C300.1	0.5	0.8		3C381.0	0.4	1.0	1.3
3C303.0	0.5	0.9	2.0	3C382.0	0.3	0.5	1.0
3C303.1	0.6	1.8		3C388.0	0.3	-.59±.19(1.8)	1.1
3C305.0	0.6	0.6	2.2	3C389.0	?	0.5	0.9
3C305.1	0.6	2.5	7.1	3C390.0	0.4	0.5	
3C306.1	0.8	0.8		3C390.3	?	0.3	?
3C309.1	0.3	0.3		3C391.0	0.3	0.4	
3C314.1	1.2	1.4	7.1	3C394.0	0.4	0.9	2.3
3C317.0	0.3	0.3		3C399.1	0.4	0.9	2.3
3C318.0	0.5	0.8		3C401.0	0.4	0.5	1.6
3C319.0	0.5	0.8	2.6	3C409.0	0.3	0.3	0.6
3C320.0	0.8	1.5	5.3	3C415.2	1.7	2.0	6.0
3C322.0	0.8	1.5	5.3	3C418.0	0.3	.61±.17(2.4)	0.8
3C323.0	1.1	2.0	7.2	3C427.1	0.4	0.8	2.1
3C324.0	0.6	1.0		3C428.0	0.8	1.0	3.2
3C325.0	0.4	0.6	3.5	3C432.0	0.9	1.4	4.0
3C327.1	0.4	0.6		3C435.0	0.7	0.8	4.3
3C332.0	0.6	1.0	2.1	3C436.0	0.4	0.6	1.8
3C334.0	0.7	1.4		3C438.0	0.3	0.4	2.1
3C337.0	0.5	0.7	3.0	3C441.0	0.5	0.8	2.5
3C338.0	0.4	0.8	4.9	3C446			0.7
3C340.0	0.7	0.7		3C449.0	0.5	0.5-1.82±.56(7.1)	
3C341.0	1.1	1.76±.36(18.4)	3.2	3C454.1	1.1	1.5	7.7
3C343.0	0.3	0.4		3C454.2	0.7	1.0	2.5
3C343.1	0.38±.10(0.7)	0.4	2.4	3C460.0	0.4	1.1	5.1
3C346.0	0.4	0.5		3C465.0	0.4	0.4	
3C348.0	0.8	0.3		3C468.1	0.4	0.6	2.3
3C349.0	0.4	0.6	2.3	3C469.1	1.1	1.2	5.5
3C351.0	0.5	1.2	1.8	3C470.0	0.8	1.1	4.3
3C352.0	0.8	1.1	3.1				
3C356.0	1.0	1.3	5.5				
3C357.0	0.6	1.0	2.2				
3C368.0	1.1	1.4	13.				

effect are 3C139.2 and 3C234.0 with such entries for both 18 and 21 cm. Another possible cause of the excessive scatter would be the linear to circular cross-talk due to phase uncertainties. Several sources with high linear polarizations (e.g., 3C284.0, 3C285.0, and 3C341.0) show question marks.

A striking feature of this list is that there are no truly convincing detections, certainly none with circular polarizations of a few percent. Any circular polarizations are much less than the average degree of linear polarization in radio sources.

CHAPTER III

DERIVED POLARIZATION PARAMETERS

A. Rotation Measure Calculations and Error Analyses

Faraday rotation of the radiation from a particular source can be determined by fitting all the available data to the equation

$$\psi = \psi_o + RM \cdot \lambda^2 \qquad (3\text{-}1)$$

in a least-squares sense. This method presupposes that all the quoted uncertainties are standard errors, that all sources of error have been included, and that the ionospheric Faraday rotation has been removed from the data. Unfortunately the authors of the various polarization observations are far from uniform in their analyses, primarily because several different observational techniques have been used and these techniques have been changing over the years since the first measurements were made. Therefore, before any attempt at calculating the rotation measure and intrinsic position angle can be made, the data must be made more homogeneous.

Several papers--e.g., Gardner, Morris and Whiteoak (1969a)--list probable errors for their results. In such cases the quoted error was increased by a factor of 1.48 to obtain the standard error, assuming a gaussian distribution. For large angular errors, this assumption is no longer valid, but observations with such large uncertainties are essen-

tially useless in determining rotation measures, as will be explained.

Other papers neglect to specify the derivation of the tabulated errors. In such cases the uncertainties were treated as standard errors. This could lead to slightly worse fits than could be obtained by treating these as probable errors, but, as Table 3-2 illustrates, most fits were quite good. Other problems, however, were not so easily resolved.

Quite often not all sources of error were considered when deriving the uncertainties published along with the data. Gardner and Davies (1966b) list two sets of errors for their observations of the degree of polarization. The first includes all instrumental effects and the r.m.s. noise of the observation; the second adds the uncertainties introduced by correction for the polarization of the galactic background. Since their observations are single-dish, these corrections and the subsequent uncertainties can be very large. Consequently the second error is generally slightly larger and often much larger than the first. Their 21.5 cm polarization for PKS 1151-34 becomes 2.4% ± 2.0% instead of 2.4 ± 0.5, and clearly the larger error is the more realistic. The angular error, however, is not similarly treated, and is quoted as 139° ± 5°. In light of the large degree error, this small uncertainty is highly suspect. One would expect a value on the order of $\Delta\psi \approx \tan(\Delta p/p)$, or about 35°, instead, making the observation useless for a reliable determination of the Faraday rotation. Therefore, rather than accepting the quoted errors at face value, a comparison of the degree and position angle errors was made. If necessary, the angular uncertainty was increased, or the entire

observation was discarded from the calculation.

Ionospheric Faraday rotations are not made in many of the earlier works--e.g., Berge and Seielstad (1967). For such data, an additional ionospheric uncertainty was determined by taking

$$\Delta\psi_I = 5\ (\lambda^2/462)\ \ [^\circ] \qquad (3\text{-}2)$$

where λ is in cm. The 5° value for 21 cm observations was determined by examining the distribution of the ionospheric corrections for the 21 cm observations of the present work. When reflected about the origin to provide for corrections of the opposite sign the distribution formed something close to a Gaussian with a standard deviation of about 5°. The additional uncertainties for all observations were then assumed to follow a similar distribution. If all data published in the future were to be supplied with ionospheric corrections, or at least with date and time of observation, this rather unsatisfying procedure could be dispensed with. For this work, no polarizations without corrections at wavelengths longer than 21 cm were used, and this additional error was not applied shortwards of 10 cm. For the remaining observations, the uncertainty was then added in quadrature to the previously determined standard error.

The beamwidths used by the various observers differ greatly depending on the instrument and frequency used. Partial resolution of the source can make the apparent polarization quite different from that of the integrated radiation. Beyond discarding those observations for which the authors claimed partial resolution or combining observations of sep-

arate components to simulate the larger beam of the low-frequency observations, no detailed beamwidth correction program was carried out. Most of the sources are fairly small so that the effects are probably minimal. The variation of beamwidth could explain some of the high-frequency scatter observed.

As described in Chapter I, there is no reason to expect the polarization position angles of a source to follow a λ^2 law once the source has been depolarized. With this in mind, an attempt was made to discard all polarization observations with frequencies below that at which the degree of polarization was reduced to one-third of the maximum degree attained at high frequency. Whenever this resulted in an unacceptably ambiguous determination of the rotation measure, the observations were not deleted and a note was included in Table 3-2 to that effect. Sources which do use depolarized data should be viewed with some skepticism as the quoted value of the rotation measure could be based on the incorrect multiple of 180°. Some sources show a marked depolarization towards both the high and low frequency ends of the data, and some show complex behavior with several plateaus. These have been treated individually and are described in the notes to Table 3-2.

Once the data were edited and the quoted errors corrected, equation 3-1 was fitted to the remaining points. In order to examine all the possible rotation measures, the position angles for all but the highest frequency observation were taken as $\psi_i = \psi_{obs_i} + n_i\pi$ where n_i was any integer and i ran between 2 and N, the number of observations; n_1 is fixed at zero. At first, all combinations leading to $|RM| \leq 300$ rad/m^2

were examined. In practical terms, this required letting n_i range between -4 or -5 and +4 or +5 at 21 cm. The basis for selecting the best set of the n_i was the χ^2 of the fit, defined as

$$\chi^2 = \sum_{i=1}^{N} \frac{|\psi_i - \psi(\nu_i)|^2}{\sigma_i^2} = \sum_{i=1}^{N} \frac{|(\psi_{obs_i} + n_i\pi) - \psi(\nu_i)|^2}{\sigma_i^2} \qquad (3\text{-}3)$$

where σ_i is the standard error of the i^{th} observation, and $\psi(\nu_i)$ is the value of the fitted line at the frequency of the i^{th} observation. This is just the weighted sum of the squares of the residuals. For a perfect fit $\chi^2 = 0$, and it increases with increasing poorness of fit.

Table 3-1 illustrates the relationship between χ^2 and the quality of the fit. If a set of N observations be made a large number of times upon a relationship which can be expressed by a certain function, in this case $\psi(\nu)$, then $P(\chi_o^2)$ is the fraction of those sets of observations which can be expected to have a χ^2 at least as high as χ_o^2. Table 3-1 gives $\chi^2(P)$ for various values of n, the number of degrees of freedom of the data. In our case, where the frequency is considered to be completely determined, n = N - 2, since we are employing a two parameter fit. As an example, if a sample of 5 measurements is fitted to equation 3-1 and results in a χ^2 of 1.21, then n = N - 2 = 3 and $\chi^2(.75) = 1.21$ from Table 3-1. This means that there is a 75% probability of obtaining a χ^2 of 1.21 or higher for our 5 measurements if the fitted curve were actually representative of the parent distribution. This relationship between χ^2 and P is based on a gaussian distribution. For the data actually used in calculating the rotation measures, this is a good

TABLE 3-2

RELATIONSHIP BETWEEN χ^2 AND GOODNESS OF FIT

$\chi^2(P)$

	P							
n	.99	.90	.75	.50	.25	.10	.05	.01
1	.0002	.016	.102	.455	1.32	2.71	3.84	6.63
2	.020	.211	.575	1.39	2.77	4.61	5.99	9.21
3	.115	.584	1.21	2.37	4.11	6.25	7.81	11.3
4	.297	1.06	1.92	3.36	5.39	7.78	9.49	13.3
5	.554	1.61	2.67	4.35	6.63	9.24	11.1	15.1
6	.872	2.20	3.45	5.35	7.84	10.6	12.6	16.8
7	1.24	2.83	4.25	6.35	9.04	12.0	14.1	18.5
8	1.65	3.49	5.07	7.34	10.2	13.4	15.5	20.1
9	2.09	4.17	5.90	8.34	11.4	14.7	16.9	21.7
10	2.56	4.87	6.74	9.34	12.5	16.0	18.3	23.2
11	3.05	5.58	7.58	10.3	13.7	17.3	19.7	24.7
12	3.57	6.30	8.44	11.3	14.8	18.5	21.0	26.2
13	4.11	7.04	9.30	12.3	16.0	19.8	22.4	27.7
14	4.66	7.79	10.2	13.3	17.1	21.1	23.7	29.1
15	5.23	8.55	11.0	14.3	18.2	22.3	25.0	30.6

assumption since departure from a gaussian takes place at large angular errors, and position angles with errors over 20° are useless. See pages 41 to 45 for a discussion of the actual distribution of the position angle measurements.

Once the χ^2's for the various combinations of the n_i were calculated the best set of n_i and hence the best rotation measure and intrinsic position angle could be established by choosing the set yielding the lowest χ^2. If one particular set of the n_i for N = 3 were to result in a χ^2 of 12.3, that set would be unlikely to be the correct one. If, however, one set yielded χ^2 = 1.32 while another gave χ^2 = 0.455, there

would be almost no basis for selecting one over the other; the observations would be ambiguous--more than one set of the n_i would give a satisfactory fit. In order to define quite clearly the relative certainty of the rotation measure for a particular source, the following quality codes were established:

Code 6.--The fit of the data to a straight line was such that $P(\chi^2)$ was greater than 1%, unless higher values of χ^2 could be accounted for by excessive scatter of the data rather than by systematic effects. At least four well-separated frequencies were available such that the removal of any one frequency would not lead to an ambiguity. There were no ambiguities for $|RM| \leq 300$.

Code 5.--Same as for code six, except that only three well-separated frequencies can be used.

Code 4.--There are no ambiguities for $|RM| < 500$ rad/m^2, but the χ^2 of the fit is so high that $P(\chi^2)$ is less than 1%. This may indicate that an individual point is in error, that the polarization is variable, that the ψ/λ^2 plot is actually curved, that the quoted errors for an observation are too optimistic, or that the rotation measure is actually higher than 500 rad/m^2.

Code 3.--There are at least three well-separated frequencies and the fit of the data to the chosen rotation measure is good. However, there is at least one other set of the n_i leading to a $|RM| < 300$ rad/m^2 with a χ^2 such that $P(\chi^2)$ is greater than 1%. This other possibility has been eliminated by the fact that $P(\chi^2)$ for the chosen set of the n_i is much greater than that for the rejected one, and because the selected

rotation measure is much lower in absolute value than the rejected one.

Code 2.--The same as for code three, but both possibilities are of comparable magnitude. Rejection is on the basis of goodness of fit only.

Code 1.--The same as for code three, except that both possibilities fit equally well. Rejection is on the basis that one has a much higher rotation measure than the other.

Code 0.--Reserved for special problems which are explained in the notes to Table 3-2.

Some of the terms used here require a more complete definition. "Well-separated" frequencies depend on the uncertainties of the observed position angles. If the change in position angle for, say, a rotation measure of 100 rad/m^2 between two frequencies is several times greater than the standard error, then the frequencies can be considered well-separated. That is, the two separate observations together help to eliminate some ambiguities with $|RM| < 300$ rad/m^2 which each taken separately cannot do. Measurements at 1640 MHz and 1680 MHz with standard errors of 15° are not significantly better than one measurement at 1660 MHz; the two frequencies are not "well-separated". Measurements at 1400 MHz and 1640 MHz with errors of 5° are. In practice, 6 cm, 10 cm, 18 cm, 21 cm and 30 cm are usually well-separated regions, while frequencies within these bands are not.

The low frequency observations at about 600 and 400 MHz are not usually helpful. Occasionally, when the error is particularly low and the circumstances are just right, one of these observations will relieve

an ambiguity; but they usually do not. For a rotation measure of 200 rad/m^2 the polarization vector has already gone through 35 turns of 180° by the time 400 MHz is reached. Often the data at 400 MHz can then be changed by one multiple of 180° in either direction without affecting the fit very severely. It is not then surprising that a n_i can be chosen to match low frequency data to almost any rotation measure. Therefore, except in unusual circumstances, data at these frequencies cannot be considered in determining whether a rotation measure determination is of code 6 or code 5 quality.

As described in the explanation of code six, a "good" fit is one for which $P(\chi^2)$ is greater than 1%. This is a somewhat arbitrary dividing line based primarily on the observations that most fits were considerably better than the 1% criterion, or considerably worse; i.e., either $P(\chi^2) > 5\%$ or $P(\chi^2) < 0.1\%$. Since there were only 354 rotation measures determined, it seemed most unlikely that such a low $P(\chi^2)$ would be indicated by a legitimate set of the n_i. Doubtlessly some of those fits with $P(\chi^2) = 1\%$ are in error, too, but there are not many with such a poor fit.

In cases where there were many points at or near the same frequency one of three conditions would apply. The points would have the same value within quoted uncertainties, leading to a good fit. One point would be notably discrepant compared with the others; it would be discarded, leading to a good fit. Finally, the points could indicate scatter in considerable excess of their errors, indicating either a variable source or over-optimistic error analysis. In such a case the $P(\chi^2)$ would be expected to be quite low. If the scatter were sufficient to explain

the value of P, the fit could still be considered "good", but a note was added to that effect.

The other criterion for rejecting a particular rotation measure was its magnitude. The distribution of the code six rotation measures provides the guideline for the rejection of possibilities on this basis. Figure 3-1 is a histogram of the distribution of the absolute values of the code six rotation measures. The most striking aspect is that 70% of the sources have an absolute value of the rotation measure less than 30 rad/m^2, 86% are below 50 rad/m^2, and only 3 (1.5%) have rotation measures greater than 300 rad/m^2. One would expect that if two possible values for the rotation measure of a given source were 5.7 and -217 rad/m^2, then the former would much more likely be the correct value; and one would be justified in eliminating the latter. If, however, the values were 5 and 25 rad/m^2, there would be little basis for making such a choice. The set of rotation measures presented in Table 3-2 does not include any for which there is no substantial reason for selecting a particular value. Certainly the practice common in some of the earlier papers of selecting a rotation measure on even a small difference in absolute value has been avoided, as has that of presenting rotation measures derived from only two polarization measurements.

The distribution of the code six rotation measurements was also used as a basis for selecting the 300 rad/m^2 limit on the initial search for fits and ambiguities. Some limit must be used merely to limit computation time. In addition, no matter how excellent the data, no matter how many points, it is always possible to find ambiguity if no limit is

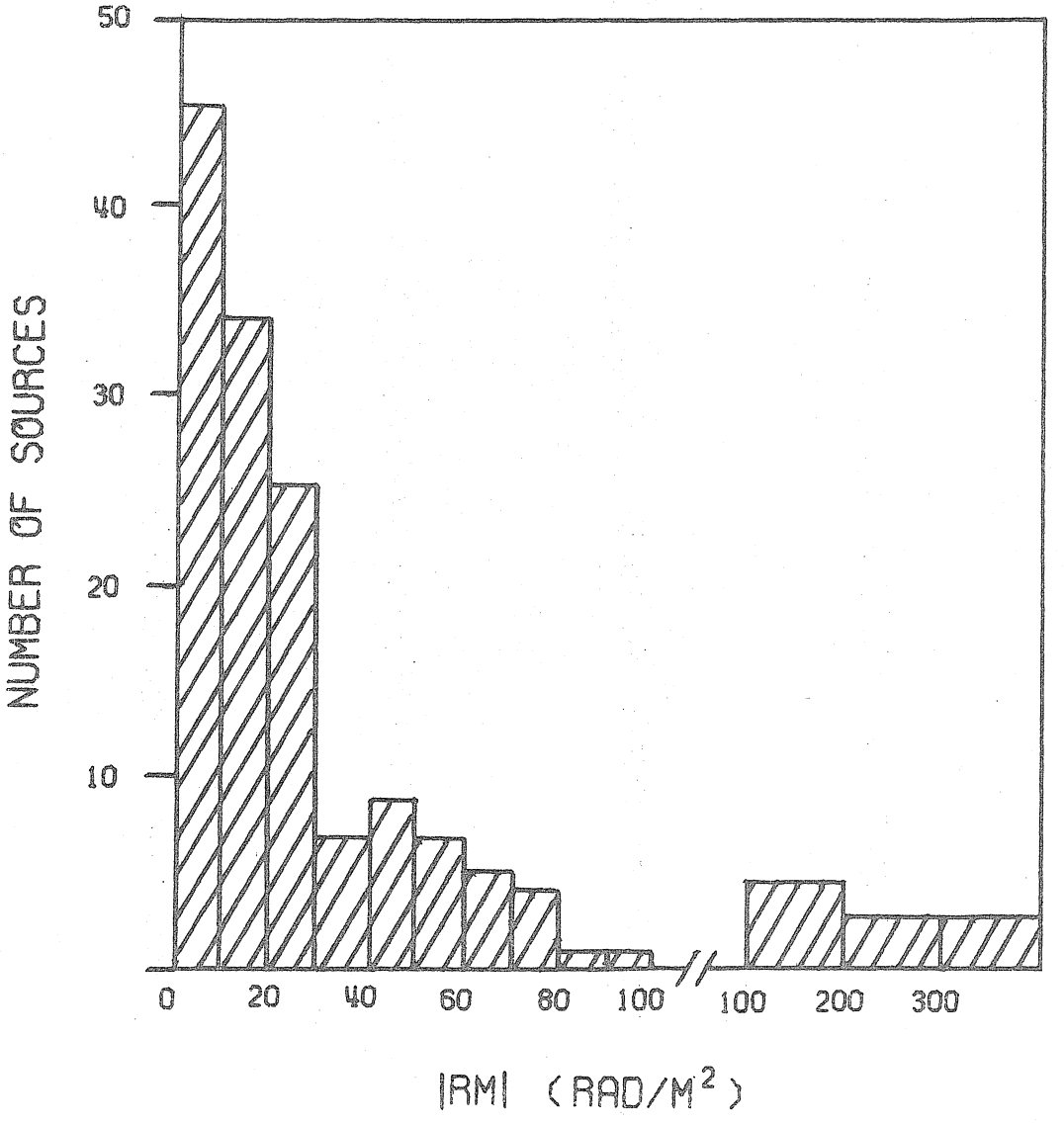

Fig 3-1.--Distribution of the code 6 rotation measures.

placed on the rotation measure. For the three frequencies observed in the present work, errors of the order of 10° lead to ambiguities at about ±250 rad/m^2. The next ambiguity occurs at well over 700 rad/m^2, and is unlikely at best. The limit of 300 rad/m^2 allows the first to be examined. Of course, if no suitable rotation measure is found under 300, the search is extended until one is found or until it becomes apparent that factors other than the magnitude are responsible for the failure. Of the 354 rotation measures of Table 3-2, only 9 are greater than 300 rad/m^2, and only two of these are greater than 400 rad/m^2. In addition, there are 5 sources for which enough data exists to allow one to expect a well-determined rotation measure, but for which none has been found. These are explained by structure effects and by curvature of the ψ/λ^2 curve and will be examined in detail later.

The distribution of the code six rotation measures is not without its selection effects. First, as seen in figure 4-3, the distribution of the code six sources in galactic coordinates is not quite the same as for the entire collection of sources. There are not as many code six sources near the galactic equator where the Faraday rotation is higher, thus one might expect a code 1 source to be more reliable if it is some distance from the plane rather than in it. In fact, all the code 1, 2 and 3 sources--the ones with ambiguities--are probably more reliable at higher galactic latitudes. This will be kept in mind in examining the various distributions in Chapter IV.

Another selection effect that may have importance is that there is a basic difference between most of the code six sources and the remaining

ones. The code six sources require at least four independent measurements, implying considerable work. In general, only those sources which are particularly strong or attracting interest by being somewhat peculiar are apt to have sufficient data to be classified with the highest reliability. There could, conceivably, be a correlation between the internal rotation measure and its flux or type. Anyone attempting careful examinations of the polarization characteristics of classes of sources should consider this as a possible effect.

More should be said about the curvature of the ψ/λ^2 plot. As described in Chapter I, internal Faraday depolarization can lead to a departure from the λ^2 law. An indication of curvature could be evidence of the internal depolarization and could provide clues to the structure of the source as discussed in detail by Burn (1966). Unfortunately determination of curvature involves at least three parameters, and the typical polarization data consist of only three points. Even apparent curvature can be caused by scatter or variability. For only a few of the sources has curvature been reliably detected, and this is indicated in Table 3-2. Later a few of the more interesting sources will be examined in detail.

B. Rotation Measure Tables

Table 3-2 lists all the sources for which an at least partially unambiguous rotation measure is known, and is based upon all available polarization data, including those presented in this work for the first time. In addition to the polarization characteristics, other parameters of interest are included for convenience and are used in various correlations

presented in Chapter IV.

The first column contains the source and an alternate name. Source names of the form '0003-00' are Parkes sources and are always in the alternate name position. Sources belonging to the 3CR list are identified by a decimal point following the three digit number; the 3C sources not on the 3CR list have no decimals (e.g., 3C032). Sources of the form M00-210 are MSH sources and B0511-30 indicates a source of the second Bologna list. The rest are self-explanatory.

The galactic coordinates l^{II} and b^{II} comprise the second column. The identification and redshifts, where known, constitute the next two columns. The first part of the identification is the visual magnitude, and the second is the optical identification. The symbols are primarily those used by Wyndham (1966) derived from the type notation of Matthews, Morgan and Schmidt (1964). Some of the symbols are defined below:

I Highly obscured region with no galaxies visible. Identification with an extra-galactic object is very unlikely.

II Obscured region with some galaxies visible. The field is usually crowded.

III No obscuration visible. There are objects within 30" of the radio source position.

IV Blank field. No obscuration and no objects within 30" of the radio position.

N N type galaxy.

E E type galaxy.

G A galaxy which is too faint to have been more completely differentiated.

C Used as a suffix and indicates that the galaxy is a member of a cluster. When used as a prefix it indicates a super-giant D galaxy in a cluster.

TABLE 3-2

THE ROTATION MEASURES

SOURCE	ALTERNATE NAME	GALACTIC COORDINATES	IDENT	ID REF	Z	Z REF	R.M.	+/-	I.P.A.	+/-	NO. POLS	FIT D	C	POLARIZATION REFERENCES	NOTES
3C002.0	0003-00	99.8 -60.2	19.4QSO	13	1.037	13	-78.2	1.1	125.9	2.0	4	2.4	5	1, 7,11,12	
3C009.0	0017+15	112.1 -46.5	18.2QSO	13	2.012	13	-23.2	1.0	34.8	1.8	6	1.9	6	3, 6, 7	
M00-29	0021-29	9.8 -83.6	20. QSO	7			+7.0	4.5	106.5	2.2	3	0.8	5	6, 7	
M00-210	0023-26	42.5 -84.2	III	14			+25.7	9.5	46.1	18.5	3	0.1	3	6, 7	
3C015.0	0034-01	114.8 -63.8	16. E1	6	0.0733	6	-14.4	0.9	50.6	1.7	5	7.6	6	6, 7,11	1660-6-1.8SD
3C016.0	0035+13	117.8 -49.4	III	21			+317.1	2.1	50.9	3.7	3	4.7	5	1, 7	
3C017.0	0035-02	115.2 -64.8	19. E	21	0.2201	18	-2.3	6.6	176.0	8.9	6	4.2	6	1, 3, 6, 7	
3C018.0	0038+09	118.6 -52.7	18.5G	14			+15.5	4.6	71.4	2.3	5	4.0	6	6, 7,12	1690-6-1.8SD
M00-410	0039-44	308.6 -72.8	III	14			-19.1	2.7	78.4	2.1	4	0.4	6	6, 7	
3C020.0	4C+51.02	121.6 -10.8	II	21			+165.6	4.8	52.0	5.6	5	2.1	2	2, 3,12,13	
M00-315	0042-35	312.3 -81.5	III	14			+4.5	6.3	77.3	1.7	3	0.6	5	6, 7	
M00-411	0043-42	306.6 -75.0	18. E	2			+2.6	0.2	135.9	0.9	7	2.9	6	5, 6, 7	
M00-222	0045-25	97.8 -88.0	7.0SC	2	0.00086	22	+90.9	5.1	117.2	3.6	4	1.0	5	7,13	
3C022.0	4C+50.04	122.9 -11.7	II	21			-82.0	4.0	26.0	9.6	3	0.0	2	1	
	0049-43	302.4 -74.0	III	14			-8.4	1.9	172.6	1.6	5	0.3	6	6, 7	
3C027.0	4C+68.02	123.3 + 5.6	I	21			-91.1	1.0	0.5	2.6	7	2.3	6	3,13,14,15	
3C029.0	0055-01	126.5 -64.2	14.1EO	17	0.0450	17	+2.4	0.5	157.6	0.9	8	6.3	6	5, 6, 7,14	
4C-00.06	0056-00	127.1 -62.4	17.3QSO	13	0.717	13	-6.5	1.3	87.5	0.5	6	2.4	6	4, 6, 7,15	
3C031.0	4C+32.05	126.9 -30.3	12.0DE3C	21			-62.0	2.9	32.1	6.5	4	0.1	3	1, 3	NOTE
3C032	0105-16	143.3 -78.3	III	14			+3.2	9.6	22.8	2.5	4	7.8	5	6, 7,12	
3C033.1	4C+72.01	124.3 +10.4	II	21			-17.3	1.6	137.8	3.7	4	1.1	3	1,11	
4C+01.02	0106+01	131.9 -61.0	18.4QSO	13	2.107	13	-20.6	0.5	127.9	2.6	5	2.2	6	4, 6, 7	
3C033.0	0106+13	129.5 -49.3	15.6D	11	0.0600	18	-12.3	0.3	93.8	0.7	13	13.4	6	3, 4, 5, 6, 7,13,14	
3C034.0	4C+31.02	127.6 -30.9	III	21			-69.3	7.5	4.0	8.7	3	0.0	1	1	
3C035.0	NRAO61	126.4 -13.3	14.5D3	21	0.0677	9	-125.9	8.8	33.6	18.0	3	4.2	5	1	
3C038	0117-15	154.1 -76.4	III	14			-2.2	0.7	110.5	2.0	5	1.3	5	3, 7,11	
3C041.0	4C+32.06	131.4 -29.1	III	21			-66.8	0.9	37.8	2.1	4	11.0	4	1,15	5000-7-3SD
M01-111	0125-14	157.5 -74.4	20. QSO?	4			+19.3	7.9	14.9	4.2	3	3.1	2	6, 7	
3C042.0	4C+28.04	132.6 -33.1	III	21			-50.8	5.9	20.3	12.8	3	0.0	3	1	
	0131-367	261.6 -77.0	14.2SO	12	0.0267	12	+5.7	0.2	105.1	0.9	6	8.6	6	5, 6, 7	
3C046.0	4C+37.05	132.4 -24.2	19.5G	21			-88.1	3.8	159.3	8.2	3	1.9	5	1	
3C047.0	0133+20	136.8 -40.7	18.1QSO	13	0.425	13	-22.9	2.2	39.7	2.4	7	11.2	6	2, 3, 6, 7,12,15	
3C052.0	4C+53.02	131.5 - 8.4	18.5GC	21			-68.1	4.1	177.4	8.6	3	2.1	1	1	
M01-217	0148-29	226.8 -76.8	III	14			-0.7	2.5	102.3	3.5	4	1.3	6	6, 7	
3C054.0	4C+43.06	135.0 -17.6	III	21			+157.9	5.9	172.5	13.3	4	4.0	5	1, 3	
3C055.0	CTA 16	139.9 -31.8	III	21			-96.2	4.7	175.3	9.1	4	1.9	5	1, 3	

TABLE 3-2--Continued

SOURCE	ALTERNATE NAME	GALACTIC COORDINATES	IDENT	ID REF	Z	Z REF	R.M.	+/-	I.P.A.	+/-	NO. POLS	FIT	C D	POLARIZATION REFERENCES	NOTES
M01-135	0157-31	231.1 -74.5	19. QSO	2			+10.9	2.7	75.1	1.3	4	2.7	6	6, 7	2650-6-1.5SD
3C057	0159-11	173.1 -67.3	16.4QSO	13	0.680	13	+9.0	0.3	20.3	3.3	7	9.0	6	4, 6, 7,11	
M02-401	0201-44	266.5 -67.9	III	14			-66.2	4.7	141.3	1.5	3	3.5	3	6, 7	DEPOLARIZED
3C058.0	CTB 8	130.7 + 3.1	I	21			-94.4	1.0	4.9	1.0	6	6.4	5	1, 8, 9,10,14	
3C062	0213-132	181.4 -65.8	18.5F0	4			+18.7	0.9	78.9	1.1	9	9.2	6	3, 6, 7,13	LOW CURVE
3C063.0	0218-02	167.1 -56.9	19.5F	4			+3.3	2.1	38.6	2.0	7	9.9	6	2, 3, 6, 7	SCATTER
3C064	0219+08	157.7 -48.2	19.5G	3			-10.9	2.1	32.1	1.5	4	2.8	6	6, 7	
3C066.0	NRAO102	140.3 -16.8	12.3ED2C	21			-291.0	4.9	133.1	9.5	4	4.4	2	1	
3C065.0	4C+39.07	141.5 -19.5	III	21			+142.6	2.3	115.6	2.6	3	1.2	3	1	
3C068.1	4C+34.08	145.6 -24.0	19.5G?	21			-63.3	2.7	80.5	5.9	3	8.7	4	1	
3C069.0	4C+58.08	136.2 - 0.9	I	21			-184.1	2.4	115.0	5.4	3	1.0	5	1	
M02-110	0235-19	201.3 -64.5	III	12			+6.3	1.6	174.6	1.5	4	2.3	6	6, 7	
	0237-23	209.8 -65.1	16.6QSO	13	2.224	13	+7.9	1.8	149.8	0.7	4	10.7	4	6, 7	VARIABLE-NOTE
	0241-51	269.2 -58.0					+10.9	2.6	73.7	1.3	4	0.4	6	6, 7	5000-COMPOSITE
3C076.1	0300+16	163.1 -36.0	14.8E	15	0.0326	6	-17.6	0.7	112.0	1.1	6	17.2	6	2, 6, 7,12	1410-6-3SD
3C078.0	0305+03	174.9 -44.5	13.2DE3	21	0.0289	18	+6.6	0.5	90.9	2.3	11	16.1	6	3, 5, 6, 7,11,13	
3C079.0	0307+16	164.1 -34.5	18.6N	15	0.2561	18	-16.9	1.2	25.5	1.1	6	3.4	6	6, 7,12	
3C083.1	4C+41.06	150.1 -13.1	12.5FD3C	21			-183.3	2.1	143.8	2.5	3	0.8	5	1	NOTE
FOR A(A)	0319-37	239.5 -57.1	10. SO	12	0.0058	12	-2.4	0.7	66.1	1.7	3	0.2	5	5, 6	
	0319-45	254.2 -55.2					+8.1	1.9	54.9	2.7	4	3.2	6	6, 7	
FOR A(B)	0322-37	239.4 -56.5	10. SO	12	0.0058	12	-3.2	0.9	111.2	2.7	3	0.6	5	5, 6	
3C086.0		143.9 - 1.1	I	21			-130.8	3.5	122.2	4.2	4	9.8	4	13	CURVE?
3C088.0	0325+02	181.0 -42.0	13.0D4	21	0.0302	18	+22.1	1.6	82.3	2.9	6	2.3	6	3, 6, 7,13	NOTE
CTA 26	0336-01	188.0 -42.5	18.4QSO	7	0.852	5	+17.1	0.6	145.7	4.9	5	1.2	3	4, 6, 7	5000-7 DIS/DEL
3C093.0	0340+04	181.9 -37.5	18.1QSO	7			+8.5	1.5	136.2	1.8	6	2.2	6	1, 6, 7	
M03-306	0344-34	234.9 -52.0	17.4E	12			+16.0	2.9	153.9	4.9	4	4.9	6	6, 7	
4C+05.16	0347+05	182.3 -35.7	III	12			+26.2	3.3	68.7	2.0	4	0.1	6	6, 7	
3C095	0349-14	205.5 -46.3	16.2QSO	13	0.614	13	-37.7	9.6	161.8	7.2	3	0.1	3	6, 7	
3C094	0350-07	196.6 -42.7	16.5QSO	13	0.962	13	+21.6	1.3	6.5	0.6	4	0.4	6	6, 7	
3C098.0	0356+10	179.9 -31.0	14.0ED3	21	0.0306	18	+73.7	1.9	59.4	5.4	5	2.3	6	3, 5,13	
3C099.0	0358+00	189.6 -36.7	18.0G	21			-35.3	2.9	123.4	3.6	3	0.0	5	1, 7	
	0403-13	205.8 -42.7	17.2QSO	13	0.571	13	+12.3	3.4	175.6	3.0	4	3.3	6	6, 7	
3C103.0	CTA 28	156.8 - 6.6	II	21			-43.1	1.6	73.4	2.6	4	2.4	5	1, 3	
3C105.0	0404+03	187.6 -33.6	III	12			-65.2	1.8	48.5	1.4	4	0.1	6	6, 7	
3C107.0	0409-01	193.2 -35.3	16.2N?	21			-30.1	7.4	91.4	15.5	3	0.7	3	1	
3C109.0	0410+11	181.8 -27.8	17.8N	15	0.3056	6	-16.0	2.0	60.5	3.1	4	0.8	6	6, 7	

TABLE 3-2--Continued

SOURCE	ALTERNATE NAME	GALACTIC COORDINATES	IDENT	ID REF	Z	Z REF	R.M.	+/-	I.P.A.	+/-	NO. POLS	FIT D	C	POLARIZATION REFERENCES	NOTES
4C+14.11	0411+14	179.3 -25.7	IV	12			-55.1	3.8	21.5	2.9	4	0.2	6	6, 7	
3C111.0	4C+37.12	161.7 - 8.8	I	21			-20.8	0.9	142.9	5.0	8	7.4	6	3,11,13,14	1665-13-1.9SD
3C114.0	0417+17	177.3 -22.2	18.5GC	21			-11.4	6.7	138.3	14.7	4	0.5	3	1	
3C119.0	4C+41.13	161.0 - 4.3	20.+QSO	7			-4.8	6.3	127.6	9.7	5	11.7	1	1,14	SCATTER
	0430+05	190.4 -27.4	15.0D	12	0.032	12	+9.3	2.6	161.2	3.2	7	5.2	6	6, 7, 9,12,14	
3C123.0	4C+29.14	170.6 -11.7	19.5G	21			-307.0	27.8	12.2	5.2	3	0.4	5	8, 9,14	NOTE
MO4-409	0438-43	248.4 -41.6	III	12			-274.1	3.2	83.7	2.6	4	2.8	6	5, 6, 7	
MO4-218	0442-28	228.5 -38.9	18.2E	12			-215.6	1.0	123.0	3.4	6	7.3	6	5, 6, 7,12	265C-6-DIS/DEL
3C130.0	NRAO196	155.4 + 5.1	16.5DE2	21			-81.5	3.3	157.7	5.9	4	8.9	5	1	SCATTER
3C131.0	4C+31.18	171.4 - 7.8	I	21			-108.3	5.2	84.8	9.4	3	0.4	1	1	
	0453-20	220.3 -34.4	14. E	12	0.0354	22	-58.7	7.2	155.9	2.5	3	2.1	5	6, 7	
	0453-30	231.6 -37.0	19.0E	15			-2.5	0.5	101.6	2.7	5	3.4	6	5, 6	5000-7 DIS/DEL
3C132.0	0453+22	178.9 -12.5	18.5GC	21			-38.5	0.7	17.7	1.0	7	6.7	6	1, 6, 7,11	
	0454-46	252.0 -38.8					+13.0	1.5	11.6	1.4	3	0.8	3	6, 7	
	0456-30	231.7 -36.4	17.6E	15			-367.0	1.6	17.9	2.1	5	6.3	6	5, 6	
3C133.0	0459+25	177.7 - 9.9	I	21			-8.4	2.0	140.2	2.1	4	0.4	5	3, 6, 7	
MO5-601	0506-61	270.5 -36.1					-200.6	4.8	27.9	3.4	3	0.2	3	6, 7	
3C135.0	0511+00	200.4 -21.1	18.0D	15	0.1270	15	+42.0	6.3	85.5	2.0	3	0.1	3	6, 7	
	0511-48	254.7 -36.0					+28.1	1.6	155.0	1.8	4	6.3	6	6, 7	HIGH CURVE
B0511-30	0511-30	233.1 -33.3	17. E	12			+2.9	2.1	159.7	4.1	3	1.4	5	6	
3C136.1	0512+24	179.7 - 7.7	17.0G	21			-170.9	2.7	110.8	2.1	3	1.5	5	6, 7	
3C137.0	4C+50.16	158.8 + 7.7	II	21			-4.2	2.7	36.8	5.8	4	6.2	1	1	
PIC A	0518-45	251.6 -34.6	15.7D	12	0.0342	18	+58.9	0.3	86.9	2.4	4	4.3	6	5, 6	960-5 DIS/DEL
3C138.0	0518+16	187.4 -11.3	18.8QSO	13	0.759	13	-1.8	0.8	169.4	0.8	11	8.3	6	3, 6, 7,13,14,15	
MO5-36	0521-36	240.6 -32.7	16.8N	12	0.061	12	+7.4	0.9	71.6	1.6	9	5.7	6	5, 6, 7	LOW CURVE
3C139.2	4C+28.15	178.1 - 4.3	I	21			+295.0	4.4	87.6	10.2	3	0.4	1	1	
3C141.0	4C+32.18	174.5 - 1.3	I	21			+0.4	3.0	35.2	6.0	3	0.9	2	1	
3C142.1	0528+06	197.6 -14.5	III	12			+84.6	3.2	42.4	3.6	4	0.5	6	6, 7	
3C144.0	TAU A	184.6 - 5.8	SNR	21			-21.1	0.7	143.2	1.1	10	18.2	6	6, 8,10,13,14	SCATTER
	0531+19	186.8 - 7.1	17.7E	12			-36.6	9.5	32.1	16.3	4	5.5	2	6, 7	
MO5-410	0547-40	246.8 -28.6	III	12			+48.2	1.9	110.9	1.8	4	1.8	6	6, 7	
	0602-31	238.2 -23.3	III	12			+63.1	7.6	35.5	3.4	3	2.8	5	6, 7	
	0605-08	215.8 -13.5	III	12			-222.8	5.9	58.7	4.5	3	0.1	2	6, 7	
	0607-15	222.6 -16.2	III	12			+60.2	7.3	160.7	6.9	3	1.3	1	6, 7	
3C154.0	0610+26	185.6 + 4.0	II	21			+2.2	4.6	14.8	2.5	5	10.4	4	1, 6, 7,12	SCATTER
MO6-307	0618-37	244.7 -21.9	16.6DB	12	0.0326	22	-1.6	0.8	73.6	1.8	4	4.3	6	5, 6, 7	

TABLE 3-2--Continued

SOURCE	ALTERNATE NAME	GALACTIC COORDINATES	IDENT	ID REF	Z	Z REF	R.M.	+/-	I.P.A.	+/-	NO. POLS	FIT D	C	POLARIZATION REFERENCES	NOTES
M06-503	0620-52	261.1 -25.6					+70.3	5.9	33.8	2.9	3	2.7	1	6, 7	
3C161	0624-05	215.4 - 8.0	III	12			+110.4	0.4	97.3	0.7	13	63.6	6	3, 6, 7,13,14	SCAT/LOW CURVE
M06-505	0625-53	262.4 -25.1					+65.0	1.9	82.4	0.9	4	1.4	6	5, 6, 7	
	0625-35	243.4 -20.0	17.6DB	12			+13.0	8.7	169.5	3.2	3	6.1	1	6, 7	
	0634-20W	229.9 -12.4	16.8E	12			+49.4	0.7	84.8	0.5	6	2.3	6	5, 6, 7	
	0634-20E	229.9 -12.4	16.8E	12			+40.4	3.1	108.3	1.1	4	4.4	6	6, 7	
	0637-75	286.4 -27.2					+21.1	1.1	0.4	3.3	5	4.2	6	5, 6	5000-7 DIS/DEL
3C165.0	0640+23	191.1 + 8.7	II	21			+60.8	1.6	68.1	1.8	6	11.9	5	1, 7	SCATTER/DEPOL
3C166.0	0642+21	193.1 + 8.3	19.5G	21			+86.9	3.9	62.8	5.4	4	3.6	3	1, 7	NOTE
	0646-39	249.4 -17.6	III	12			+44.6	2.5	58.3	2.8	4	7.1	6	6, 7	
3C169.1	4C+45.12	171.1 +18.8	III	21			+9.0	7.7	61.5	16.7	3	1.2	2	1	
3C171.0		162.2 +22.2	18.8G	21	0.2387	18	+54.9	1.7	79.4	4.9	5	2.2	6	2, 3,12,13,15	
M06-216	0656-24	235.5 - 9.2	III	12			+222.3	2.8	11.5	2.0	3	0.0	5	6, 7	
3C173.0	4C+38.19	179.0 +18.3	18.0N?	21			+20.4	11.6	109.7	24.0	3	3.1	2	1	
3C172.0	0659+25	191.5 +13.3	17.2QSO	7			+18.9	2.2	96.1	4.3	4	0.0	5	3, 6	
3C173.1	4C+74.12	140.0 +27.3	18.5GC	21			-33.1	2.8	58.9	6.1	3	0.8	5	1	
3C175.0	0710+11	204.8 +10.1	16.6QSO	13	0.768	13	+11.6	5.2	4.5	6.4	6	5.0	5	2, 3, 6,12	
3C175.1	0711+14	202.3 +11.5	18.0QSO	7			+93.8	1.4	135.8	4.6	4	2.1	1	1, 4, 7	DEPOLARIZED
B0715-24	0715-25	238.2 - 5.9	III	12			+155.6	2.8	5.6	4.5	6	11.5	6	6, 7	LOW CURVE
3C177.0	0721+15	202.8 +14.1	15.5N	21			+66.9	2.4	11.4	5.5	3	0.3	5	1	
3C180.0	0724-01	218.9 + 7.0	19.0G	21			+46.1	6.1	142.0	12.4	3	1.9	2	1, 7	
3C181.0	0725+14	203.8 +14.6	18.9QSO	13	1.382	13	+40.9	3.0	93.2	8.8	4	3.0	6	1,15	
3C184.0	4C+70.06	145.1 +29.5	IV	21			+229.1	0.8	128.3	1.9	5	5.9	5	1, 3, 5	
3C184.1	NRAO271	133.6 +28.9	17.0DC	21	0.1187	9	-18.3	6.2	73.5	15.1	3	0.6	3	1	
DA 237	0735+17	201.9 +18.1		10			+1.9	2.6	25.0	2.3	4	8.9	6	6, 7	2650-6-2.5SD
OI+061	0736+01	217.0 +11.4	17.5QSO	13	0.191	13	+19.6	0.9	72.7	1.5	6	11.0	6	6, 7,15	
3C187.0	0742+02	217.3 +12.8	19.5G?	21			+26.9	5.0	46.3	8.2	3	1.2	2	1	DEPOLARIZED
3C192.0	0802+24	197.9 +26.4	15.0DE1C	21	0.0599	15	+20.8	2.6	70.8	2.9	7	2.5	6	2, 6, 7,12,13	
	0806-10	231.4 +12.0	18.8E	4	0.107	15	-37.3	2.3	112.8	4.1	4	1.8	3	5, 6, 7	
3C196.0	NRAO285	171.2 +33.2	17.8QSO	13	0.871	13	+305.1	3.9	64.5	3.3	11	11.2	3	1, 3,13,14	
3C197.1	4C+47.28	172.7 +34.5	16.5DE1C	21	0.1302	8	-4.4	5.0	166.3	11.7	3	0.1	3	1	
B0819-30	0819-30	249.8 + 3.7	18.2E3	12			-77.9	11.1	142.7	11.3	3	2.9	2	6, 7	
3C198.0	0819+06	218.1 +22.9	17.0D4C	21	0.0809	18	+25.1	3.8	98.5	8.6	3	0.2	5	1	DEPOLARIZED
3C200.0	4C+29.29	194.0 +32.6	20.0G	21			+13.3	4.0	37.3	8.8	3	1.0	3	1	
M08-24	0825-20	242.4 +10.3	18. QSO	7			-100.8	1.0	134.6	1.5	4	3.5	1	4, 6, 7	
3C205.0	4C+58.16	159.3 +36.9	17.6QSO	13	1.534	13	-11.5	0.5	65.7	1.8	6	3.9	6	1, 3, 4,15	

TABLE 3-2--Continued

SOURCE	ALTERNATE NAME	GALACTIC COORDINATES	IDENT	ID REF	Z	Z REF	R.M.	+/-	I.P.A.	+/-	NO. POLS	FIT D	C	POLARIZATION REFERENCES	NOTES
3C207.0	0838+13	213.0 +30.1	18.2QSO	13	0.684	13	+26.2	1.3	23.7	1.6	4	2.8	3	6, 7,15	
	0842-75	289.4 -19.9	III	12			+6.5	1.3	156.9	3.3	4	1.8	6	5, 6, 7	
M08-308	0843-33	255.7 + 5.7	12.3E3	12	0.00732	22	+70.2	1.1	154.8	0.8	5	1.9	6	6, 7	
3C208.1	0851+14	213.6 +33.6	III	21			+33.2	5.9	102.7	10.3	3	1.2	2	1	
3C212.0	0855+14	214.0 +34.5	19.0N	21			+139.5	3.4	51.0	4.5	5	4.9	6	1, 2, 7,12	
3C213.1	4C+29.33	196.5 +39.7	19.0GC	21			+262.9	6.4	110.3	14.0	3	2.5	5	1	
M08-219	0859-25	251.8 +13.4	III	12			+69.4	2.2	28.5	4.1	6	6.3	6	6, 7,12,13	
	0859-14	242.3 +20.7	17.8QSO	13	1.327	13	+15.9	0.6	72.3	1.3	4	3.2	3	4, 6, 7	
	0903-57	276.1 - 7.0	III	12			+183.7	2.9	61.2	0.8	3	0.0	5	6, 7	DEPOLARIZED
3C215.0	0903+16	211.9 +37.3	18.3QSO	13	0.411	13	+29.1	1.8	71.0	5.0	4	0.8	2	1, 4	
3C217.0	4C+38.26	185.2 +42.6	18.5QSO	7			+6.4	0.9	8.9	3.4	4	3.5	2	1, 4	
	0916-54	275.4 - 3.9					-280.7	3.9	147.1	2.8	3	0.6	5	6, 7	
3C219.0		174.4 +44.8	17.5CD5	21	0.1745	18	-13.7	0.5	145.2	4.1	5	4.0	5	11,13	
3C220.2	4C+36.15	188.1 +46.8	18.2G?	21			+31.3	8.7	160.4	19.2	3	2.0	2	1	
3C223.0	NRAO328	188.4 +48.6	17.1E2	6	0.1370	6	+16.0	0.1	77.7	0.8	5	1.1	6	1, 3, 4	
3C225.0	0939+14	220.0 +44.0	III	21			-22.8	4.3	103.5	9.4	5	2.6	6	1, 6	
3C226.0	0941+10	225.2 +42.7	19.5G	21			+15.0	2.0	60.0	3.2	3	1.6	5	1, 7	
3C227.0	0945+07	228.6 +42.3	14.5N1	21	0.0855	15	-6.5	0.6	157.7	1.8	11	6.1	6	3, 5, 6, 7,13,14	
3C228.0	0947+14	220.4 +46.0	III	21			+3.7	0.8	110.1	1.9	6	3.3	6	6, 7,11,15	
3C230.0	0949+00	237.6 +39.1	18.5N	15			-17.6	3.1	69.6	2.4	4	6.4	6	6, 7,15	DEPOLARIZED
3C234.0	NRAO343	200.2 +52.7	17.5N1	21	0.1846	18	-183.9	8.7	60.2	21.0	4	2.0	3	1, 3	
3C236.0	NRAO344	190.1 +54.0	15.0DE4	21	0.0988	17	-187.9	6.0	133.7	11.5	3	1.8	5	1	
3C238.0	1008+06	234.1 +46.7	IV	21			+36.1	4.1	76.0	5.3	4	4.8	1	6, 7,15	
3C239.0	4C+46.20	170.5 +53.2	17.5QSO	7			+18.3	15.4	102.1	30.9	4	3.6	2	1	
M10-404	1018-42	275.6 +11.8	III	12			-32.1	9.2	103.1	18.4	3	2.2	2	6	
3C244.1	4C+58.21	151.0 +50.7	19.0GC	21			-234.4	3.4	4.9	8.2	5	5.9	5	1, 3	
3C245.0	1040+12	233.1 +56.3	17.3QSO	13	1.029	13	+28.1	1.8	25.4	1.7	8	4.1	6	2, 3, 6, 7,12,14	LOW CURVE
4C+20.24	1055+20	222.5 +63.1	17.1QSO	13	1.110	13	+43.1	0.3	112.2	2.7	4	2.4	3	4, 7,15	
4C+01.28	1055+01	251.5 +52.8	18.3QSO	5			-123.6	2.1	141.6	0.6	4	1.7	5	6, 7, 9	4995-14 DIS/DEL
3C247.0	4C+43.20	170.7 +62.2	18.4QSO	21			+245.8	4.8	134.9	9.2	3	1.9	2	1	
3C249.0	1059-01	255.7 +51.3	IV	21			+17.0	2.0	29.6	2.7	8	3.9	6	2, 3, 6, 7,12	
3C249.1	4C+77.02	130.4 +38.6	15.7QSO	13	0.311	13	-29.9	0.6	16.2	2.6	4	1.5	3	1, 4	
3C250.0	1106+25	212.4 +66.9	III	21			-47.2	15.2	26.7	30.3	3	3.9	1	1	
3C252.0	4C+35.25	184.8 +67.1	III	21			-16.1	7.0	107.8	9.9	3	0.1	1	1	
3C254.0	4C+40.28	172.6 +65.9	18.0QSO	13	0.734	13	-18.2	2.7	125.4	9.4	5	0.8	2	2, 3,12,15	
	1116-46	286.7 +13.4	QSO	20	0.71	20	+5.3	9.5	171.0	2.7	3	0.1	5	6, 7	

TABLE 3-2--Continued

SOURCE	ALTERNATE NAME	GALACTIC COORDINATES	IDENT	ID REF	Z	Z REF	R.M.	+/-	I.P.A.	+/-	NO. POLS	FIT D	C	POLARIZATION REFERENCES	NOTES
4C+12.39	1116+12	242.3 +63.9	19.2QSO	13	2.118	13	-5.2	12.5	106.2	4.4	3	0.0	5	6, 7	
3C257.0	1120+05	254.8 +59.8	IV	21			+229.9	5.5	124.9	12.2	3	0.6	1	1	NOTE
	1127-14	275.3 +43.7	16.9QSO	13	1.187	13	+120.5	0.8	103.3	1.7	4	4.6	1	4, 6, 7	
M11-604	1136-67	296.2 - 6.2					-99.6	3.4	135.6	1.1	3	0.1	5	6, 7	
M11-108	1136-13	277.5 +45.4	17.8QSO	13	0.554	13	-18.6	0.5	42.3	2.7	7	11.6	6	4, 6, 7,12	408-4-2SD
3C263.0	4C+66.13	134.2 +49.8	16.30SO	13	0.652	13	-197.7	8.6	55.8	18.4	3	3.3	5	1	1414-3 DIS/DEL
M11-208	1139-28	285.0 +31.6	III	12			-63.3	2.1	104.4	2.2	4	0.2	6	6, 7	
3C263.1	1140+22	227.3 +73.8	20.0G	21			+22.2	2.1	79.4	1.7	6	4.1	6	1, 6, 7	
3C264.0	1142+19	235.8 +73.0	13.0DE1	21	0.0206	18	+6.1	4.4	132.5	1.9	6	8.9	6	1, 6, 7,14	1640-1-2.2SD
3C265.0	4C+31.37	191.9 +75.0	20.0G?	21			+1.6	2.6	31.3	3.1	3	1.5	5	1	
3C267.0	1147+13	254.9 +69.7	III	21			+2.3	3.2	149.8	3.6	3	0.1	5	6, 7	
4C+00.47	1148-00	272.3 +59.1	17.6QSO	13	1.982	13	-0.5	0.9	160.1	1.9	4	0.0	6	6, 7,15	LOW CURVE
3C268.1	4C+73.11	128.0 +43.6	III	21			-2.9	5.7	169.3	12.7	3	4.9	2	1,14	
3C268.2	4C+31.39	188.0 +78.2	19.0G	21			+16.7	4.3	85.8	9.5	3	0.0	5	1	
3C268.4	4C+43.23	147.5 +71.4	18.4QSO	13	1.400	13	+0.5	3.1	36.2	6.9	3	5.2	5	1	
	1216-10	289.8 +51.7	III	12			-2.9	2.5	113.3	2.3	3	4.3	5	6, 7	
3C270.0	1216+06	281.8 +67.4	11.7ED3C	21	0.00697	12	+8.5	0.5	98.9	1.0	8	6.1	6	3, 5, 6, 8,14	8000-8 DIS/DEL
3C270.1	4C+33.29	166.4 +80.6	18.6QSO	13	1.519	13	+2.9	2.4	87.2	5.2	4	10.3	2	1	
3C272.0	4C+42.35	141.4 +74.0	III	21			-3.3	3.1	114.9	6.5	3	0.3	5	1	
4C+21.35	1222+21	255.2 +81.7	17.5QSO	13	0.435	13	-8.9	0.5	127.6	4.3	4	0.0	1	4, 7,15	
3C272.1	1222+13	278.3 +74.5	11.3E2C	21	0.00293	12	-7.0	1.4	146.1	0.8	9	20.1	6	6, 7,13,14	SCAT/LOW CURVE
3C273.0	1226+02	290.0 +64.3	12.8QSO	13	0.158	13	+2.1	0.5	151.7	0.8	14	21.5	6	3, 5, 6, 7, 9,13,15	
3C274.1	1232+21	270.0 +83.2	20.0G	21			-5.0	0.9	165.9	0.6	3	0.3	5	6, 7	
	1237-10	298.2 +52.4	18.2QSO				+5.9	0.4	39.7	1.6	4	6.3	6	4, 6, 7	
3C275.0	1239-04	298.6 +58.0	III	21			-16.1	1.2	90.4	3.7	5	2.1	6	1, 6, 7,11	
3C275.1	1241+16	293.4 +79.1	19.0QSO	13	0.557	13	-14.0	0.4	132.6	2.5	5	2.3	6	4, 6, 7,15	
3C277.0	4C+50.35	122.8 +66.6	III	21			-12.4	8.7	32.8	20.1	3	0.7	2	1	
3C277.2	1251+15	305.5 +78.6	IV	21			+21.1	5.5	100.6	12.4	3	7.2	4	1	
3C277.3	COM A	71.4 +89.2	15.5D2	21	0.0857	18	+4.9	3.7	179.5	6.8	3	6.2	2	1	
3C278	1252-12	304.2 +50.3	13.2D8	4	0.0143	12	-14.3	0.9	16.1	0.8	9	13.4	6	6, 7,13,14	1690-6-2.5SD
3C279	1253-05	305.1 +57.1	17.8QSO	7	0.536	13	+22.1	0.9	86.0	2.6	8	13.2	6	3, 5, 6,13	NOTE
3C280.0	4C+47.36	120.2 +69.8	IV	21			-14.9	1.3	39.5	3.2	7	8.2	6	1, 2, 3,12,14,15	DEPOLARIZED
3C280.1	4C+40.32	115.2 +76.8	19.4QSO	7	1.659	13	-18.8	5.1	26.6	9.4	4	1.2	3	1	
3C284.0	NRAO421	38.4 +85.6	18.5GC	21	0.2394	9	-3.2	3.1	13.3	6.8	4	3.7	3	1, 3	
4C+11.45	1318+11	328.0 +72.5	19.5QSO	15			-6.7	2.1	86.1	2.2	3	0.2	3	6, 7	
3C285.0	NRAO422	103.3 +73.4	15.5D:	21	0.0797	17	-15.4	5.2	75.3	10.3	3	3.8	3	1	

TABLE 3-2--Continued

SOURCE	ALTERNATE NAME	GALACTIC COORDINATES	IDENT	ID REF	Z	Z REF	R.M.	+/-	I.P.A.	+/-	NO. POLS	FIT	C D	POLARIZATION REFERENCES	NOTES
	1323-61	307.1 + 1.3					+187.8	1.1	9.7	1.0	6	13.8	6	6, 7	LOW CURVE
3C287.0	1328+254	22.3 +81.0	17.7QSO	13	1.055	13	-58.5	3.5	167.0	1.1	10	50.2	4	3, 6, 7,13,14,15	NOTE
3C286.0	4C+30.26	56.4 +80.7	17.2QSO	13	0.846	13	-1.1	0.9	31.0	3.3	6	1.5	6	4,13,15	14500-9 DIS/DEL
3C287.1	1330+02	326.3 +63.0	19. N	12	0.2156	12	+0.1	2.7	147.7	2.9	3	0.1	5	6, 7	
	1334-33	313.7 +27.7	11.9E	12	0.0114	12	-38.3	0.3	125.7	0.9	4	6.3	5	5, 6, 7	
4C-06.35	1335-06	323.2 +54.6	17.7QSO	13	0.625	13	-97.4	1.9	28.5	1.3	4	2.7	1	5, 6, 7	
	1343-60	309.7 + 1.9	SNR	15			-402.4	0.7	147.7	3.0	6	12.4	6	5, 6, 7	500C COMPOSITE
3C293.0	NRAO433	54.6 +76.1	14.3S/D6	6	0.0452	6	-10.5	2.7	77.6	6.4	7	32.9	4	1, 2, 3,12,15	SCATTER
3C293.1	1352+16	359.6 +71.7	19.0G	21			+8.5	5.0	127.3	10.3	3	0.1	3	1	
M13-115	1354-17	324.3 +42.4	III	12			-30.7	11.9	26.2	3.4	3	0.0	3	6, 7	
4C+19.44	1354+19	8.9 +73.0	16.0QSO	13	0.720	13	+4.1	0.7	70.6	0.7	5	4.0	6	6, 7,15	
M13-405	1355-41	316.2 +19.3	16. QSO	20	0.313	20	-28.5	2.4	77.8	2.3	5	0.1	6	6, 7	
	1414+11	357.9 +64.1	13.3F3	12	0.0237	12	-3.1	1.7	37.7	3.3	4	0.7	6	6, 7	
M14-208	1420-27	326.7 +31.1	18. QSO	12			-10.0	3.6	36.6	2.8	4	4.5	3	6, 7	2650-6-2SD
3C300.0	1420+19	18.1 +67.7	18.0G	21	0.27	19	-3.9	4.7	94.3	10.0	6	0.3	6	1, 3, 6, 7	
	1424-41	321.5 +17.3	17.5QSO	20			-200.4	4.2	82.4	7.7	4	1.2	3	6, 7	
4C+03.30	1434+03	354.3 +55.4	III	12			-39.9	3.3	28.1	1.7	4	0.6	1	6, 7,15	DEPOLARIZED
	1437-62	315.3 - 2.0	SNR	15			+72.2	3.5	148.3	6.3	3	0.0	5	6	5000-7 DIS/DEL
3C303.0	4C+52.33	90.5 +57.5	16.0DEC	21			+14.8	2.4	43.6	5.8	3	0.4	5	1	
M14-308	1451-36	328.8 +20.0	III	12			+2.9	3.1	61.7	2.1	4	0.5	6	6, 7	
3C306.1	1452-04	351.1 +46.6	19.0GC	21			-5.6	2.2	86.9	4.9	3	0.3	5	1, 7	
3C309.1	4C+71.15	110.0 +42.1	16.8QSO	13	0.905	13	+76.9	5.0	12.2	10.6	3	0.4	5	1,14	
3C310.0	1502+26	38.5 +60.2	14.5G	21	0.0543	18	+11.3	1.5	35.7	2.8	7	7.1	6	3, 5, 6, 7,13	
	1508-05	353.9 +43.0	III	12			-23.9	3.1	76.1	2.8	4	5.5	6	6, 7	
3C313.0	1508+08	9.2 +51.8	III	12			+14.3	5.7	2.4	4.6	3	0.5	3	6, 7	
	1510-08	351.3 +40.1	16.5QSO	13	0.361	13	-17.1	2.6	72.9	2.0	4	8.9	6	6, 7,14	
3C315.0	1511+26	39.3 +58.3	16.6DBC	21	0.1086	18	-1.0	1.8	116.3	2.8	6	6.0	6	2, 6, 7	
4C+00.56	1514+00	1.4 +46.0	18.8QSO	5			-11.9	2.8	162.9	3.7	4	0.2	6	6, 7	
	1514-24	340.7 +27.6	15.2N	15			-18.8	2.1	46.4	1.8	4	2.4	6	6, 7	
3C319.0	4C+54.34	88.1 +51.1	18.5GC	21			+5.3	4.3	95.8	9.0	3	5.6	3	1	
	1526-42	331.7 +11.7					+35.3	2.0	52.4	3.6	4	4.0	3	5, 6, 7	
3C321.0	1529+24	37.2 +53.9	III	21			+9.9	0.6	1.5	1.0	5	3.2	5	3, 6, 7,11	
3C323.1	1545+21	33.9 +49.5	16.7QSO	13	0.264	13	+22.3	4.8	124.5	3.0	4	0.4	5	3, 6, 7	
3C324.0	1547+21	34.9 +49.2	IV	21			+333.1	1.5	113.1	3.3	5	8.3	6	1, 6, 7	
	1547-79	310.8 -19.7					+38.0	1.3	123.4	0.8	4	5.6	6	6, 7	
3C325.0	4C+62.25	96.3 +44.1	III	21			-13.3	2.4	92.3	5.5	3	0.0	5	1	LOW CURVE

TABLE 3-2--Continued

SOURCE	ALTERNATE NAME	GALACTIC COORDINATES	IDENT	ID REF	Z	Z REF	R.M.	+/-	I.P.A.	+/-	NO. POLS	FIT D	C	POLARIZATION REFERENCES	NOTES
3C326.0	1550+20	33.3 +48.2	18.5GCL	21			+24.3	2.4	11.1	2.0	3	0.0	3	6, 7	
NRAO488	1553+20	33.7 +47.3					+59.5	5.3	155.6	5.5	3	0.2	2	6, 7	
3C327.0	1559+02	12.5 +37.8	15.0DE3C	21	0.1041	18	+9.3	0.6	161.6	0.9	10	12.9	6	3, 6, 7,13,14	101C-5 DIS/DEL
	1602-63	322.8 - 8.4	17.5DB	12			+214.3	2.9	168.6	3.1	3	0.9	5	6	NOTE
M16-001	1602-09	1.9 +30.5	III	12			-7.8	1.3	27.5	1.9	6	7.4	6	6, 7	
3C330.0	4C+66.17	98.9 +40.7	III	21			+27.5	4.7	97.0	10.1	5	2.7	3	3,13	
	1610-77	313.4 -18.8					+102.4	3.7	86.0	0.9	3	0.2	2	6, 7	
	1614+21	36.9 +43.1					+15.3	4.4	75.5	3.1	3	3.2	3	6, 7	
3C332.0	NRAO498	52.6 +45.4	16.0DE3C	21	0.1520	9	+2.6	1.7	120.7	3.1	3	0.9	5	1	
3C334.0	1618+17	33.2 +41.1	16.4QSO	13	0.555	13	+41.1	1.8	45.2	3.0	4	2.2	5	1, 7	
3C336.0	1622+23	41.4 +42.1	17.5QSO	13	0.927	13	+26.1	1.3	136.1	1.0	5	0.7	6	3, 6, 7,15	
3C341.0	4C+27.33	46.8 +42.3	19.5G	21			+19.8	0.8	143.5	1.9	4	1.2	5	1	
3C337.0	4C+44.28	69.5 +43.6	III	21			+39.7	3.5	61.7	8.0	3	0.1	5	1	
3C340.0	1627+23	41.3 +40.9	III	21			+21.9	1.2	179.5	1.8	3	0.0	5	1, 7	
	1637-77	314.4 -19.9	16. D3	12	0.0438	22	+49.5	3.5	124.7	4.7	3	0.0	2	6, 7	
3C345.0	4C+39.48	63.4 +40.9	16.0QSO	13	0.594	13	+18.2	0.2	46.5	2.0	9	1.0	6	3, 9,13,15	610-11 DIS/DEL
3C346.0	1641+17	35.3 +35.8	16.0G	21			-35.2	1.1	175.2	3.2	6	6.3	6	1, 6,11,15	NOTE
3C348.0	HER A	23.1 +28.9	18.0CD4:	21	0.154	12	-10.0	1.0			10		6	1, 6, 7, 8,13,14	NOTE
3C349.0	4C+47.45	73.0 +38.2	19.0G	21			+10.7	2.6	40.8	6.1	3	0.3	5	1	
3C352.0	4C+46.34	71.8 +36.2	IV	21			+22.3	8.3	41.4	18.6	3	2.4	2	1	
3C353.0	1717-00	22.9 +20.5	15.0D2	21	0.0307	18	+50.7	2.7	75.8	1.0	6	5.3	6	6, 7,10,13,14	
4C-02.74	1722-02	20.2 +17.9	III	12			+55.2	7.2	83.4	4.7	3	0.8	5	6, 7	
3C356.0	4C+51.36	77.9 +34.2	15.3N?	21			+8.4	4.3	128.3	9.2	3	1.3	3	1	
3C360	1730-13	12.0 +10.8	III	12			-49.7	1.5	58.9	1.6	5	1.2	6	6, 7,14	
	1732-09	15.6 +12.3	III	12			+54.2	1.3	170.7	0.8	4	1.3	6	6, 7	
	1737-30	358.5 + 0.4					+90.8	2.6	10.0	2.5	4	2.7	3	5, 6, 7	
	1737-60	331.7 -15.6					-4.5	2.5	68.5	4.0	4	1.5	6	6, 7	
3C371.0	4C+69.24	100.1 +29.2	14.2N1	21	0.0508	16	+7.9	4.5	1.6	10.1	3	1.7	2	1,14	
	1817-64	330.7 -21.1					+69.3	1.8	155.1	2.0	4	3.6	6	6, 7	
	1819-67	327.4 -22.4					+7.4	1.6	39.8	1.8	4	1.3	6	6, 7	
3C379.1	4C+74.23	105.3 +27.8					-37.2	4.2	120.7	10.2	4	5.4	2	1	
3C380.0	4C+48.46	77.2 +23.5	16.8QSO	13	0.691	13	+270.0	0.3	68.5	4.3	8	9.5	3	4, 5, 9,13,15	
3C381.0	NRAO568	76.1 +22.5	17.0ND:	21	0.1614	17	+25.3	0.8	71.2	2.3	5	3.4	3	1,11	1655-1-1.5SD
3C382.0	CTA 80	61.3 +17.4	14.5D3:	21	0.0586	18	-148.6	3.5	85.2	7.6	3	0.1	2	1	
3C386.0	1836+17	47.0 +10.5	13.0DE2	21	0.0008	18	-212.1	1.2	66.5	3.9	8	3.2	6	2, 3, 6, 7,11	1390-13 DIS/DEL
M18-404	1840-40	355.3 -15.9	III	12			+79.2	4.9	5.0	4.0	3	0.2	2	6, 7	

TABLE 3-2--Continued

SOURCE	ALTERNATE NAME	GALACTIC COORDINATES	IDENT	ID REF	Z	Z REF	R.M.	+/-	I.P.A.	+/-	NO. POLS	FIT	C D	POLARIZATION REFERENCES	NOTES
3C388.0	NRAO577	74.7 +20.2	14.5CD3	21	0.0917	18	-115.9	4.6	14.1	7.8	4	1.9	2	1,15	
3C390.0	1843+09	41.1 + 5.8	I	21			-424.5	2.4	161.8	4.1	4	11.4	4	1, 7,13	
3C389.0	4C-03.70	29.7 - 0.3	I	21			+48.4	4.3	73.5	9.1	3	1.2	5	1	
3C390.3	NRAO582	111.4 +27.1	13.8N	21	0.0569	16	-6.0	0.9	18.7	1.8	3	2.7	5	1	LO CURVE
3C396.0	1901+05	39.2 - 0.3	I	21			-110.5	8.2	101.1	6.3	3	0.9	1	6, 7	
3C399.1	4C+30.35	62.7 + 8.5	I	21			+61.1	0.8	75.1	2.0	5	8.7	6	1,15	
	1922-62	333.9 -28.0	III	12			+44.4	2.4	131.0	4.2	4	0.8	6	6, 7	
M19-111	1938-15	24.4 -17.8	III	12			-72.2	1.7	43.0	2.0	6	5.7	6	6, 7	
3C403.0	1949+02	42.3 -12.3	14.5DE3	21			-37.3	0.6	45.8	1.7	9	8.4	6	2, 3, 5, 6, 7,12,13	
M19-507	1954-55	342.8 -31.4	16.5E	12			0.0	3.6	100.1	18.2	3	0.9	2	5, 6	NOTE
M19-305	1955-35	5.2 -28.4	III	12			-81.6	3.7	68.2	2.8	3	1.7	3	6, 7	
3C409.0	2012+23	63.4 - 6.1	I	21			+16.6	2.7	87.0	2.5	6	2.8	1	1, 7,13	
3C410.0	4C+29.60	69.2 - 3.8	I	21			-219.8	6.4	176.6	14.7	4	6.0	5	13	
3C411.0	2019+09	52.8 -15.0	III	21			-112.9	2.5	170.7	3.1	8	16.3	6	3, 6, 7,15	SCATTER
M20-505	2020-57	340.1 -35.0					+23.1	2.6	119.4	3.5	4	3.6	6	6, 7	2650-6-1.6SD
M20-208	2030-23	21.7 -32.0	20. D	12			-26.4	1.4	153.8	2.1	5	0.7	6	6, 7	1690-6 DIS/DEL
3C415.2	4C+53.46	90.3 + 8.2	II	21			-82.9	5.3	149.5	8.7	4	5.1	5	1	1400-SCAT
M20-307	2032-35	7.9 -35.6	III	12			+1.7	1.5	93.6	1.6	5	2.0	6	6, 7	
3C418.0	4C+51.42	88.8 + 6.0	II	21			-267.0	2.3	146.6	5.4	5	7.3	5	1, 3	
M20-212	2040-26	18.3 -35.3	15.4E	12			-18.1	2.9	157.3	4.1	4	0.5	6	6, 7	
NRAO639	2044-02	44.6 -26.8	III	12			-22.4	10.0	162.8	7.5	3	0.6	2	6, 7	
3C424.0	2045+06	53.8 -22.0	18.0GC	21			-53.1	4.0	66.4	2.0	5	3.9	6	2, 3, 6, 7	LOW CURVE
	2052-47	352.6 -40.4					+39.5	3.3	168.5	1.6	4	2.2	6	6, 7	
M20-214	2053-20	27.1 -36.0	17.8E2	12			-7.3	7.3	135.4	12.2	3	0.2	1	6, 7	
M20-215	2058-28	17.8 -39.6	15.6E	12			+17.2	7.3	63.0	3.4	3	1.5	5	6, 7	
3C428.0	4C+49.36	90.5 + 1.3	I	21			-356.4	3.3	54.9	6.0	5	17.7	4	1	DEPOLARIZED
M21-203	2113-21	28.0 -40.9	17.5QSO	12			-22.1	2.4	77.4	2.4	4	1.4	6	6, 7	
	2115-30	15.8 -43.6	16.5QSO	13	0.980	13	+27.2	2.4	86.4	2.6	4	4.9	6	6, 7	1660-6-1.8SD
3C430.0		99.7 + 8.0	15.0ED4:	21	0.0549	9	-168.5	4.1	150.4	9.4	5	2.5	1	13,15	
3C433.0	2121+24	74.5 -17.7	16.0D4:	21	0.1025	18	-75.8	0.9	166.6	1.1	10	5.8	6	3, 5, 6, 7,13	LOW CURVE
3C435.0	2126+07	60.7 -30.0	19.5QSO	7			-228.7	3.0	29.0	3.6	5	1.6	1	1, 7	
PHL1657	2135-14	38.4 -43.3	15.5QSO	13	0.200	13	+22.2	1.4	0.8	1.6	4	1.2	6	6, 7	
M21-407	2140-43	357.3 -49.0	III	12			+6.2	1.9	85.0	2.5	4	5.0	6	6, 7	2650-6-2SD
3C436.0	NRAO665	80.2 -18.8	19.0G	21	0.2154	18	-49.2	1.3	162.7	2.8	3	0.2	5	1	
3C437.0	2144+15	70.9 -28.4	III	12			-12.1	3.0	46.0	4.6	4	3.7	6	6, 7	2650-6-1.6SD
4C+06.69	2145+06	63.7 -34.1	16.5QSO	13	0.367	13	-0.1	2.1	24.7	2.3	5	0.4	3	4, 6, 7, 9,14	

TABLE 3-2--Continued

SOURCE	ALTERNATE NAME	GALACTIC COORDINATES	IDENT	ID REF	Z	Z REF	R.M.	+/-	I.P.A.	+/-	NO. POLS	FIT D	C	POLARIZATION REFERENCES	NOTES
NRAO668	2148+14	70.9 -29.5	III	12			-21.7	4.2	145.6	6.5	3	0.8	3	6, 7	
	2149-28	20.2 -50.5	III	12			-43.1	3.2	139.4	3.0	4	1.5	6	6, 7	
M21-208	2150-52	343.9 -48.8					-67.1	4.5	107.0	5.7	3	1.4	5	6, 7	
	2152-69	321.3 -40.7	13.8D	12	0.0266	12	+37.1	1.7	23.3	1.6	4	4.5	6	6, 7	LOW CURVE
M21-203	2154-18	36.0 -49.0		5			+17.8	2.7	54.2	3.0	5	5.5	6	6, 7	
3C441.0	4C+29.65	84.9 -20.9	19.4G?	21			-123.6	1.6	175.4	3.5	4	2.7	5	1	
	2209+08	69.8 -37.6	18.5QSO?	12	0.486	15	-20.1	3.0	95.4	2.3	4	2.7	6	6, 7	
3C442.0	2212+13	75.1 -34.1	13.0D	21	0.02618	12	-30.9	4.0	146.7	4.3	5	6.7	6	6, 7	
3C445.0	2221-02	61.9 -46.7	15.3N	21	0.0568	18	-310.7	4.1	163.6	1.7	5	4.5	0	2, 6, 7	NOTE
3C446	2223-05	59.0 -48.8	18.4	13	1.404	13	-25.9	1.4	1.7	0.7	6	7.8	6	1, 3, 7,13	SCATTER
3C449.0	NRAO692	95.5 -15.9	12.5CDE4	21	0.0181	17	-170.3	2.8	99.7	5.1	6	16.6	4	1	SCATTER
CTA 102	2230+11	77.4 -38.6	17.3QSO	13	1.037	13	-45.6	1.4	47.0	2.1	8	7.7	6	3, 5, 6,13	NOTE
3C452.0		98.1 -17.1	16.0ED1	21	0.0820	18	-271.2	1.1	2.0	0.7	4	0.1	5	2, 3,13,14	
	2247+11	81.6 -41.3	14.4E	12	0.0268	15	-20.0	3.2	52.2	3.9	4	1.3	6	6, 7	
3C454.0	2249+18	87.4 -35.7	18.4QSO	13	1.757	13	-88.0	0.8	105.6	1.1	7	2.8	6	6, 7,15	DEPOLARIZED
M22-406	2250-41	355.7 -62.0	III	12			+14.8	2.1	65.3	2.1	4	0.3	6	6, 7	
3C454.3	2251+15	86.1 -38.2	16.1QSO	13	0.859	13	-53.8	1.4	16.5	1.5	7	21.8	6	6, 7, 9,14,15	SCATTER
3C455.0	2252+12	84.3 -40.8	19. QSO	1	0.543	1	+1.5	6.6	157.6	6.3	4	2.6	6	6, 7	
M22-504	2252-53	335.0 -56.6					-1.8	4.4	44.3	2.3	4	1.7	6	6, 7	
	2253-52	336.0 -57.2					+35.8	10.9	111.6	4.3	4	1.5	2	6, 7	DEPOLARIZED
3C458.0	2310+05	82.9 -49.8	20.0G	21			+3.2	3.0	31.0	2.9	4	0.4	6	6, 7	
3C459.0	2313+03	83.0 -51.3	17.7N	21	0.2201	6	-6.9	0.8	7.8	2.2	9	37.3	6	2, 3, 5, 6, 7,12	SCATTER
	2317-27	26.7 -69.7	18. E	12			+9.9	1.5	90.4	1.6	4	0.5	6	6, 7	
3C460.0	2318+23	97.7 -34.7	III	21			+14.5	7.6	94.9	10.7	5	4.0	1	1, 7	
	2338-58	319.6 -56.5					+0.3	4.7	88.1	3.4	4	1.1	6	6, 7	
4C+09.74	2344+09	97.5 -50.1	16.0QSO	13	0.677	13	-0.5	0.8	148.3	5.5	3	0.1	1	4, 7,15	
3C468.1	4C+64.25	116.5 + 2.5	I	21			+5.4	10.5	157.9	19.9	4	2.8	2	1, 3	
3C469.1	4C+79.23	120.4 +17.3	III	21			+6.5	4.0	86.5	8.1	4	1.6	5	1	
3C470.0	4C+43.59	113.0 -17.8	19.5G	21			-20.1	2.1	130.5	4.3	3	2.7	5	1	
	2356-61	314.0 -55.1	16. D	12			+17.4	1.3	20.7	2.2	6	7.2	6	6, 7	

QSO Quasi-stellar object.

SNR Supernova remnant.

HII Ionized hydrogen region.

PN Planetary nebula.

For a more detailed description of galaxy-type symbols see Matthews, Morgan and Schmidt (1964). The references for the identification and redshift data are given below. These references are not always the original observation papers but are often compilations.

TABLE 3-3

IDENTIFICATION AND REDSHIFT REFERENCES

FOR TABLE 3-2

Number	Reference	Number	Reference
1	Arp et al. (1972)	12	CSIRO Radiophysics Staff (1969)
2	Bolton, Clarke and Ekers (1965)	13	DeVeny, Osborn and Janes (1971)
3	Bolton and Ekers (1966a)	14	Gardner, Morris and Whiteoak (1969a)
4	Bolton and Ekers (1966b)	15	Gardner, Whiteoak and Morris (1969)
5	Bolton and Wall (1970)	16	Sandage (1966)
6	Burbidge (1967a)	17	Sandage (1967)
7	Burbidge (1967b)	18	Schmidt (1965a)
8	Burbidge (1970)	19	Schmidt (1972)
9	Burbidge and Strittmatter (1972a)	20	Tritton (1972)
10	Burbidge and Strittmatter (1972b)	21	Wyndham (1966)
11	Clarke, Bolton and Shimmins (1966)	22	Burbidge and Burbidge (1972)

The next column contains the rotation measure and its standard error, and is followed by the intrinsic position angle and its uncertainty. These quantities and their derivation are fully explained in the first section of this chapter. The next to last column contains information pertinent to the quality and reliability of the determination of the Faraday rotation parameters. "No. Pols" indicates the number of polarization measurements actually used in the determination of the rotation measure. There may well have been more data points available which had been discarded prior to the calculation because they lay in excessively depolarized frequency regions, because their errors were far larger than those of the data actually used and contributed no additional information, or because they were in conflict with other, substantiated data. The process of selection has been thoroughly described in the preceding section.

"Fit" refers to the χ^2 of the fit of the data to the best Faraday rotation parameters. Its use in conjunction with the number of polarization measurements to determine the quality of the fit has been discussed in the foregoing section, as has "CD", the quality code. The codes divide the rotation measures into seven classes in this manner:

6 Good fit involving data at at least four distinct frequencies. No ambiguities.

5 Same as code 6, but data is available at only three frequencies.

4 No ambiguities for $|RM| < 500$ rad/m^2, but the fit is poorer indicating that a larger RM or curvature is possible.

3 An ambiguity with $|RM| < 300$ rad/m^2 has been eliminated by size and quality of fit.

2 The ambiguity has been eliminated on basis of fit alone.

1 The ambiguity has been eliminated on basis of absolute value of the rotation measure alone.

0 Special case, discussed in the notes to Table 3-2.

The final column lists the references for the polarizations used in the rotation determinations and provides notes describing certain circumstances. Again, the references listed are only for those polarization measurements actually used in the calculations. Other references with data on the given source may have been eliminated if their observations were deleted in accordance with the discussion above.

TABLE 3-4

POLARIZATION MEASUREMENT REFERENCES

FOR TABLE 3-2

Number	Reference	Number	Reference
1	The present work	9	Hobbs and Hollinger (1968)
2	Berge and Seielstad (1967)	10	Hollinger and Hobbs (1968)
3	Bologna, McClain and Sloanaker (1969)	11	Kronberg and Conway (1970)
4	Conway *et al.* (1972)	12	Maltby and Seielstad (1966)
5	Gardner and Davies (1966b)	13	Morris and Berge (1964b)
6	Gardner, Morris and Whiteoak (1969a)	14	Sastry, Pauliny-Toth and Kellermann (1967)
7	Gardner, Whiteoak and Morris (1969)	15	Conway (1972)
8	Hobbs and Haddock (1966)		

The word "NOTE" in the Notes column indicates an entry in Notes to Table 3-2, below, for the source in question. "HIGH CURVE" or "LOW CURVE" indicates that there is evidence, as discussed in the preceding section, of curvature towards the high or low frequency end, respectively, of the polarization data. Entries of the form "1660-6-1.8SD" indicate that a polarization data point at 1660 MHz from reference 6 is 1.8 standard deviations from the fitted line. All cases in which a point deviates by more than 1.5 standard deviations have been indicated. In the extreme case, the point may be indicated by "DIS/DEL", which means that the point is discrepant and has been deleted for the purpose of performing the calculation. Points are not discarded unless their residuals are greater than three standard deviations and the actual value at that frequency has been well-established by the other data. All points discarded for poor fit have been indicated.

"DEPOLARIZED" indicates that the source has been depolarized to less than one-third of its maximum degree of polarization within the range of data used for the calculation. This may make the derived values suspect. The omission of the word "DEPOLARIZED" does not in any case indicate that the source was not observed to depolarize, but merely that any depolarization occurring within the range of data used was not excessive. Depolarizations of the sources are discussed in the following section. "COMPOSITE" means that the data point at the frequency shown was formed by combining data of two or more observations of separate components of the source in order to make the point compatible with lower frequency and lower resolution data.

Notes to Table 3-2

3C031.0 The two measurements listed in Table 2-4 at 1640 MHz have been averaged for this source.

0237-23 This source is variable according to Berge and Seielstad (1972). This may explain the poor fit.

3C083.1 The two measurements listed in Table 2-4 at 1640 Mhz have been averaged for this source.

3C088.0 There is a large amount of scatter in the 21 cm data, necessitating the deletion of all but reference 6.

3C119.0 The scatter at 18 and 21 cm is so large that the source may well not be polarized at these frequencies. The rotation measure shown could be completely in error.

3C123.0 The source is depolarized as high as 2830 MHz. Only 14500, 8000, and 4995 MHz data were used.

3C166.0 The point at 1414 MHz (reference 3) was totally discrepant in both degree of polarization and position angle and was discarded.

3C257.0 A rotation measure of either +229.9 or -288.1 rad/m^2 provides a satisfactory fit, but nothing of smaller absolute value does.

3C279 This source is complex. Polarization rises, then falls with wavelength. The high frequency data shows much scatter, and the low is curved. See Figure 3-2.

3C287.0 Depolarization, curvature and scatter all contribute to the high χ^2.

1602-63 Addition of a point at 5000 MHz composed of the PKS 1602-63W

and PKS 1602-63E data of reference 7 gives no fit for $|RM| < 500$ rad/m^2. Curvature, variability or scatter could explain this.

3C346.0 Data above 2950 MHz appears highly variable. This was deleted in computing the rotation measure.

3C348.0 This source depolarizes from 8000 MHz to 2650 MHz, has a plateau from 1665 to 1000 MHz, then depolarizes further. The high frequency data fit a RM of +28 rad/m^2, $\psi = 15.7°$ quite well. The low frequency data fit a RM of -9.9, $\psi = 67.5°$. No RM will fit all the data. The quoted value is for the low frequency only. The value of ψ has been deleted. See Fig. 4-3.

1954-55 This is based on 960 to 1660 MHz data. The high frequency data shows marked depolarization to a plateau in this range. No fit is obtainable for all points.

3C445.0 The degree of polarization drops rapidly between 5000 and 2830 MHz. Deleting 5000 MHz makes the RM ambiguous, and small RM's are then possible.

2230+11 There is marked scatter at 5000 MHz. This data has been deleted.

In addition to the 354 sources for which rotation measures have been computed, there are seven sources for which no value could be determined, even though there appeared to be sufficient data. For two of these, 3C274.0 (VIR A) and PKS 1322-42 (CEN A), it proved impossible to sort out the structure effects on the various polarizations. Mitton (1972) has claimed a value of +500 rad/m^2 for the radiation from the core

of 3C274.0, and -4 rad/m^2 for the halo. The five remaining sources are:

3C394.0 My 1665 and 1640 MHz data disagree, indicating an error, variability, or an extremely large rotation measure. There is no way to decide which, if any, is the most valid; and taking only one or an average value yields an ambiguous answer.

2104-25 Six observations at four separate frequencies are available. No satisfactory fit could be obtained below $|RM| = 1000$ rad/m^2. There is no marked depolarization.

2141-81 Four observations at four frequencies are available. There is no depolarization.

2323-40 This is a highly depolarized source--18% at 5000 MHz and 3.5% at 1660 MHz. No fit could be found with all the data, and the calculation was ambiguous when points were eliminated.

3C465.0 There is considerable scatter in the data, but even averaging the discrepant data gives no satisfactory fit. This source appears to be depolarized below 18 cm.

All five of these sources were searched for fits with rotation measures between +1000 and -1000 rad/m^2 to no avail. The remarkable fact is that only these five out of the 361 sources for which sufficient polarization data exists could not be fit with a straight line for at least a portion of the wavelengths available. This indicates that most of the Faraday rotation occurs external to the emitting regions. The following chapter will examine the origin of the Faraday rotation more closely.

C. DEPOLARIZATION MEASUREMENTS

Many attempts have been made to characterize the depolarization of radio sources by means of a single parameter, such as the derivative of p with respect to ψ, or by the frequency at which the polarization first drops to one-half its maximum value. Efforts to correlate these "depolarization measures" with any quantity such as type of source, galactic coordinates, redshifts, spectral index, maximum degree of polarization, etc., have been uniformly unsuccessful. The most likely explanation for this failure is that depolarization is extremely complex, caused by the many possibilities explained in Chapter I, and that each of these mechanisms of depolarization must be characterized by many parameters. Therefore it is unrealistic to expect a single depolarization parameter to be effective in describing the process, especially when derived for sources with no more than three or four polarization measurements. The ideal would be to examine individual sources in detail with many observations at many frequencies. This data could then be combined with other sources of information for the source to provide a powerful tool for understanding the source structure and energy process.

In conjunction with inquiries into the magnetic field structure of the local spiral arm, it is useful to ask whether significant depolarization of extragalactic radio sources occurs within our own galaxy. This has been answered in the negative before (e.g., see Gardner and Whiteoak, 1966) as well as in the positive (Bologna, McClain and Sloanaker, 1969), but always by means of the rather ineffective depolarization measure.

Table 3-5 lists various polarization parameters for the sources for which rotation measures have been derived. That there is a very severe selection effect must be pointed out. Any source which either has a low degree of polarization or which depolarizes so rapidly that it is not possible to obtain three polarization determinations cannot have a reliable rotation measure and will therefore not be included. Table 3-5 will display an excess of sources with either high polarizations or slight depolarizations and a dearth of those with intrinsically low polarizations or strong depolarizations. This fact must be considered carefully in making any statistical analyses of the data of Table 3-5. Since the depolarization mechanisms are so complex it is not possible to be as systematic as in the derivation of the rotation measures. Therefore a fairly loose classification system was adopted. If the source was observed to depolarize with increasing wavelength the classification 'D" was assigned. If the source polarization increased (very rare) 'I' was the basic character. If there appeared to be no change in the source polarization of more than 50% of the maximum for the entire frequency range of observations, the symbol 'L' for 'level' was applied. Many sources showed a plateau in the polarization at either the high or the low frequency end, or both. Such plateaus were indicated by PH, PL, or PHL, respectively. Any source which was more complex, perhaps rising then falling, was denoted by 'C' either alone or as a suffix to the general trend.

These classifications are not simply a matter of the actual depolarization characteristics of the sources, but include dependencies

on the range and number of polarization data points available. A source with no data at wavelengths longer than 21 cm might be claimed as an 'L' when it actually depolarizes completely at 1 GHz. Similarly, it is nearly impossible to decide if a plateau region exists when only three data points are available. Finally, a source with a low polarization, say 1%, may depolarize without any indications since the various measurements may have errors on the same order as the depolarizations. The classifications I, D, and L presented here must therefore be treated with a measure of skepticism.

The first two columns of Table 3-5 give the source name and alternate as described in the explanation for Table 3-2. The third gives the range of the data in GHz. The fourth column gives the maximum polarization of the source in the frequency range shown. If the source depolarizes to a low plateau, the polarization of this plateau is also shown. All values are in percent. The fifth column is the source depolarization classification as discussed above. For those sources which depolarize, column six gives either the frequency at which p drops to one-half its maximum, or the frequency of the beginning of the plateau. For sources with increasing polarizations, this column is the frequency for which the degree of polarization first climbs to one-half its maximum. This frequency, both for depolarizing and increasing sources, is very dependent upon the range of the data available and probably is, in most cases, not a very reliable indicator.

The polarization curves of a few representative sources are presented in Figures 3-2 through 3-7.

TABLE 3-5

DEPOLARIZATION CHARACTERISTICS

SOURCE	ALTERNATE NAME	RANGE (GHZ)	POL S (%)	TYPE	FRQ (GHZ)	SOURCE	ALTERNATE NAME	RANGE (GHZ)	POL S (%)	TYPE	FRQ (GHZ)
3C002.0	0003-00	5-0.4	3	D	2.0	3C076.1	0309+16	5-0.6	18	DPH	0.6
3C009.0	0017+15	5-0.4	18	DC	2.0	3C078.0	0305+03	5-0.6	3	L	
M00-29	0021-29	5-0.6	4 2	DPL	1.6	3C079.0	0307+16	5-0.4	8	DPH	1.0
M00-210	0023-26	5-1.0	1	L		3C083.1	4C+41.06	5-1.4	8	D	1.6
3C015.0	0034-01	5-0.6	6	D	0.6	FOR A(A)	0319-37	3-0.6	15	D	0.8
							0319-45	5-1.4	6	L	
3C016.0	0035+13	5-1.4	7	L		FOR A(B)	0322-37	3-0.4	10	DPH	0.7
3C017.0	0035-02	5-0.4	1	L		3C086.0		3-1.4	6 2	DPL	2.0
3C018.0	0038+09	5-0.6	2	L		3C088.0	0325+02	5-1.4	5	L	
M00-410	0039-44	5-1.4	5	D	1.5	CTA 26	0336-01	5-0.6	3	L	
3C020.0	4C+51.02	5-1.4	2	L							
						3C093.0	0340+04	5-0.6	8 2	DPL	2.0
M00-315	0042-35	5-1.4	7	D	>3	M03-306	0344-34	5-1.4	5	L	
M00-411	0043-42	5-0.4	13	DPH	0.6	4C+05.16	0347+05	5-1.4	3	L	
M00-222	0045-25	5-1.0	2	L		3C095	0349-14	5-1.4	1	L	
3C022.0	4C+50.04	5-1.4	4	L		3C094	0350-07	5-0.4	12	DC	
	0049-43	5-1.4	0	D	1.6						
						3C098.0	0356+10	3-0.6	7	L	
3C027.0	4C+68.02	5-1.4	6	L		3C099.0	0358+00	5-1.4	4	DPH	1.5
3C029.0	0055-01	5-0.4	13	DPH	0.7		0403-13	5-0.4	3	DPH	1.0
4C-00.06	0056-00	5-0.6	7 2	DPL	1.0	3C103.0	CTA 28	5-1.4	11 3	DPL	>2
3C031.0	4C+32.05	5-1.4	3	L		3C105.0	0404+03	5-1.4	5	L	
3C032	0105-16	5-0.6	11	D	3.0						
						3C107.0	0409-01	5-1.4	4	L	
3C033.1	4C+72.01	5-0.6	3	L		3C109.0	0410+11	5-1.4	5	L	
4C+01.02	0106+01	5-0.4	8	C		4C+14.11	0411+14	5-1.4	8	L	
3C033.0	0106+13	5-0.4	9 4	DPHL	0.8	3C111.0	4C+37.12	5-0.6	3	L	
3C034.0	4C+31.02	5-1.4	9	D	2.0	3C114.0	0417+17	5-1.4	6	L	
3C035.0	NRA061	5-1.4	3	L							
						3C119.0	4C+41.13	5-0.6	2	D	2.0
3C038	0117-15	5-0.6	6	D	3.0		0430+05	15-1.	4	L	
3C041.0	4C+32.06	5-1.0	7	L		3C123.0	4C+29.14	15-1.	7	D	5
M01-111	0125-14	5-1.4	3	L		M04-409	0438-43	5-1.0	1	L	
3C042.0	4C+28.04	5-1.4	3	L		M04-218	0442-28	5-1.0	3	I?	
	0131-367	5-0.4	20 7	DPL	1.5						
						3C130.0	NRA0196	5-1.4	6 2	DPL	2.0
3C046.0	4C+37.05	5-1.4	10	L		3C131.0	4C+31.18	5-1.4	4	D?	
3C047.0	0133+20	5-0.6	5	DC			0453-20	5-1.0	4	D	2.0
3C052.0	4C+53.02	5-1.4	3	L			0453-30	5-0.6	7 4	DPL	1.0
M01-217	0148-29	5-1.4	6	IPL?	3.0	3C132.0	0453+22	5-0.6	8	D	1.6
3C054.0	4C+43.06	5-1.4	5	L							
							0454-46	5-1.4	6	I	2.0
3C055.0	CTA 16	5-1.4	6	L			0456-30	5-0.6	8	L	
M01-135	0157-31	5-1.0	6	D	2.0	3C133.0	0459+25	5-0.6	4	DPH	0.8
3C057	0159-11	5-0.4	3	L		M05-601	0506-61	5-1.4	3	L	
M02-401	0201-44	5-1.4	10	D	2.4	3C135.0	0511+00	5-1.4	4	L	
3C058.0	CTB 8	14-1.	6	DPH	2.0						
							0511-48	5-1.4	11	L	
3C062	0213-132	5-0.6	8	DPH	0.6	B0511-30	0511-30	3-1.4	10	L	
3C063.0	0218-02	5-0.6	7	DC		3C136.1	0512+24	5-1.4	16	D	1.4
3C064	0219+08	5-1.4	7	L		3C137.0	4C+50.16	5-1.4	9 4	DPL	1.5
3C066.0	NRA0102	5-0.6	3	DPH	1.0	PIC A	0518-45	3-0.4	3	DPH	0.5
3C065.0	4C+39.07	5-1.4	14	D	>2						
						3C138.0	0518+16	5-0.4	11	D	1.0
3C068.1	4C+34.08	5-1.4	6	L		M05-36	0521-36	5-0.4	4	L	
3C069.0	4C+58.08	5-1.4	5	L		3C139.2	4C+28.15	5-1.4	8	D?	
M02-110	0235-19	5-1.0	8	C		3C141.0	4C+32.18	5-1.4	6	L	
	0237-23	5-0.4	5	D	2.0	3C142.1	0528+06	5-1.4	5	L	
	0241-51	3-1.4	7	D	1.5						

TABLE 3-5--Continued

SOURCE	ALTERNATE NAME	RANGE (GHZ)	POLS (%)	TYPE	FRQ (GHZ)
3C144.0	TAU A	9-1.0	7	D	2.2
	0531+19	5-1.4	2	L	
M05-410	0547-40	5-1.4	13	I	
	0602-31	5-1.4	2	L	
	0605-08	5-1.4	2	L	
	0607-15	5-1.4	3	I?	
3C154.0	0610+26	5-1.4	4	D	2.0
M06-307	0618-37	5-1.0	12	L	
M06-503	0620-52	5-1.4	4	D	2.0
3C161	0624-05	5-0.6	10	C	
M06-505	0625-53	5-1.0	5	D	2.5
	0625-35	5-1.0	3	D	1-2
	0634-20W	5-1.0	15 6	DPL	3
	0634-20E	5-1.4	19 6	DPL	2.0
	0637-75	5-0.6	4	L	
3C165.0	0640+23	5-1.4	9 3	DPL	>2
3C166.0	0642+21	5-1.4	3	D	1.5
	0646-39	5-1.4	6	L	
3C169.1	4C+45.12	5-1.4	6	L	
3C171.0		3-0.4	7	D	1.4
M06-216	0656-24	5-1.4	18	D	2.0
3C173.0	4C+38.19	5-1.4	4	L	
3C172.0	0659+25	3-0.6	8	DPH	1.0
3C173.1	4C+74.12	5-0.6	7	DPH	1.0
3C175.0	0710+11	5-0.4	10	DC	3
3C175.1	0711+14	5-0.6	10	D	>2
B0715-24	0715-25	5-0.4	3	L	
3C177.0	0721+15	5-1.4	21	D	<2
3C180.0	0724-01	5-1.4	2	L	
3C181.0	0725+14	5-0.4	2	L	
3C184.0	4C+70.06	5-0.6	6	L	
3C184.1	NRAO271	5-1.4	3	L	
DA 237	0735+17	5-1.4	4	L	
OI+061	0736+01	5-0.4	6	L	
3C187.0	0742+02	5-1.4	10	D	2.0
3C192.0	0802+24	5-1.4	4	L	
	0806-10	5-1.0	2	L	
3C196.0	NRAO285	5-0.6	4	D	2.0
3C197.1	4C+47.28	5-1.4	4	L	
B0819-30	0819-30	5-1.4	2	I	
3C198.0	0819+06	5-1.4	14 4	DPL	>2
3C200.0	4C+29.29	5-1.4	6	L	
M08-24	0825-20	5-0.6	4	DPH	1.0
3C205.0	4C+58.16	5-0.4	7	DPHL	1.0
3C207.0	0838+13	5-0.6	3	L	
	0842-75	5-1.0	4	L	
M08-308	0843-33	5-1.4	20	L	
3C208.1	0851+14	5-1.4	4	L	
3C212.0	0855+14	5-0.6	3	D?	2
3C213.1	4C+29.33	5-1.4	4	L	
M08-219	0859-25	5-1.0	8	D	2.0
	0859-14	5-0.4	3	L	
	0903-57	5-1.4	8	D	2.0
3C215.0	0903+16	5-0.6	7	D	2
3C217.0	4C+38.26	5-0.6	6 2	DPL	2.0
	0916-54	5-1.4	3	L	
3C219.0		3-0.4	3	DPH	0.5
3C220.2	4C+36.15	5-1.4	5	L	
3C223.0	NRAO328	5-0.4	8	L	
3C225.0	0939+14	5-0.6	5 1	DPL	2.0
3C226.0	0941+10	5-1.4	9	D	1.4
3C227.0	0945+07	5-0.4	6	DPH	0.5
3C228.0	0947+14	5-0.6	7	D	1.5
3C230.0	0949+00	5-0.6	7	D	.2
3C234.0	NRAO343	5-0.4	2	L	
3C236.0	NRAO344	5-1.4	3	L	
3C238.0	1008+06	5-1.0	2	DPH	1.0
3C239.0	4C+46.20	5-0.6	3	DPH?	1
M10-404	1018-42	3-1.0	4	L	
3C244.1	4C+58.21	5-0.6	6	DPH	1.1
3C245.0	1040+12	5-0.4	11	D	1.5
4C+20.24	1055+20	5-0.4	4	L	
4C+01.28	1055+01	15-1.	7	L	
3C247.0	4C+43.20	5-1.4	7	D	1.4
3C249.0	1059-01	5-0.6	8	DPH	1.0
3C249.1	4C+77.02	5-0.4	4	DPH	0.5
3C250.0	1106+25	5-1.4	4	L	
3C252.0	4C+35.25	5-1.4	12 1	DPL	>2
3C254.0	4C+40.28	3-0.6	4	DPH	1.0
	1116-46	5-1.4	5	L	
4C+12.39	1116+12	5-0.6	2	DPH	1.0
3C257.0	1120+05	5-1.4	6	L	
	1127-14	5-0.4	3	DPH	1.0
M11-604	1136-67	5-1.4	11	L	
M11-108	1136-13	5-0.4	6	C	
3C263.0	4C+66.13	5-0.6	2	DPH	1.0
M11-208	1139-28	5-1.4	10	D	1.6
3C263.1	1140+22	5-1.4	9 2	DPL	3
3C264.0	1142+19	5-0.6	11	D	>3
3C265.0	4C+31.37	5-1.4	6	L	
3C267.0	1147+13	5-1.4	4	L	
4C+00.47	1148-00	5-0.4	4	L	
3C268.1	4C+73.11	5-1.4	2	L	
3C268.2	4C+31.39	5-1.4	6	L	
3C268.4	4C+43.23	5-0.6	11	DPH	1.0
	1216-10	5-1.4	6	L	
3C270.0	1216+06	8-0.4	12	D	1.0
3C270.1	4C+33.29	5-0.6	11	D	1.2
3C272.0	4C+42.35	5-1.4	12 5	DPL	2
4C+21.35	1222+21	5-0.4	3	L	

TABLE 3-5--Continued

SOURCE	ALTERNATE NAME	RANGE (GHZ)	POLS (%)	TYPE	FRQ (GHZ)	SOURCE	ALTERNATE NAME	RANGE (GHZ)	POLS (%)	TYPE	FRQ (GHZ)
3C272.1	1222+13	5-0.6	8	DPLC			1547-79	5-1.4	10	L	
3C273.0	1226+02	14-.4	3	I		3C325.0	4C+62.25	5-0.6	3	DPH	0.8
3C274.1	1232+21	5-1.4	17	C		3C326.0	1550+20	5-1.4	8	L	
	1237-10	5-0.6	6	L		NRAO488	1553+20	5-1.4	3	L	
3C275.0	1239-04	5-0.6	2	C			1602-63	3-1.4	9	D	2
3C275.1	1241+16	5-0.4	3	DPH	1.0	M16-001	1602-09	5-1.0	10	L	
3C277.0	4C+50.35	5-1.4	4	L		3C330.0	4C+66.17	3-0.6	5	DPH	1.0
3C277.2	1251+15	5-1.4	6	L			1610-77	5-1.4	7 3	DPL	3
3C277.3	COM A	5-0.6	5	D	2.0		1614+21	5-1.4	5	L	
3C278	1252-12	5-0.6	7	DPH	1.0	3C332.0	NRAO498	5-0.6	9	D	1.5
3C279	1253-05	14-.4	7	IC		3C334.0	1618+17	5-0.4	6 2	DPL	1.4
3C280.0	4C+47.36	5-0.6	10 2	DPL	3.0	3C336.0	1622+23	5-0.4	7 1	DPL	1.4
3C280.1	4C+40.32	5-0.4	7	D	1-2	3C341.0	4C+27.33	5-1.4	22	L	
3C284.0	NRAO421	5-1.4	12	L?		3C337.0	4C+44.28	5-1.4	5	L	
4C+11.45	1318+11	5-1.4	6	I		3C340.0	1627+23	5-1.4	11 5	DPL	2
3C285.0	NRAO422	5-1.4	7	L			1637-77	5-1.4	2	L	
	1323-61	5-0.6	7	D	1.5	3C345.0	4C+39.48	14-.4	7	IC	
3C287.0	1328+254	5-0.4	5	D	2.0	3C346.0	1641+17	8-0.6	3	D	1.3
3C286.0	4C+30.26	14-.4	15	C		3C348.0	HER A	8-0.6	11	DPL	2.5
3C287.1	1330+02	5-1.4	4	L		3C349.0	4C+47.45	5-1.4	4	L	
	1334-33	5-0.6	36	D	1.8	3C352.0	4C+46.34	5-1.4	3	L	
4C-06.35	1335-06	5-0.6	4	D	1.2	3C353.0	1717-00	14-.6	7	DC	2
	1343-60	3-0.6	2	L		4C-02.74	1722-02	5-1.4	4	L	
3C293.0	NRAO433	5-0.6	3	DPH	0.7	3C356.0	4C+51.36	5-1.4	6	L	
3C293.1	1352+16	5-1.4	7	L		3C360	1730-13	5-1.4	4	L	
M13-115	1354-17	5-1.4	4	D	2.0		1732-09	5-1.4	10	L	
4C+19.44	1354+19	5-0.4	8 1	DPHL	1.0		1737-30	5-1.0	2	D	3
M13-405	1355-41	5-1.4	6	L			1737-60	5-1.4	6	L	
	1414+11	5-1.4	14	L		3C371.0	4C+69.24	5-0.4	4	L	
M14-208	1420-27	5-1.4	4	L			1817-64	5-1.4	10	L	
3C300.0	1420+19	5-0.6	2	L			1819-67	5-1.4	9	L	
	1424-41	5-0.6	4	L		3C379.1	4C+74.23	5-1.4	4	L	
4C+03.30	1434+03	5-1.0	3	D	2.0	3C380.0	4C+48.46	14-.4	2	L	
	1437-62	5-1.4	5	L		3C381.0	NRAO568	5-0.6	4	L	
3C303.0	4C+52.33	5-1.4	7	L		3C382.0	CTA 80	5-0.4	2	DPH	1.0
M14-308	1451-36	5-1.4	9	L		3C386.0	1836+17	5-0.6	2	L	
3C306.1	1452-04	5-1.4	11	L		M18-404	1840-40	5-1.4	4	D	2
3C309.1	4C+71.15	5-0.6	2	DPH	1.2	3C388.0	NRAO577	5-0.6	2	D	1.5
3C310.0	1502+26	5-1.0	4	DPL	2.5	3C390.0	1843+09	5-1.4	2	L	
	1508-05	5-1.4	3	L		3C389.0	4C-03.70	5-1.4	2	L	
3C313.0	1508+08	5-1.4	2	L		3C390.3	NRAO582	5-0.6	6	DPH	0.7
	1510-08	5-0.4	5	I		3C396.0	1901+05	5-1.4	1	L	
3C315.0	1511+26	5-1.4	7	L		3C399.1	4C+30.35	5-1.0	15	D?	1.0
4C+00.56	1514+00	5-1.4	8	L			1922-62	5-1.4	10	L	
	1514-24	5-1.4	5	L		M19-111	1938-15	5-1.4	6	L	
3C319.0	4C+54.34	5-1.4	5 3	DPL	2.0	3C403.0	1949+02	5-1.0	6	C	
	1526-42	5-1.0	2	I		M19-507	1954-55	5-0.6	17 2	DPL	2.6
3C321.0	1529+24	5-0.6	10	I		M19-305	1955-35	5-1.4	7	L	
3C323.1	1545+21	5-1.4	7 2	DPL	2	3C409.0	2012+23	5-0.4	2	L	
3C324.0	1547+21	5-0.6	8	C		3C410.0	4C+29.60	3-1.4	3	L	

TABLE 3-5--Continued

SOURCE	ALTERNATE NAME	RANGE (GHZ)	POLS (%)	TYPE	FRQ (GHZ)	SOURCE	ALTERNATE NAME	RANGE (GHZ)	POLS (%)	TYPE	FRQ (GHZ)
3C411.0	2019+09	5-0.6	6 2	DPL	3.0	M21-203	2154-18	5-1.4	7	C	
M20-505	2020-57	5-1.4	6	DPH	1.5	3C441.0	4C+29.65	5-0.6	10	D	1.5
M20-208	2030-23	5-1.4	8	L			2209+08	5-1.4	5	L	
3C415.2	4C+53.46	5-1.4	9	D	1.7	3C442.0	2212+13	5-0.6	10	C	
M20-307	2032-35	5-0.4	7	L		3C445.0	2221-02	5-1.4	8 1	DPL	2.0
3C418.0	4C+51.42	5-1.4	2	L		3C446	2223-05	5-0.4	5	DPH	1.0
M20-212	2040-26	5-1.4	7	L		3C449.0	NRAO692	5-1.4	7	D	1.5
NRAO639	2044-02	5-1.4	1	L		CTA 102	2230+11	5-0.4	7	D	1.0
3C424.0	2045+06	5-1.4	4	L		3C452.0		5-0.6	10	D	1.5
	2052-47	5-1.4	5	L			2247+11	5-1.4	10 4	DPL	2.0
M20-214	2053-20	5-1.4	1	L		3C454.0	2249+18	5-0.6	10	D	1.5
M20-215	2058-28	5-1.6	2	L		M22-406	2250-41	5-1.4	4	D	1.5
3C428.0	4C+49.36	5-1.4	12	D	2	3C454.3	2251+15	14-.4	7	C	
M21-203	2113-21	5-1.4	12	L		3C455.0	2252+12	5-1.4	2	L	
	2115-30	5-0.6	6	DPH	1.0	M22-504	2252-53	5-1.4	4	DPH?	1.5
3C430.0		3-0.6	4	DPH	0.8		2253-52	5-1.4	5	D	2.0
3C433.0	2121+24	5-0.4	7	DPH	0.9	3C458.0	2310+05	5-1.4	4	L	
3C435.0	2126+07	5-0.6	5	D	3	3C459.0	2313+03	5-0.4	3	DPH	0.6
PHL1657	2135-14	5-1.4	11	L			2317-27	5-1.4	17	L	
M21-407	2140-43	5-1.4	8	D	1.5	3C460.0	2318+23	5-1.4	2	L	
3C436.0	NRAO665	5-1.4	7	L			2338-58	5-1.4	3	L	
3C437.0	2144+15	5-1.4	7	L?		4C+09.74	2344+09	5-0.4	4	C	
4C+06.69	2145+06	14-.6	1	L		3C468.1	4C+64.25	5-1.4	1	L	
NRAO668	2148+14	5-1.4	3	L		3C469.1	4C+79.23	5-1.4	7	L	
	2149-28	5-1.4	5	L		3C470.0	4C+43.59	5-1.4	13	L	
M21-208	2150-52	5-1.4	1	L			2356-61	5-0.6	7	DPH	1.0
	2152-69	5-0.4	4 1	DPHL	1.0						

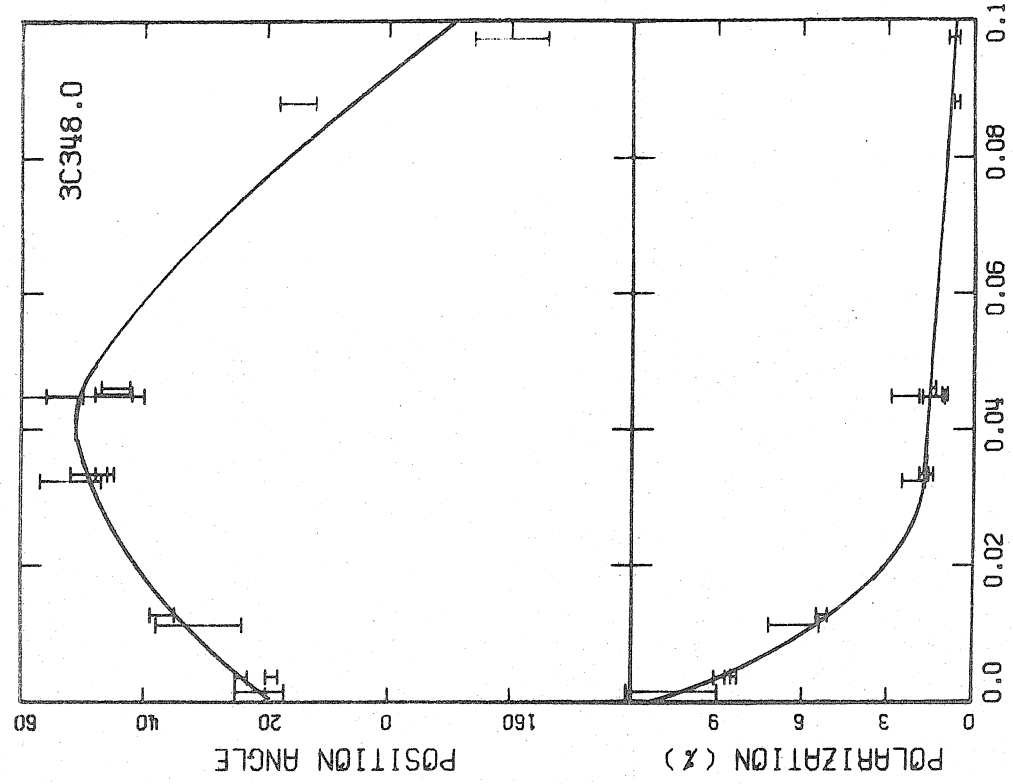

Fig. 3-3.--Polarization of 3C348. The depolarization classification for this source is 'DPL' because of the low plateau in polarization.

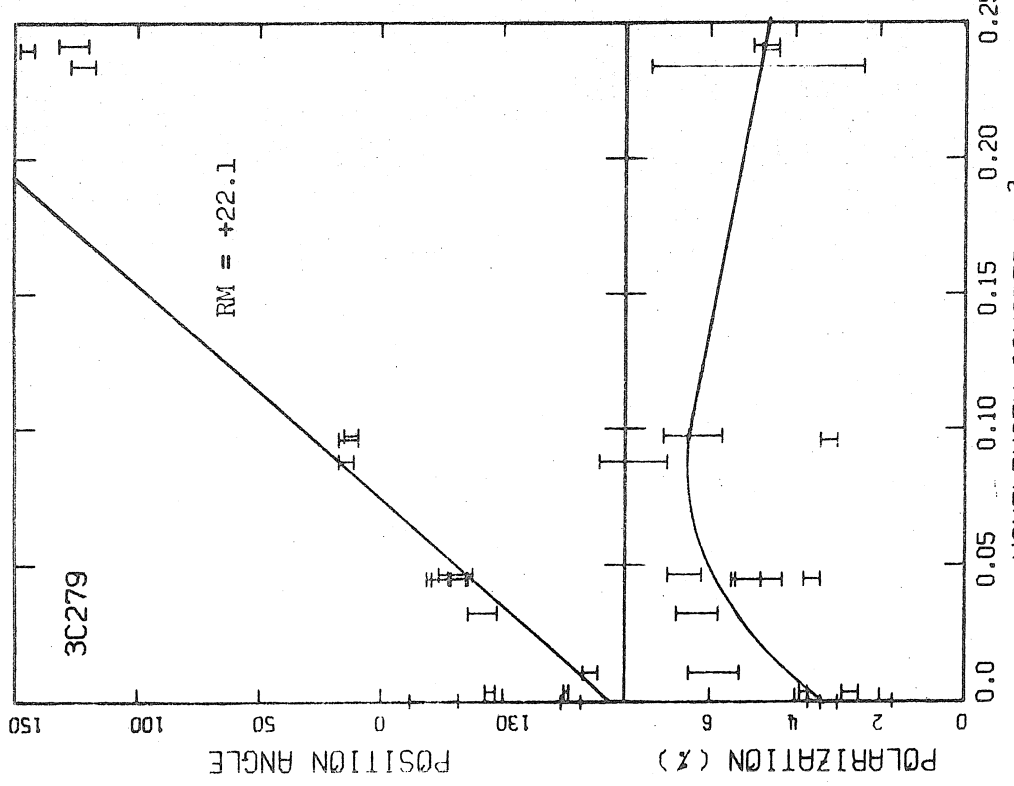

Fig. 3-2.--Wavelength dependence of polarization of 3C279. Note scatter, probably indicating variability and extreme complexity.

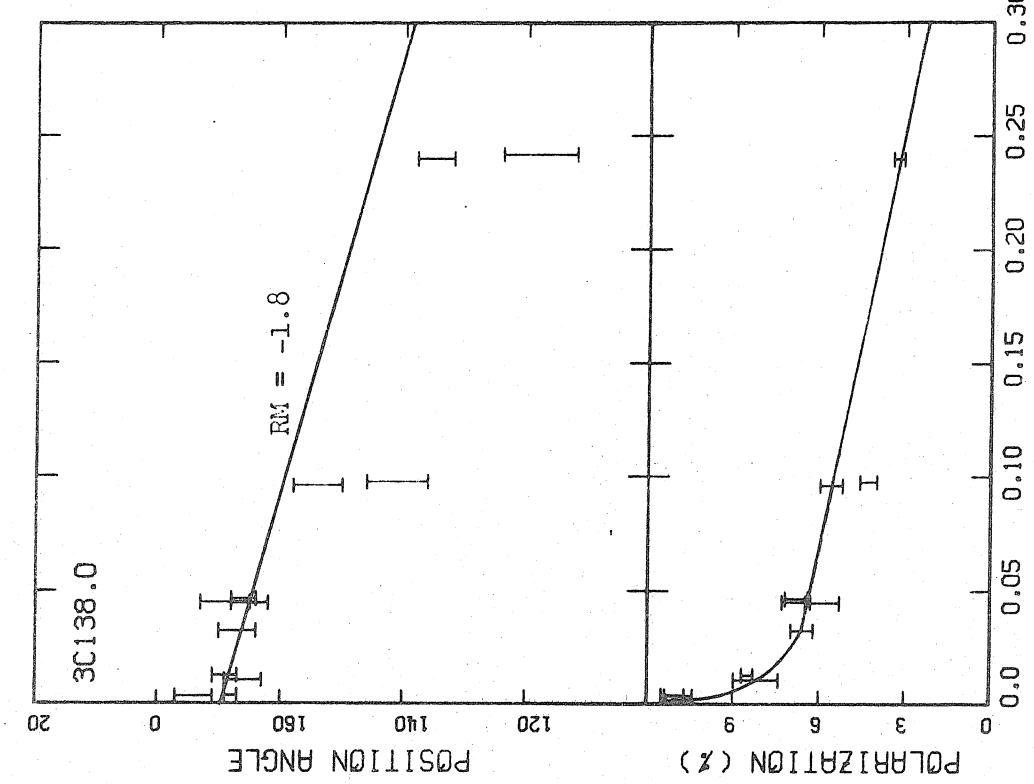

Fig. 3-5.--Polarization of 3C138.0 showing a simple depolarization ('D') profile.

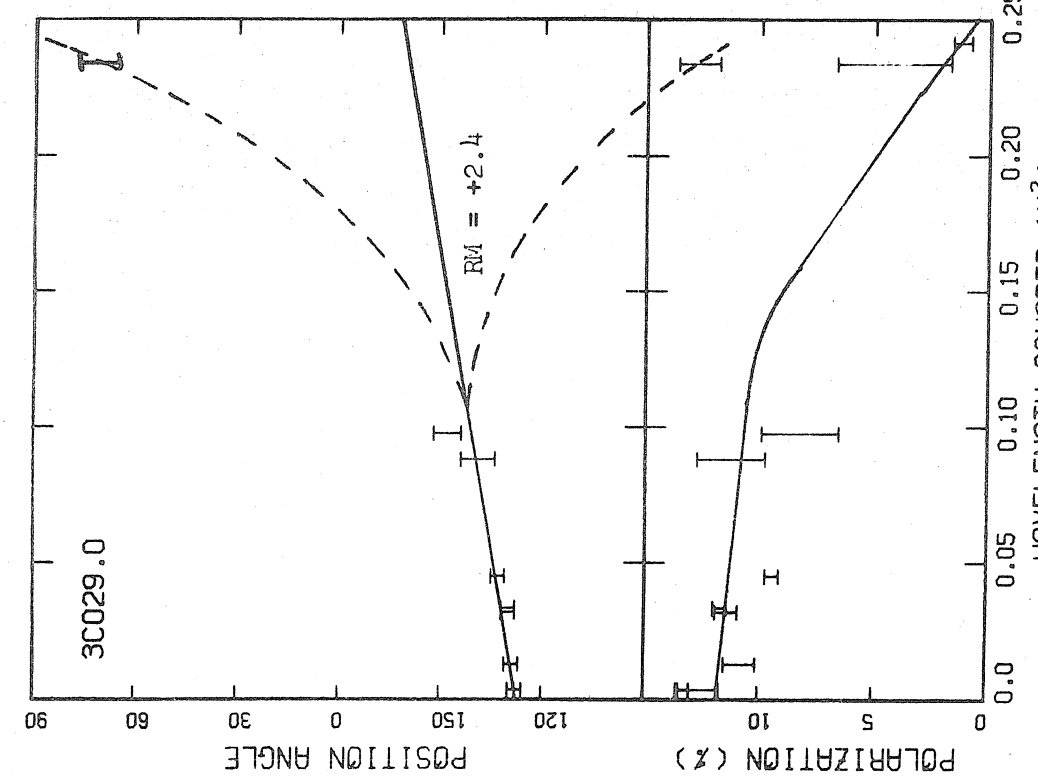

Fig. 3-4.--Polarization of 3C029.0. The broken lines indicate possible position angle curves. The source is classified "DPH" due to the high plateau.

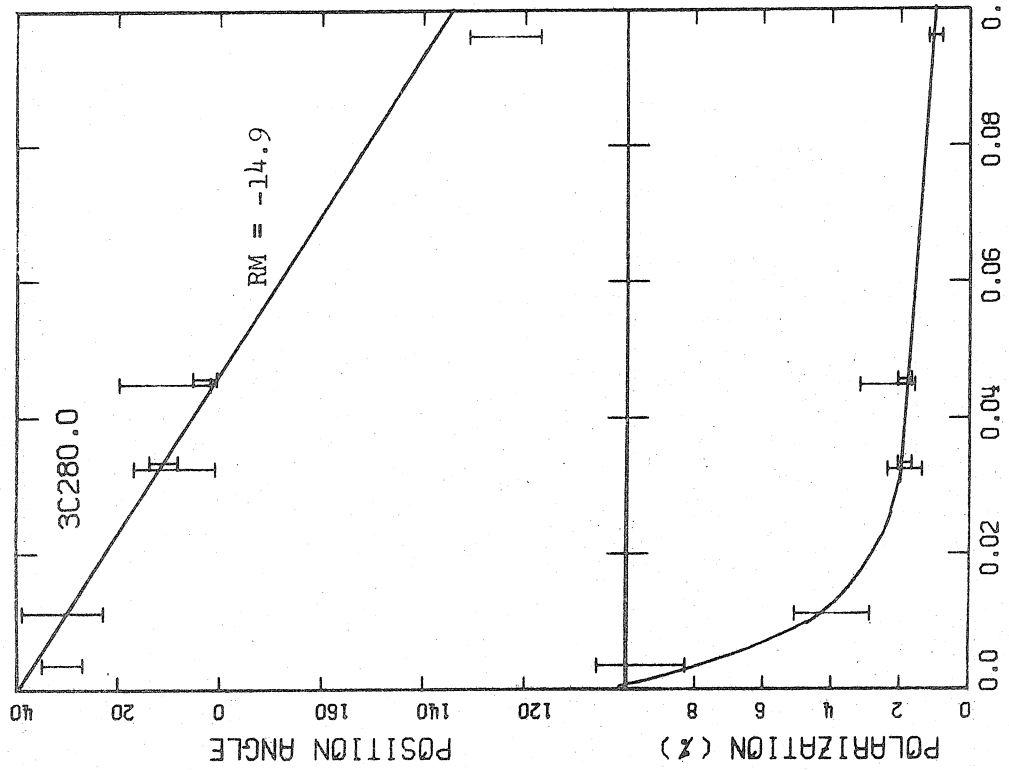

Fig. 3-7.--Polarization of 3C280.0. The low plateau gives rise to the depolarization classification 'DPL'.

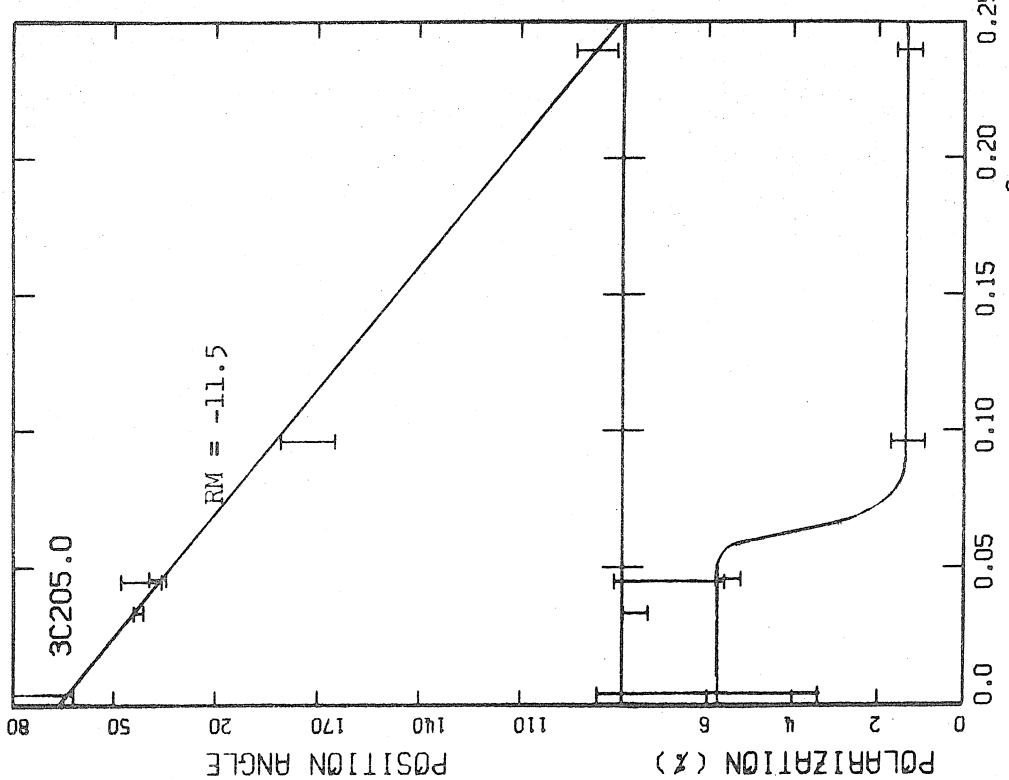

Fig. 3-6.--Polarization of 3C205.0. Both high and low plateaus are possible, and the depolarization classification is 'DPHL'.

CHAPTER IV

INTERPRETATIONS OF THE ROTATION MEASURES

A. The Galactic Magnetic Field and the Rotation Measures

The distribution of the absolute values of the rotation measures with respect to galactic latitude is shown in Figures 4-1 and 4-2 for various combinations of the rotation measure quality codes discussed in the preceding chapter. The progression of the figures is such that increasing numbers of less certain rotation measures are included. The curve in each figure is given by $|RM| = 10 + 18|\cot b|$, rad/m^2, and is the outer envelope for all rotation measures obtained from a model in which the sun is at the center of a uniform disk of electrons with a linear magnetic field in the plane of the disk. It also assumes that the intrinsic Faraday rotation for extragalactic sources is limited to 10 rad/m^2. The particular parameters used here are those for a model for which $DBn = 4.5 \times 10^{-5}$, where D is the thickness of the disk in parsecs, B is the field strength in gauss, and n is the electron density in cm^{-3}. For example, taking D = 200 pc and n = 0.06 cm^{-3} yields a magnetic field strength of 3.7 μgauss, all within acceptable ranges (Spitzer, 1968). These parameters have not been derived from the rotation measures of Chapter III, and the envelope lines are included only to show certain suggestive behavior of the data.

Several facts are evident from the various distributions represented

by Figures 4-1 and 4-2. First, there is clearly a strong dependence of the observed rotation measure upon galactic latitude; in general, the absolute value of the rotation measure decreases with increasing galactic latitude. There are, however, some rather strong exceptions to this. The arrows at the tops of the four figures indicate sources with rotation measures larger than 200 rad/m^2; even for the code six observations there are some of these sources found at moderate to high galactic latitudes, although the great majority of sources have rotation measures lying below the envelope. The distribution of the values of the rotation measures is far from gaussian whether plotted for all sources or for those in certain ranges of galactic latitude. Figure 3-1 on page 90 shows this distribution for all code six sources and indicates a narrow central peak with an extended tail and individual sources with rotation measures 10 to 20 times the width of the central region. The markedly non-gaussian behavior of this distribution is evident for all quality codes and for all regions of the sky. Since the wildly discrepant sources are more-or-less evenly distributed among the sources with the lower values, as can be seen in Figures 4-3, 4-4, and 4-5, no simple model with only a few parameters can be made to fit the entire collection of rotation measures with any substantial degree of significance. Clearly some editing procedure will be necessary so that the core and wings of this distribution may be treated separately. This procedure will occupy a considerable portion of this chapter.

The second fact which can be observed from Figures 4-1 and 4-2 is that sources at negative galactic latitudes tend to have somewhat greater

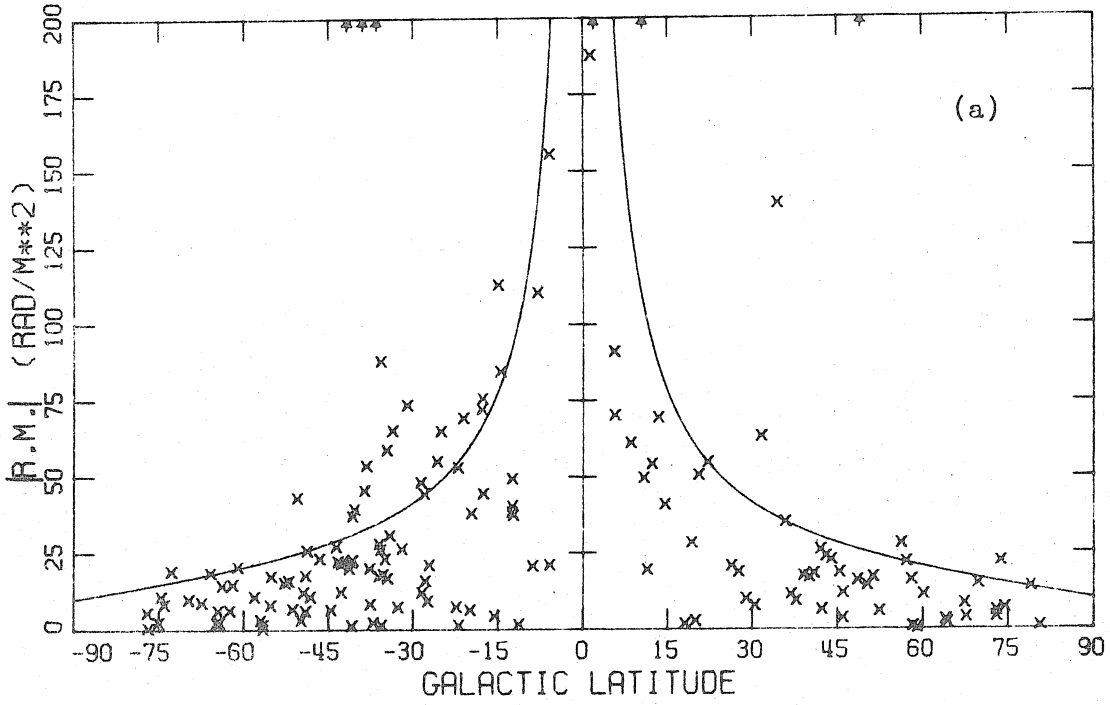

Fig. 4-1(a).--Distribution of the code 6 rotation measures with respect to galactic latitude.

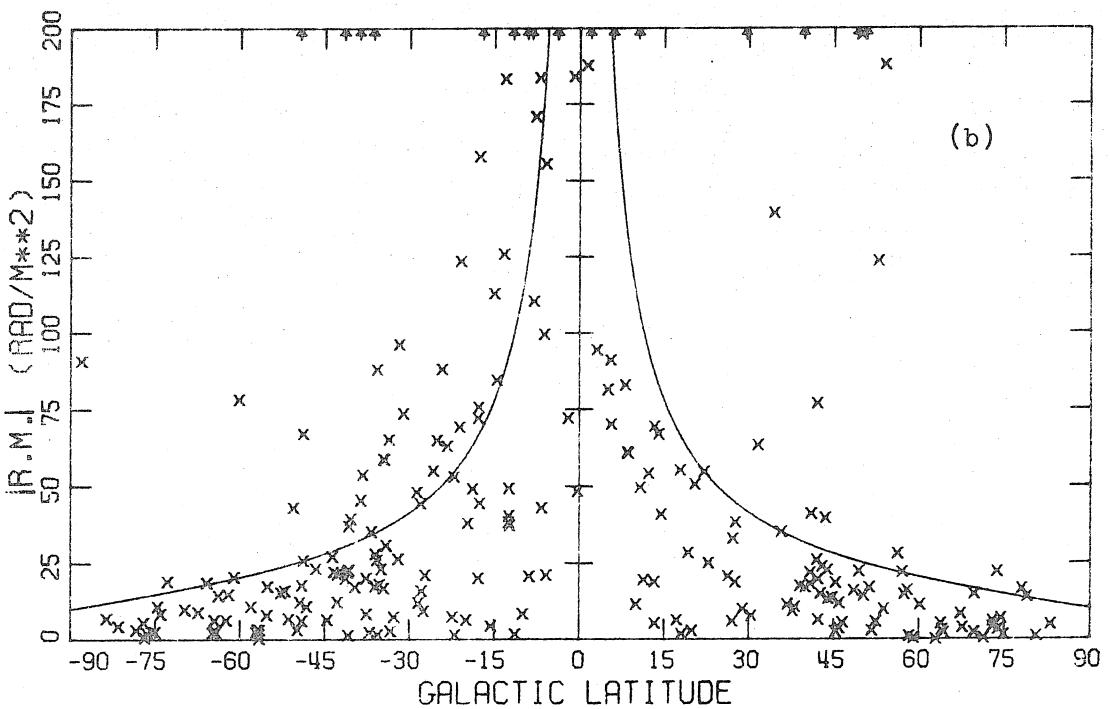

Fig. 4-1(b).--Distribution of rotation measures with quality codes 5 and 6. The arrows at the top of the figure indicate rotation measures in excess of 200 rad/m^2.

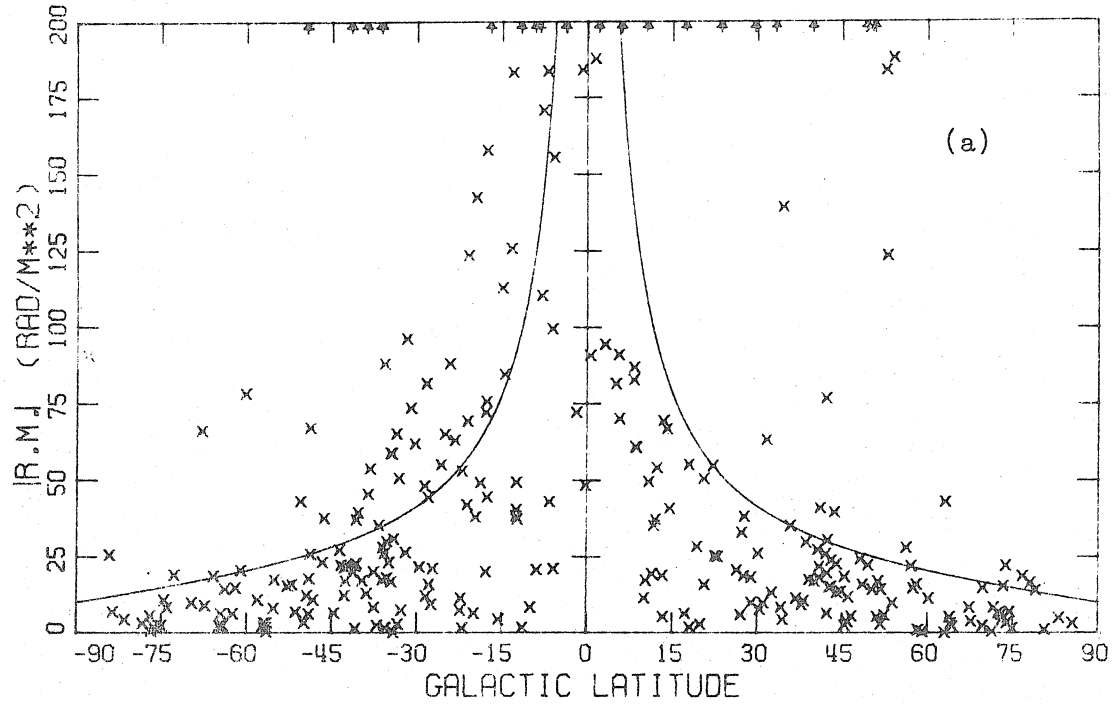

Fig. 4-2(a).--Galactic latitude distribution of the rotation measures with quality codes 3, 5, and 6.

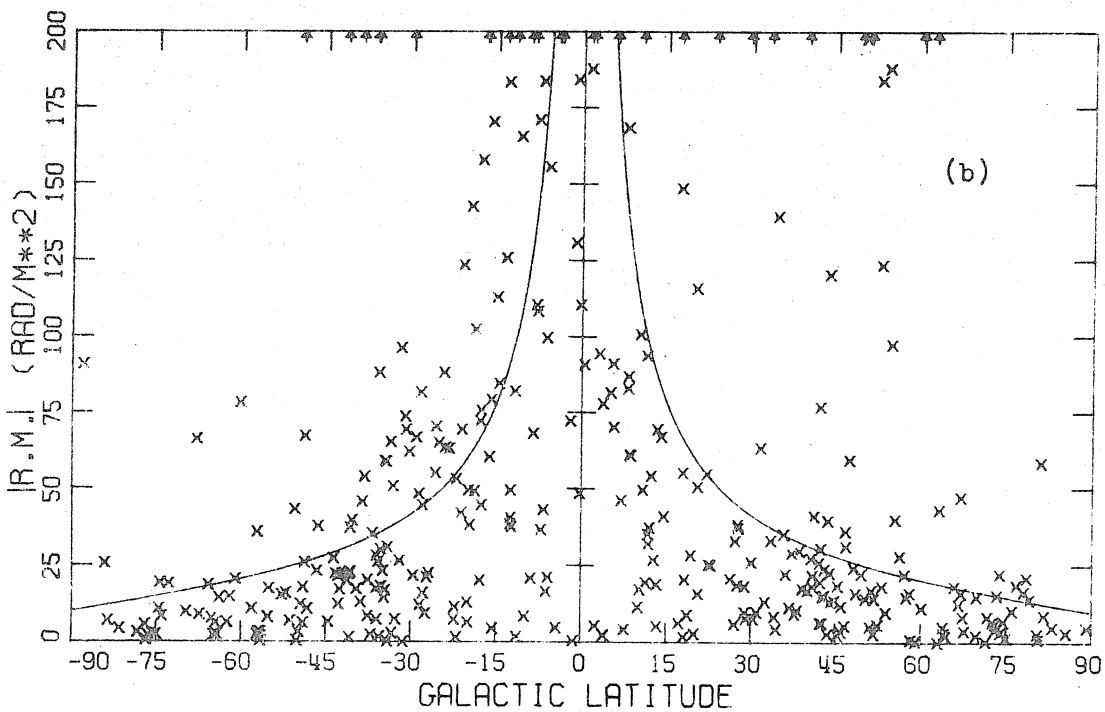

Fig. 4-2(b).--Galactic latitude distribution of the rotation measures with quality codes 1, 2, 3, 4, 5 and 6.

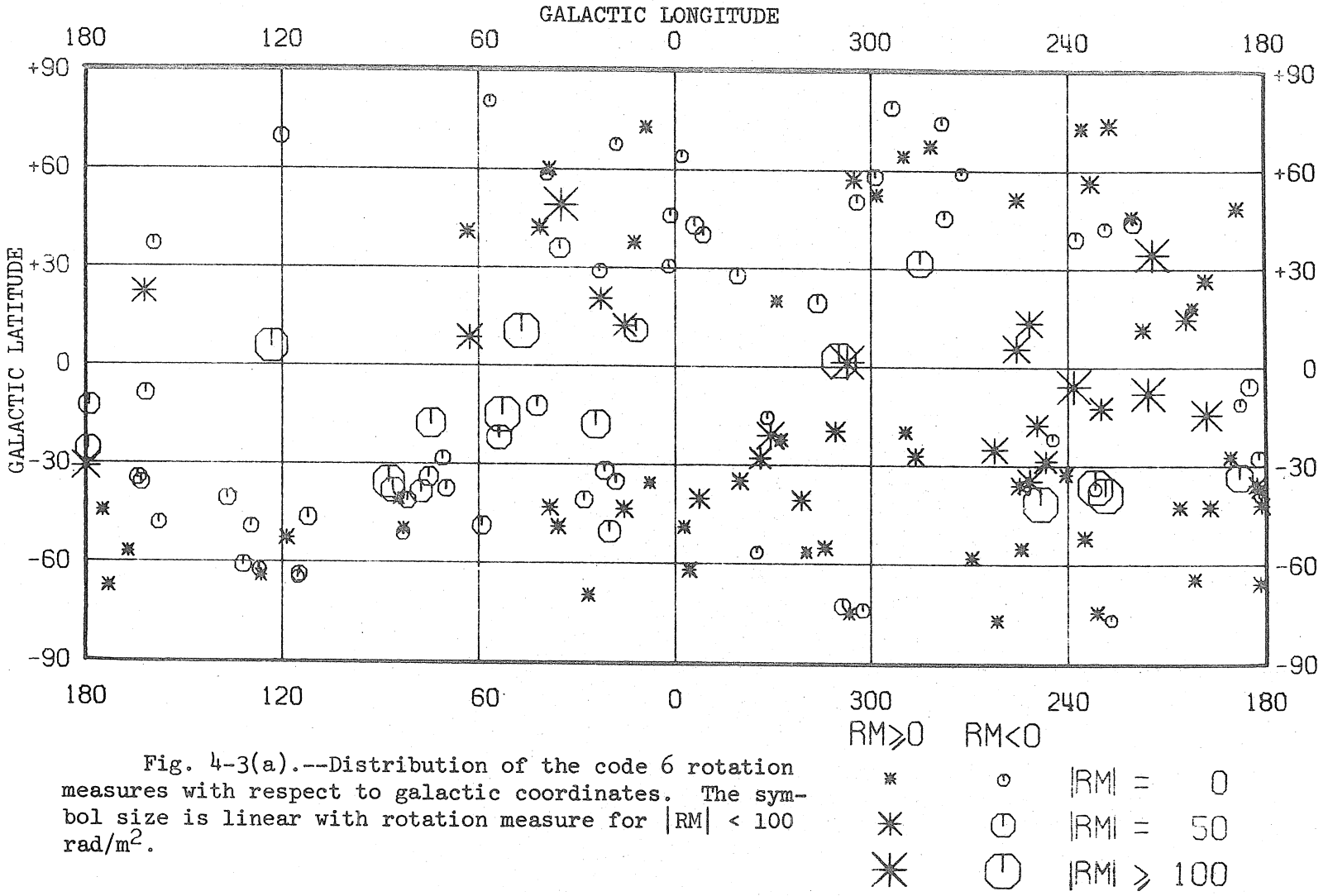

Fig. 4-3(a).--Distribution of the code 6 rotation measures with respect to galactic coordinates. The symbol size is linear with rotation measure for $|RM| < 100$ rad/m^2.

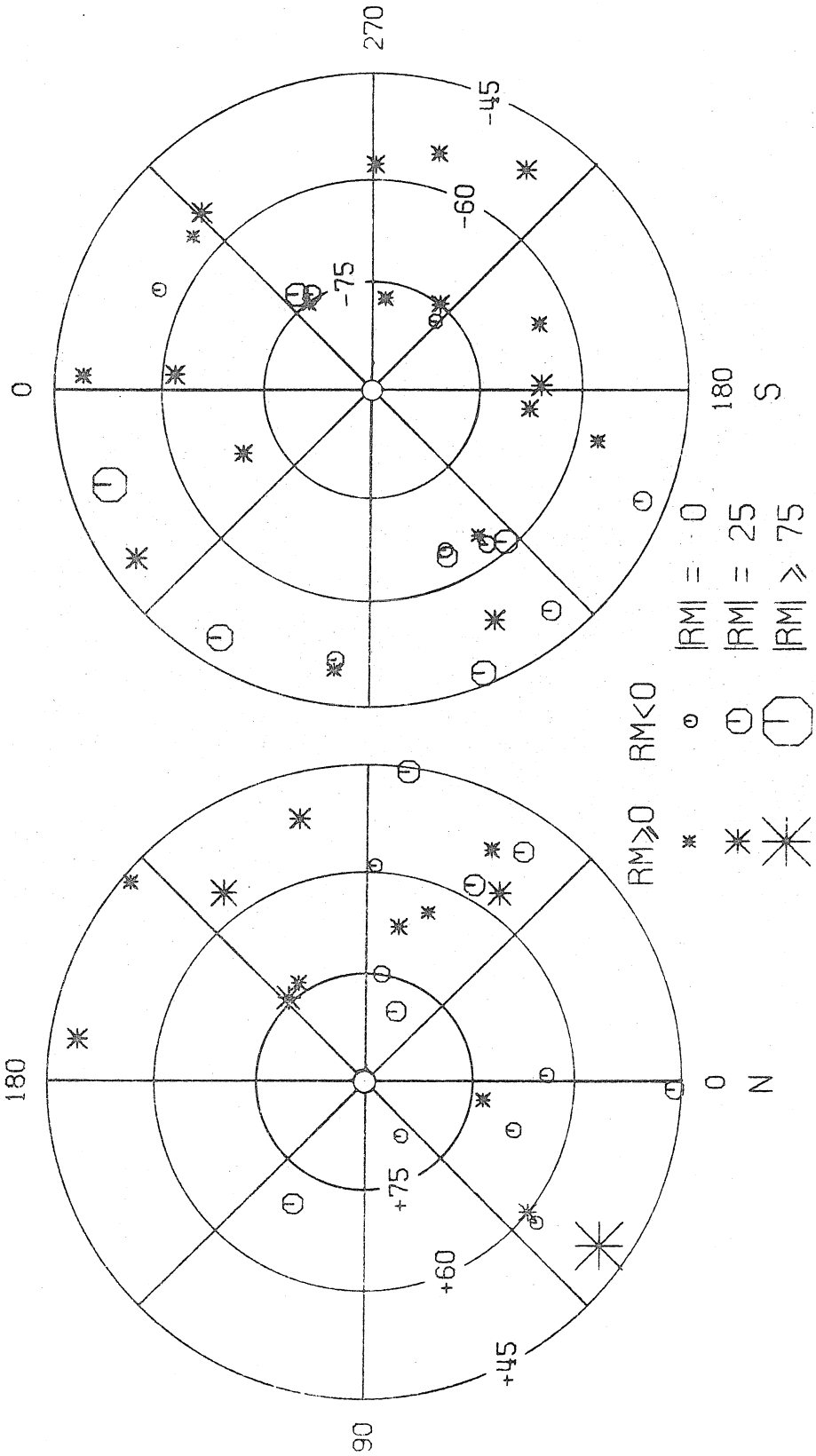

Fig. 4-3(b).--Distribution of the code 6 rotation measures near the galactic poles.

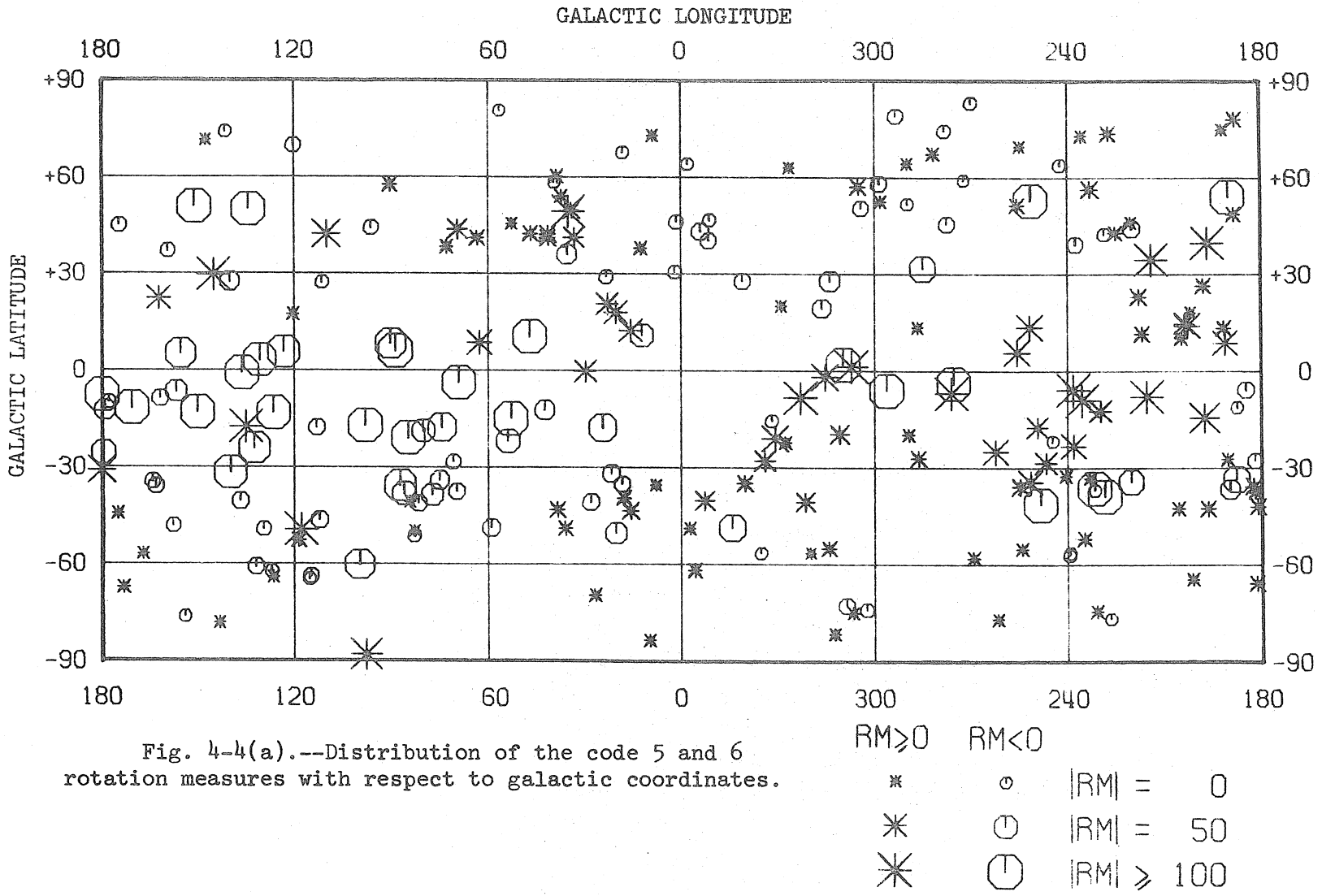

Fig. 4-4(a).--Distribution of the code 5 and 6 rotation measures with respect to galactic coordinates.

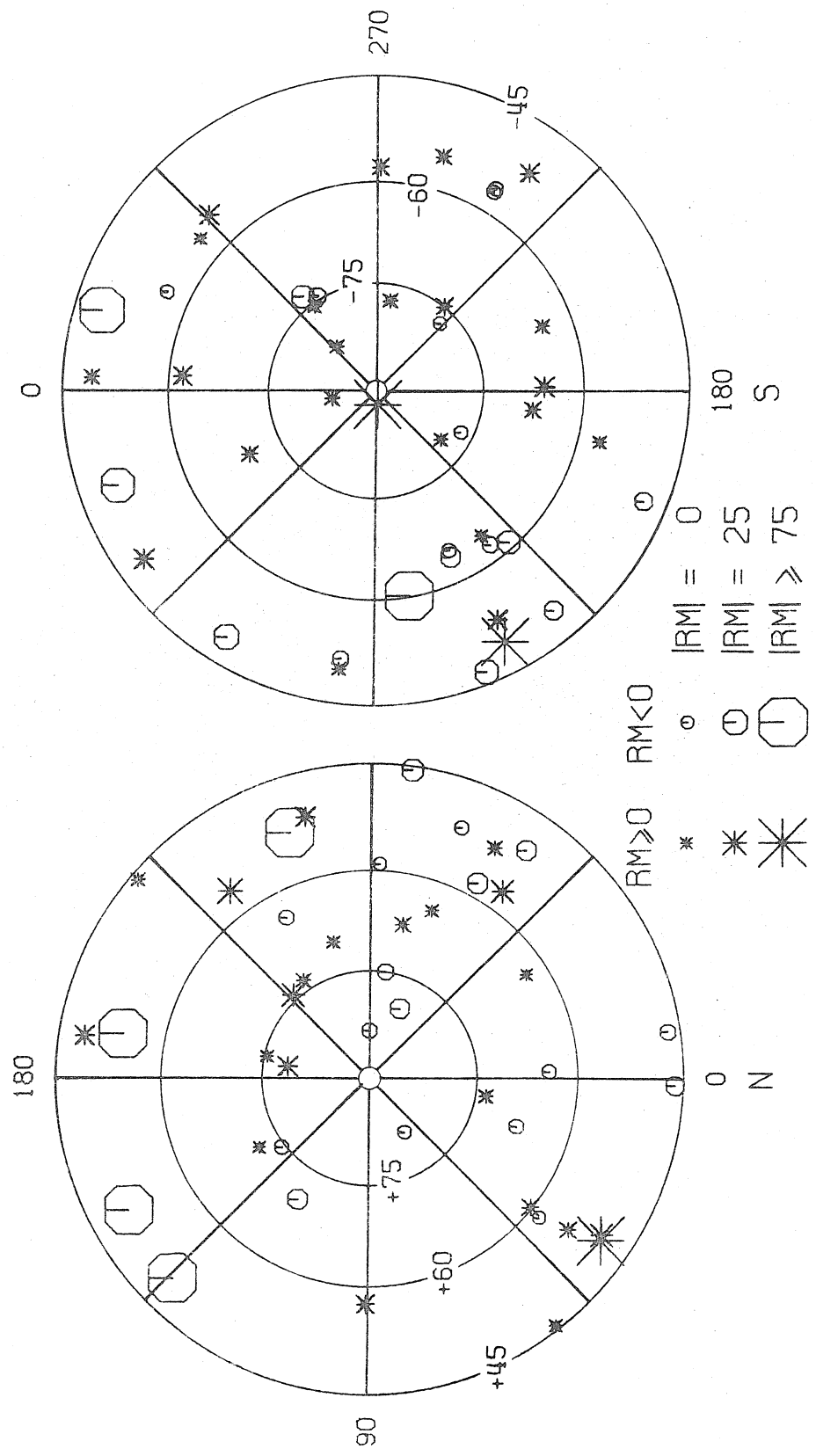

Fig. 4-4(b).--Polar distributions of the code 5 and 6 rotation measures.

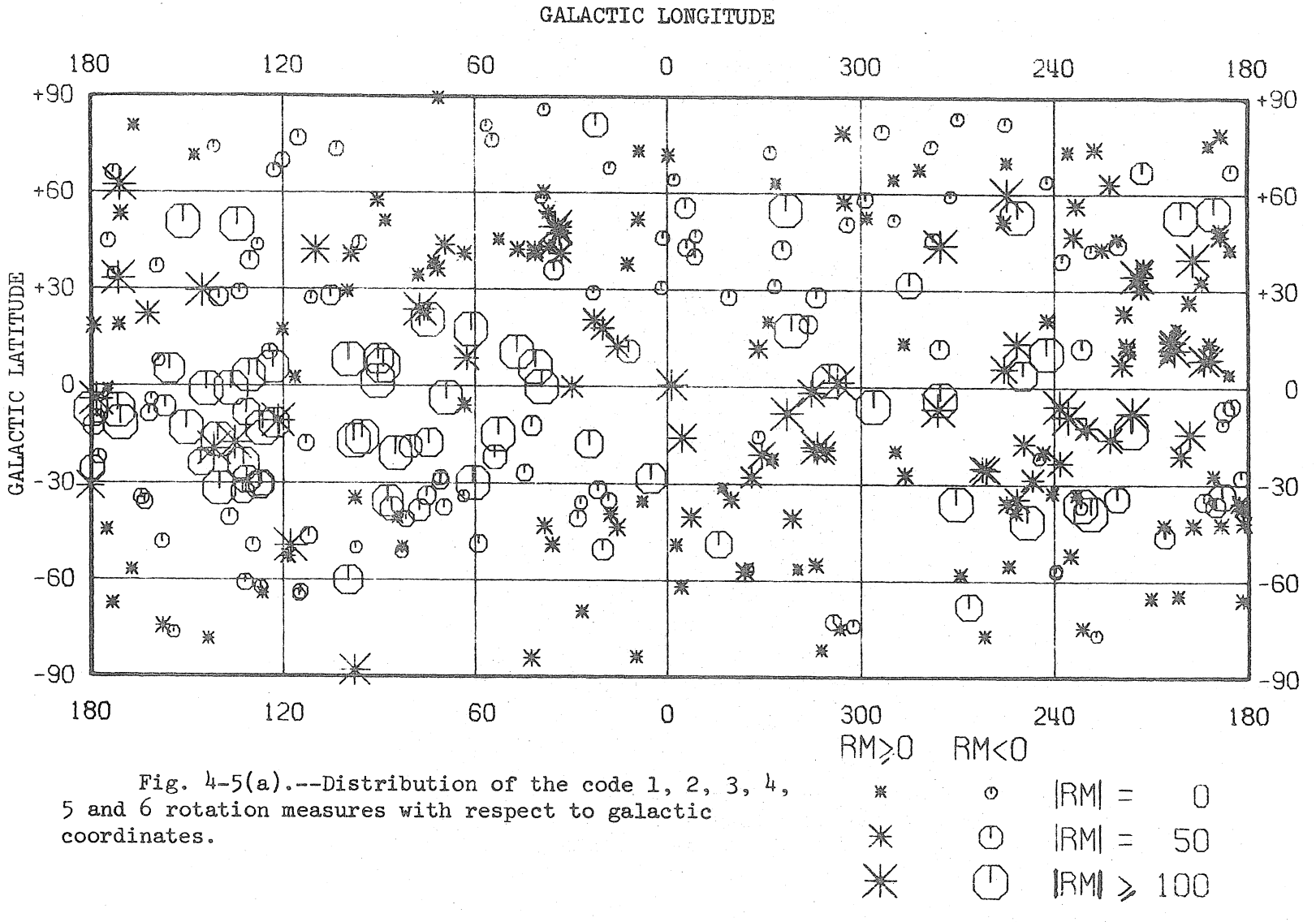

Fig. 4-5(a).--Distribution of the code 1, 2, 3, 4, 5 and 6 rotation measures with respect to galactic coordinates.

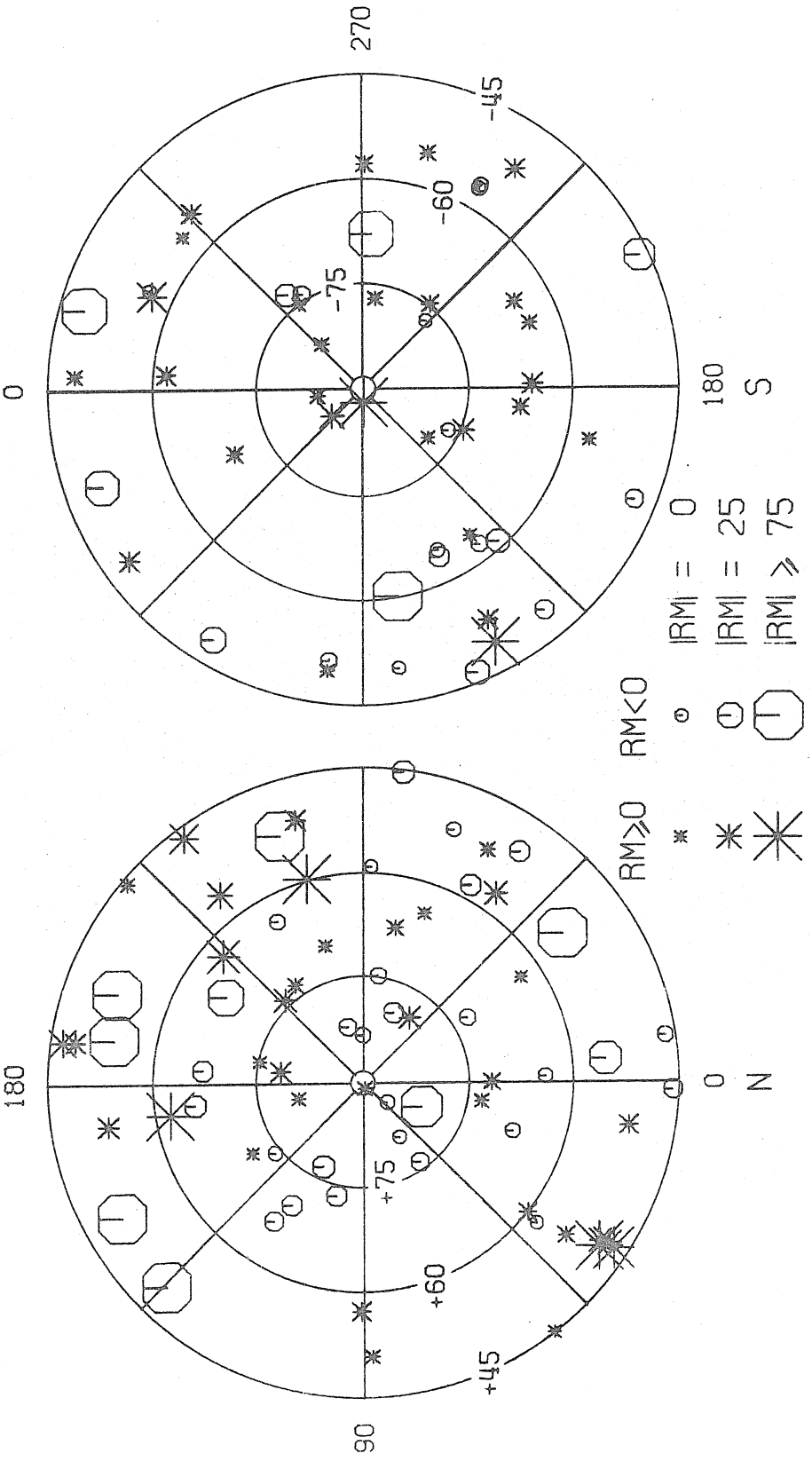

Fig. 4-5(b).--Polar distribution of the code 1, 2, 3, 4, 5 and 6 rotation measures.

rotation measures. This is most apparent as a bulge in the data between -10° and -45°. This anomaly is evident in all four distributions and must certainly be accounted for by any tenable model.

Figures 4-3 through 4-5 depict the distributions of the observed rotation measures with respect to galactic coordinates. These distributions again indicate the decrease in rotation measure toward high galactic latitudes and show that rotation measures to the south of the equator are somewhat larger than those to the north, as mentioned above. Another striking feature is the clustering of negative rotation measures near the equator for $30^\circ < l < 180^\circ$ and the not-quite-so-convincing clustering of positive values for $180^\circ < l < 330^\circ$. The negative cluster is not apparent on the code six plot (Figure 4-3) since code six data are few in this region. Most of the information in this area is due to the present work and based upon only three frequencies, ruling out code six qualities.

All of these distributions strongly suggest the following model for the rotation measures: Faraday rotation is largely caused by the electrons and magnetic field of the galaxy. Intrinsic rotation measures are generally quite small, although a few sources may have intrinsic Faraday rotation of a few hundred rad/m^2. (At this point "intrinsic Faraday rotation" refers to any rotation occurring outside the galaxy. The question of intergalactic Faraday rotation will be dealt with later. An alternative to intrinsic rotation is the possibility of concentrations of a high degree in the galactic electrons or field. This possibility will be discussed after the present model is developed.) The model

represents the local regions of the galaxy by a disk with uniform electron density and with a uniform magnetic field, not necessarily parallel to the plane. The sun is located along the axis of the disk although not necessarily midway between the faces. The radius of the disk is taken to be about 10 times the thickness so that sources below ±3° galactic latitude are deleted. There are very few such sources so that the effect is not large.

The rotation measure due to such a model can be computed as a function of galactic coordinates and is given by

$$RM = \begin{cases} -(1-\alpha)\ C \cos\theta \csc|b| & b \geq 0 \\ -(1+\alpha)\ C \cos\theta \csc|b| & b < 0 \end{cases} \qquad (4\text{-}1)$$

where $\alpha D/2$ is the distance of the sun above the midplane of the disk. The larger rotation measures at negative galactic latitudes can then be explained with positive α. The angle between source and field directions, θ, contains the two parameters, l_B and b_B, the coordinates of the field direction. The constant C is given by $4.06 \times 10^5\ nD|B|$ where n is the electron density in cm^{-3}; B, the field strength in gauss; and D, the thickness of the disk in pc.

As a preliminary step all the data, without any editing, were examined for correlations with this model. Since the distribution of the code six sources is far from uniform, all code 3, 5 and 6 sources were used as the sample. Equation 4-1 was used as a linear recursion relation. The galactic longitude of the field direction was varied at ten degree intervals; the galactic latitude of the field direction, also at ten

throughout the entire range of 90° to -90°; and α was varied from -1.0 to +1.0. The maximum correlation coefficient was +0.209 for the sample of 279 sources. The probability of a random sample of 279 sources having a coefficient this high was well under 0.1%. The values of the parameters giving the highest correlation were C = 10.11, α = 0.33, l_B = 100°, and b_B = -60°. To repeat, this was based on <u>all</u> of the most trustworthy data with no selection on the basis of magnitude of the rotation measure. Attempts to derive uncertainties for the parameters met with failure at this point, primarily due to the very unusual distribution of the magnitudes of the rotation measures as discussed above. The few very high rotation measure sources affect the model very strongly and make all the parameters very uncertain. The one affected the worst is b_B, the latitude of the field direction. The model is not very sensitive to the vertical component of the magnetic field since the disk is postulated to be so thin. Any source at high galactic latitude with an unduly large rotation measure can affect the field latitude very strongly. Even after all the editing procedures the field latitude was still quite poorly determined relative to the other parameters.

The first procedure adopted to remove the tail of the rotation measure distribution was fairly simple. First, all sources with rotation measures in excess of 200 rad/m^2 were eliminated. Then, on the basis of Figures 4-1 and 4-2, sources with $|RM| > 100$ rad/m^2 and $|b| > 30°$ and those with $|RM| > 50$ rad/m^2 and $|b| > 60°$ were eliminated. As before, known galactic sources and sources with $|b| < 3°$ were discarded. The same correlation program was run on this reduced sample, which still con-

tained 250 sources. The parameters were not greatly changed: C = 10.00, $\alpha = +0.20$, $l_B = 100°$ and $b_B = -30°$. As would be expected, the correlation was very greatly improved with r = 0.528 for the 250 sources. This provided encouragement for a more sophisticated editing of the data. Based on these parameters, the residuals were calculated for all sources. When the distribution of these residuals was examined, it was found to be similar to the original rotation measure distribution with the exception that the central peak was somewhat narrower. The postulate that two populations of sources existed was made. One population, consisting of those in the narrow peak with small residuals, included the sources with small intrinisic rotations and which fit the model. The other population included a few sources with residuals of up to 25 times the r.m.s of the central peak and comprised those with high intrinsic rotation measures. Since 90% of the sources lay within the central peak, the division seemed very clear-cut. Further correlations and parameter determinations were based on the 95%, 90%, 80% or 70% of the sources with the smallest residuals--presumably the population one sources. The determinations at the 90%, 80% and 70% levels all agreed within computed levels of uncertainty, but the 95% sample departed and demonstrated the same large uncertainties in the parameters since not all population two sources had been eliminated. All those sources eliminated by the first means (those with $|RM| > 200$ rad/m^2, etc.) were among those eliminated by the time the 80% level was reached. This method of removing the high intrinsic rotation sources is superior to the first since it also eliminates the source with a low RM in a region where the model predicts

a high one, whereas the first does not. The intrinsic rotation measure could easily be of opposite sign and sufficient magnitude to cancel the galactic rotation and produce a low net rotation measure which would not be eliminated by the first method.

Before the detailed analysis of the model is described, the reasons for the elaborate editing of the data should be summarized. First, the distribution of the rotation measures is such that there is a central core containing most of the sources with exceptionally broad wings containing the remaining 10%. Since the basic form of this distribution holds in any direction of the sky, no simple magnetic field model with few parameters can possibly suffice to explain the behavior. Therefore any attempt to fit the narrow core with some sort of uniform model requires that the wings be deleted. The editing method used here seems to be valid since the final answers obtained are not really very different from those obtained for all sources, and since only 10% of the sources have to be eliminated before the solution becomes independent of the number of sources deleted. Apparently only 10% of the sources show the very discrepant rotation measures. These sources will be considered as a class shortly.

Based on the 70% sample of 198 sources, a least-squares fit yields $C = 9.49 \pm 0.13$, $\alpha = +0.31 \pm 0.03$, $l_B = 94° \pm 3°$ and $b_B = -8° \pm 8°$. The correlation coefficient was now increased to 0.661 for the 198 sources; and, as described above, the larger 80% and 90% samples provided essentially the same results. These parameters, with the exception of b_B, are quite similar to those obtained for the entire sample of 279 sources. To

repeat an important point, the model is not very sensitive to b_B, or the vertical component of the magnetic field. The r.m.s. deviation of the 198 sources for the parameters given was about 16.8 rad/m^2. In comparison, the lowest 70% of the rotation measures have an r.m.s value of 20.0 rad/m^2. The reduction of this number to 16.8 with a model employing only four parameters with a sample of 200 measurements illustrates that the significance of the fit is quite high. For these reasons the existence of a linear, uniform component of the local galactic magnetic field is well-established. Such a uniform field and uniform electron distribution are not sufficient to explain galactic Faraday rotation completely as can be observed by examining the detailed distribution of the residuals obtained from the model.

Figure 4-6 shows all 279 rotation measures for quality codes 3, 5 and 6. The contour lines are for the rotation measures predicted by the model with the final set of parameters. On the basis of the model, all sources lying below the zero-contour should have negative rotation measures while those lying above it should have positive values. This is clearly not the case. Figure 4-7 displays the distributions of the residuals for the 198 (70%) of the sources which fit the model best, and Figure 4-8 shows the 30% highest residuals. It should be pointed out that 70% of the sources have residuals less than 38 rad/m^2. Several observations can be made about these distributions. First, there are some large-scale regions which seem to have residuals with consistent signs. In particular, the region $30° < l < 90°$, $+30° < b < +60°$ has consistently positive rotation measures and residuals, suggesting a field

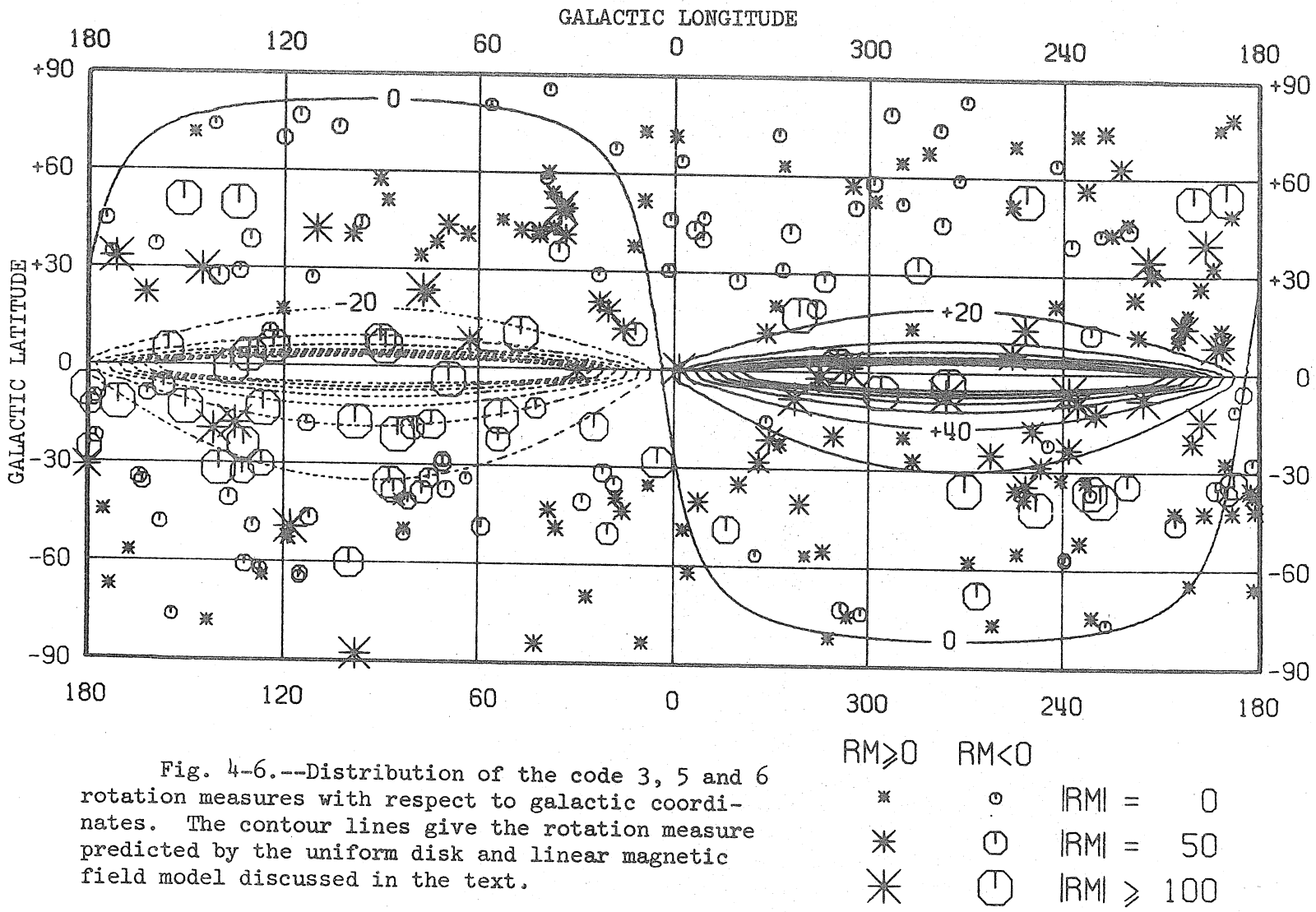

Fig. 4-6.--Distribution of the code 3, 5 and 6 rotation measures with respect to galactic coordinates. The contour lines give the rotation measure predicted by the uniform disk and linear magnetic field model discussed in the text.

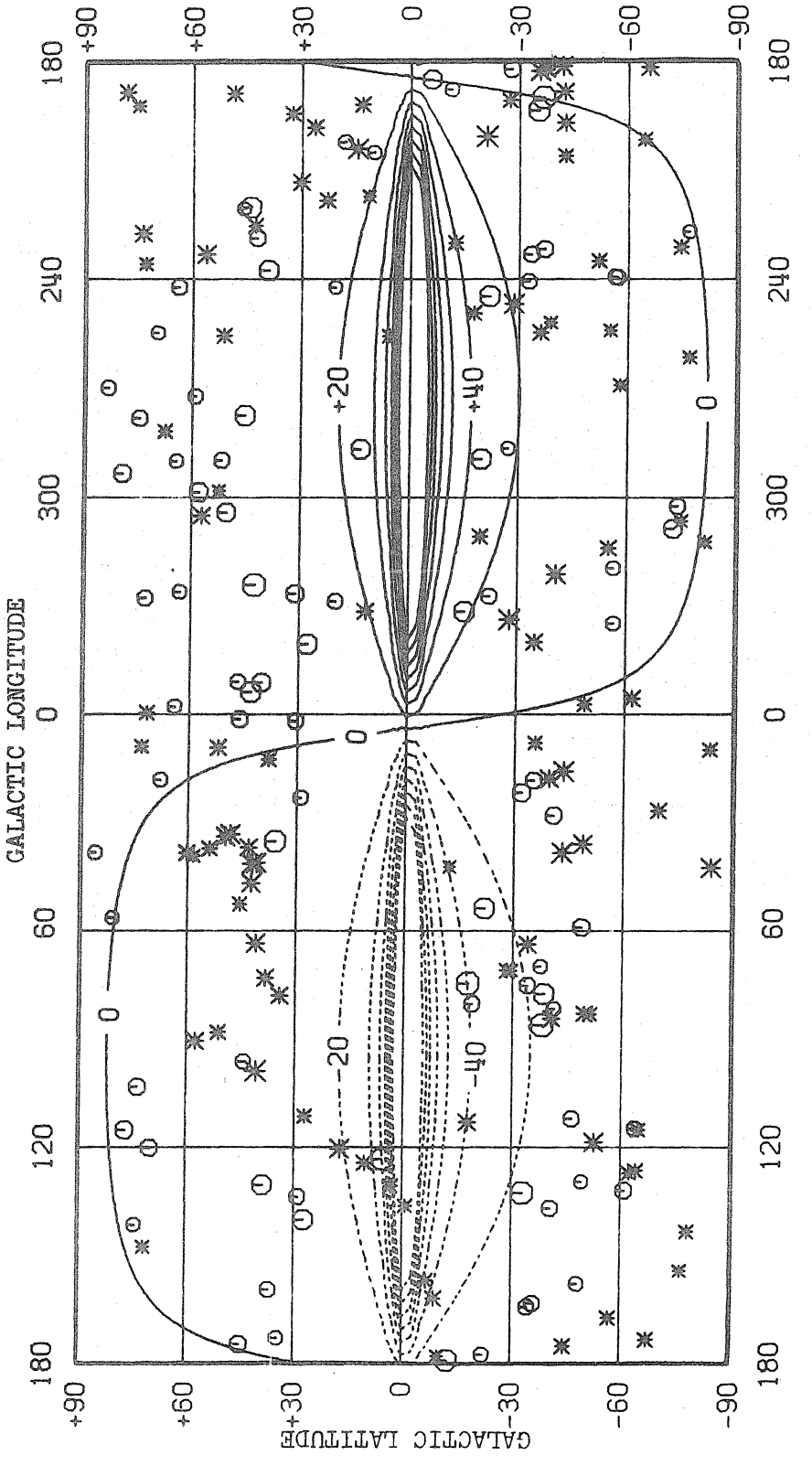

Fig. 4-7.--Distribution of the residuals of the 70% code 3, 5 and 6 sources which fit the model best. The contour lines give the predicted rotation measures. The contour interval is 20 rad/m^2.

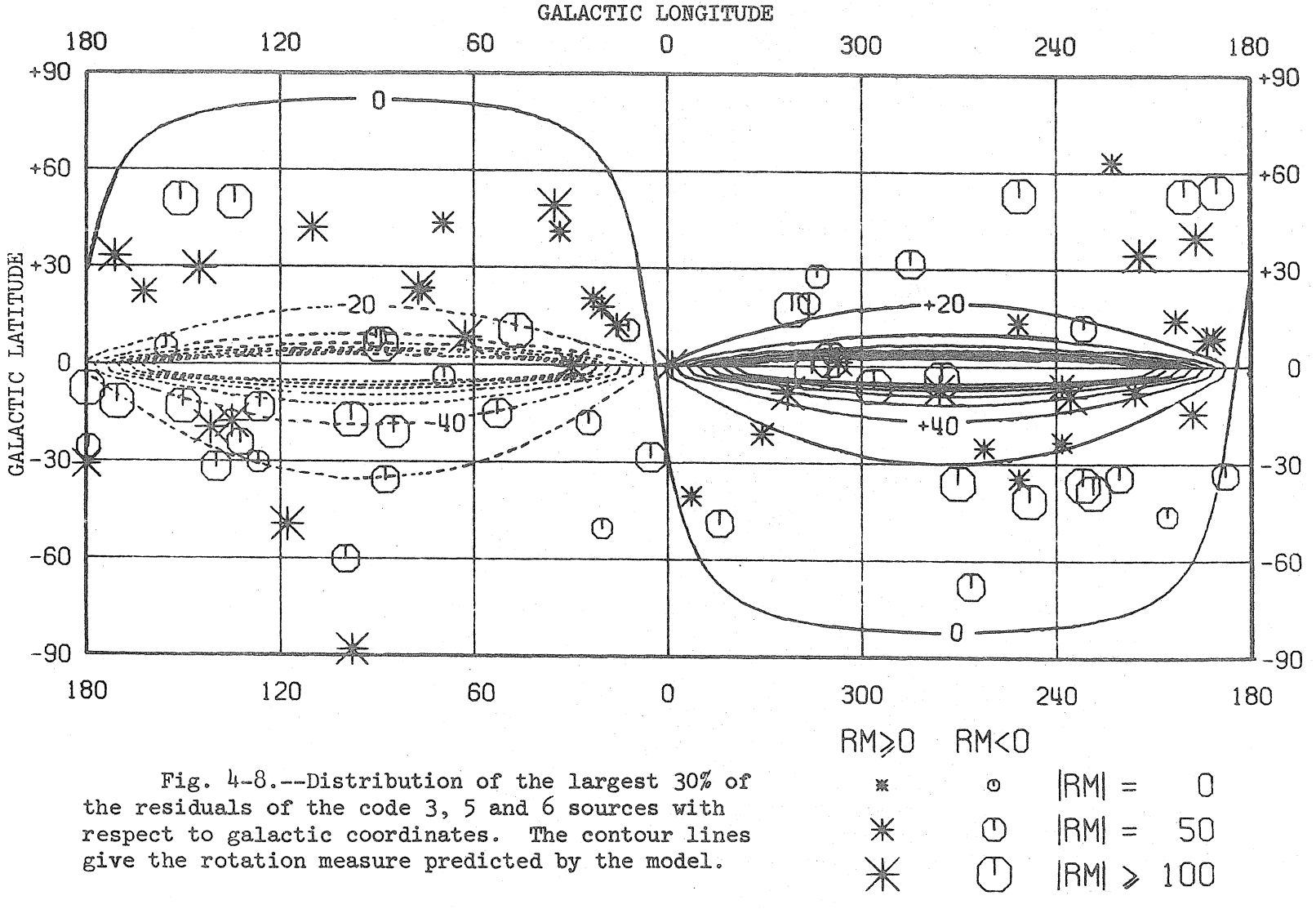

Fig. 4-8.--Distribution of the largest 30% of the residuals of the code 3, 5 and 6 sources with respect to galactic coordinates. The contour lines give the rotation measure predicted by the model.

reversal since rotations should be negative on the basis of the model. The region $240° < l < 30°$, $+30° < b < +60°$ shows a reversal of the opposite sense. These anomalies may be explained by either a loop in the field as suggested by Gardner, Morris and Whiteoak (1969b) or by a region above the plane where the general field is in the opposite direction. The former has particular appeal in the first region mentioned, which includes the north galactic spur. The second explanation can hold true only in the immediate solar neighborhood--a few hundred parsecs at most--since the sign reversal would continue down to $b \sim 0$ if the field reversal were more extended. This latter view supports the idea of a helical field, but only in the regions closest to the solar system. This close-in helical field has been supported by optical observations and will be discussed later.

Another fact evident from the figures is that the average residual increases as the line-of-sight approaches the galactic plane. Apparently the deviation from the model increases with the path length through the galactic medium. This would be expected if the deviations were due to inhomogeneities in either the electron density or the magnetic field. Table 4-1 presents the r.m.s. deviations for the 70% best-fit sources in each of several regions of galactic latitude. A similar difference in the r.m.s. deviation is seen between northern and southern sources, with the southern sources having generally higher residuals. The model predicts that the path length is 1.89 times longer for southern sources, so this variation is also explainable on the basis of inhomogeneities. The data of Table 4-1 clearly indicate that the r.m.s. intrinsic rotation

TABLE 4-1

LATITUDE DEPENDENCE OF DEVIATION FROM THE MODEL

$\|b\|$	Number of Sources	r.m.s Deviation of best 70%	Average Path Length
60°-90°	50	6.59 rad/m^2	0.60 D
40°-60°	80	14.7	0.74 D
20°-40°	82	20.1	1.1 D
0°-20°	67	38.9	2.8 D

measure for 'ordinary' sources--the 70% sample--is less than 6.6 rad/m^2. Therefore, at galactic latitudes of about 30°, the r.m.s. deviation due to inhomogeneities in the galaxy is between $\sqrt{20.1^2 - 6.6^2}$ = 19.0 rad/m^2 and 20.1 rad/m^2. For the same portion of the sky, $|b|$ = 20° to 40°, the r.m.s. of the rotation measures predicted by the model is only 10.3 rad/m^2. Thus it appears that the actual average value of $n|B|$ is three times that of the uniform field component alone. The actual factor is difficult to determine since it is not possible to decide whether the random part of the field structure is due to variations of the electron density, field strength, field direction, or various combinations. A non-random field direction would have angular characteristics different from those of a completely random field component, and the angular integration would be different and would therefore affect the average value of $n|B|$. An increase of the total field over the uniform field of 2 to 3 times seems reasonable.

Another way this factor may be determined is by examining the

entire sample of the 70% best-fitting sources. The r.m.s. deviation of this sample from the model is 16.8 rad/m^2, and the intrinsic Faraday rotation again has little affect on this number. The r.m.s. rotation measure calculated for this sample from the model is 7.3, and the total value of $n|B|$ is again perhaps three times the value for the uniform field alone. Since the uniform field has been found to be given by $C = 4.06 \times 10^5$ nBD, the total field can be given by $n_t B_t D \sim 6 \times 10^{-5}$ gauss-pc/cm^3. A D of 200 pc and n of 0.06 would then make the uniform component of B equal to 1.9 μgauss and the total field strength, B_t, equal to 5.7 μgauss. Again, it must be pointed out that the separation of the random field as being due to a random magnetic field could be specious as the variation may be due mostly to fluctuations in the electron density. The large-scale regions of field reversal do, however, indicate some substantial departures of the field direction from the uniform so that the above analysis is probably not far wrong.

The scale size of the fluctuations may also be somewhat crudely determined from the information of Table 4-1. Since the number of coherent regions is proportional to the pathlength, d, the r.m.s. deviation might be expected to increase as $\sqrt{d}$. This does appear to be the case for relatively low galactic latitudes as shown by the last two entries of the table, but the first two entries are probably unduly affected by the intrinsic rotations and errors in the rotation measure determinations. In any case it is not far wrong to set the r.m.s. deviations due to the fluctuations at

$$\langle \Delta RM \rangle = \beta \sqrt{Nd/D} \sim 20 \sqrt{d/D} \quad [rad/m^2] \qquad (4\text{-}2)$$

where N is the number of fluctuations in the distance D, and β is the average Faraday rotation due to one such coherent region. The latter is given by

$$\beta = 2 \times 8 \times 10^5 \, n \, B \, \frac{D}{N} = \frac{4 \, C}{N} \qquad (4\text{-}3)$$

where D/N is the diameter of one region and the approximate factor of two comes from the fact that the random rotation contribution is about twice that of the uniform, and we are interested in the random component. Substituting this into equation 4-2 yields

$$\beta\sqrt{N} = \frac{4 \, C}{\sqrt{N}} \sim 20$$

$$\text{or} \qquad N \sim (4 \, C)^2/20^2 \sim 4 \qquad (4\text{-}4)$$

That is, the scale size of the fluctuations is of the same order as D. This calculation is quite critically dependent upon the knowledge of the factor of two and of C but is probably sufficient for an order-of-magnitude estimate. The two field reversal regions are of approximately this size so that the entire r.m.s. deviation could be explained by field reversal regions of dimensions of about 50 to 200 pc. That is, the data are consistent with a uniform electron distribution and a uniform magnetic field component with magnetic field loops and reversals on a scale of 100 pc with field strengths of about twice the uniform component. It should be noted that the scatter of the residuals within a particular field-reversal area can be quite low. In the positive rotation measure area around l = 60°, b = +45° the residuals are essentially the

same within 8 rad/m^2. Regions smaller than 10 tO 20 pc probably have no appreciable effect on the scatter of the best-fitting 70%.

Jokipii and Lerche (1969) have derived a model for the latitude dependence of the observed r.m.s. scatter of the rotation measures based upon a disk with regions of correlation length L for which nB is essentially constant. Using the rotation measure data available at the time, they deduced a value of about 250 pc, the assumed thickness of the disk, for L. Since they had the incomplete data available then and since they failed to consider the peculiar distribution of the rotation measures (the few sources with the very high deviations), the exact numbers derived can no longer be considered valid. The main point, that the scale size of the fluctuations is of the same order as the thickness of the disk, is still reliable and confirms the somewhat less rigorous analysis above.

The 30% of the sources with the greatest deviations are an entirely different matter, bringing us to the third fact which can be deduced from the three figures, 4-6, 4-7, and 4-8. It was first postulated that the very highest rotation measures, since they had rotations far in excess of those of the majority of sources, were intrinsic to the source. Such a postulate would require an isotropic distribution of these sources in galactic coordinates. Figure 4-8 shows the distribution of the 30% largest residuals and clearly indicates that these are more concentrated near the plane. For example, of the 279 sources in the full sample, 50 are located such that $|b| \leq 60°$. If the top 30% of the residuals were isotropically distributed, 15 ± 4 should lie above $|b| = 60°$. There are

only 4. There should be 20 ± 5 for $|b| \leq 20°$ whereas there are 37. This shows considerable concentration towards the plane. If the magnitudes of the residuals are considered, the anisotropy is even more pronounced. The average value for the four high latitude residuals is 69 rad/m^2; that for the 37 residuals below 20° is 126 rad/m^2. Intrinsic rotation measures are insufficient to explain the behavior, and other mechanisms must be considered. The first is that the rotation measures may be incorrect. This is supported by the fact that, while 5% of the code six sources have residuals greater than 100 rad/m^2, 19% of the code five sources have such high residuals. The less certain the rotation measure determination, the more likely a high residual becomes. Surely, therefore, some of these extremely high residuals are due to errors. Such errors are most likely to occur for sources which have high rotation measures. Since these lie close to the plane, more errors are expected near the plane than at the poles. But this is not the only explanation of the phenomenon. Some of the code six sources do have high residuals, and these are very well determined, as explained in Chapter III.

Another factor which may cause large deviations would be small scale regions in the galaxy with intense magnetic fields and/or high electron densities. Compressed field regions around very old and therefore optically invisible supernova remnants could constitute such areas. Recently Michel and Yahil (1973) have postulated strong magnetic field trails behind stars, and these also could be a cause of the very highest rotation measure residuals. Large scale regions could not explain the phenomenon since a high residual often exists in the midst of sources

with very low residuals. The separation of the effects of such small-scale regions from that of errors in the rotation measure determinations does not appear possible with the present data.

The question of the intrinsic nature of the residuals must still be considered. Gardner, Morris and Whiteoak (1969b) have suggested that the galaxies tend to have higher intrinsic rotation measures than the quasars. The present work fails to substantiate that correlation. The distribution of source types--quasars, galaxies, or unidentified extra-galactic sources--for the sources with the highest residuals was essentially the same as for the entire sample of 279. Table 4-2 shows the r.m.s. residuals for the 70% of the sources with the lowest residuals as a function of galactic latitude and source type. This table shows

TABLE 4-2

RESIDUALS FOR DIFFERENT SOURCE TYPES

Type	$\|b\| \geq 60°$		$\|b\| < 60°$	
	Number	$\sqrt{\langle \Delta RM^2 \rangle}$	Number	$\sqrt{\langle \Delta RM^2 \rangle}$
QSO	11	7.8 rad/m^2	15	16.7 rad/m^2
GALAXY	16	6.3	25	13.7
UNKNOWN	8	5.2	16	14.2

that the average 'intrinsic' rotation measure is the same for each classification, within statistical limits. Since the r.m.s. intrinsic rotation has been shown to be less than 6 or 7 rad/m^2, and since the typical uncer-

tainty in the rotation measures of Table 3-2 is nearly that high, it is doubtful whether most sources have any intrinsic rotation. A few individual sources may, however, have large intrinsic Faraday rotations.

Since the entire development of the model started with the premise that sources with exceptionally high rotation measures are not really representative of the galaxy and were therefore discarded from the model calculation, the legitimacy of the entire procedure might now reasonably be questioned. The contention is that the procedure was valid because the high rotation sources did differ from the majority by being non-representative either because the measurement was in error and therefore discardable, or because of some intervening small-scale, high rotation region. In the latter case, the source is of no importance because the model is not sensitive to such small-scale regions, and the deviations of the majority of the sources have been attributed to large-scale structure. Such small-scale structure cannot have had any effects on the calculations. Finally, inclusion of all the data did not significantly affect any of the derived parameters except the galactic latitude of the magnetic field direction.

A brief summary of the important results is in order before proceeding. All data are consistent with the combination of a linear field in the direction $l = 94^\circ$ and parallel to the galactic plane with loops and field reversals on the scale of 100 or 200 pc. The uniform field component is given by $C = 4.06 \times 10^5$ $nBD = 9.49 \pm 0.13$ where D is the thickness of the galactic disk in pc. The total field strength, being the sum of the uniform field and the loops, is around three times as

great. The integral of nB is about 1.9 times as great for directions in the southern galactic hemisphere as for northern directions, corresponding to a height above midplane of 0.15 D for the sun for a uniform field and electron distribution. Small-scale inhomogeneities do not affect the rotation measures of the great majority of the sources, although a few undoubtedly are so affected.

If even smaller scale inhomogeneities existed over any significant portion of the sky, some depolarization of the sources as pathlength increases is to be expected. That is, if the source is partially covered by more than one very small scale inhomogeneity with random rotation measures, their contributions would be expected to cancel partially. Therefore some correlation of the depolarization characteristics with galactic latitude might be expected. Attempts were made to find a correlation between either the existence or maximum frequency of depolarization as defined by Table 3-5 and the galactic latitude. Samples were drawn from the worst 30% of the sources, the best 70%, or all of them for various combinations of the quality codes. No significant correlations were discovered; the depolarization characteristics of the radio sources seem to be independent of galactic coordinates, so that such characteristics are probably entirely internal to the source. Therefore very fine scale fluctuations in the galactic medium probably do not exist to any great degree. Since the definition of depolarization is not very rigid, as explained in the previous chapter, it is not possible to be more quantitative about this effect.

Other field models were also examined for significant correlations.

One possibility was that all the rotation occurred very near the sun and the thickness of the galactic disk had no effect. In such a case the rotation measure distribution would be given by RM = C' $\underline{B}\cdot\hat{r}$ where $\hat{r}$ is a unit vector in the direction of the line-of-sight. The same behavior might be expected for Faraday rotation external to the galaxy caused by intergalactic fields and electrons. This model did show some correlation due to the $\underline{B}\cdot\hat{r}$ dependence of the actual model, but not with such strong significance. For example, for the complete sample of 279 sources this model provided a maximum correlation coefficient of only 0.121 compared with the 0.209 for the original model and had negligible success in lowering the r.m.s. residuals. The field direction derived from this was always about 100°, -10°, the same as calculated for the adopted version.

Another model tried was the helical field. This has been one of the more popular models since early data indicated such a field was not impossible and confirmation seemed to be present in the optical data. The highest correlations for helical fields were obtained where the pitch angle, shear and axis direction were such that the field closely approximated the linear model, and the correlations were consistently lower than those obtained for the linear model. The helical field does not seem adequate to explain the rotation measure data. In the past there was almost no information available for $0° < l < 180°$ and $0° < b < +30°$, and what little there was indicated that the region had positive rotation measures. This apparent reversal with respect to the data below the galactic equator was the strongest evidence for the helical field. The

presented work has added a large number of data points in the region and shows that the negative rotation measure region does extend above the equator. While the helical field model is ruled out on the larger scale, it is still an acceptable possibility for the more local regions, as has been discussed before in connection with the 100 to 200 pc loops and reversals. The subject of a local helical field will be taken up again when the polarization of starlight is considered.

B. Comparisons with Other Data

Pulsar Rotation and Dispersion Measures

Pulse dispersion measurements on pulsars allow the line-of-sight electron content to be determined. The dispersion measure, DM, is defined as

$$DM \equiv \int n_e dl \qquad (4\text{-}5)$$

where n_e is the electron density in cm^{-3} and l is in parsecs. The integral is along the line-of-sight. If the rotation measure can also be measured for the pulsar, a partial separation of the line-of-sight integrals of the electron density and the longitudinal component of the magnetic field may be made. In particular,

$$B_{l,e} = \frac{\int n_e \underline{B} \cdot d\hat{l}}{\int n_e \, dl} \qquad (4\text{-}6)$$

where B_l is the longitudinal field in microgauss. This gives the average field only in the case where the distributions of $\underline{B}$ and n_e are not correlated as is believed to be the case. Based on 21 pulsars for which

both RM and DM are known, Manchester (1972) has derived a linear field of about 3.5 μgauss directed towards $l = 90°$. There is also indication that sources farther than 200 or 300 pc show a reduction in their Faraday rotation. This is quite consistent with the model proposed in the first section. The 3.5 μgauss field is that of the local region, and the more distant pulsars have contributions from other areas with a generally differently oriented field. The observed field strength is in good agreement with the value predicted for the homogeneous regions of 100 pc extent. Assuming an average electron density of 0.06 cm^{-3} (Spitzer, 1968) and a thickness of 200 pc (Woltjer, 1965), equation 4-1 puts the uniform field component at 2.0 μgauss. This would give total fields of 4 to 6 μgauss for the coherence regions, only slightly higher than Manchester's local field value.

The derivation of the form of the local field--linear or helical--and its axial direction from the pulsar data is not so definite. Manchester feels that the helical model is ruled out, but there is actually insufficient coverage of the sky to confirm that.

Stellar Polarizations

Starlight has long been observed to be partially polarized. The polarization is attributed to the alignment of the interstellar grains by a magnetic field in accordance with the model of Davis and Greenstein (1951), which predicts a plane of polarization in the direction of the transverse component of the magnetic field. The degree of the polarization is related to grain structure and material, grain and gas tempera-

tures, and other factors, as well as to the strength of the magnetic field. It is therefore difficult to deduce much about the strength of the magnetic field from the interstellar polarizations, though the best estimates at present give a lower limit of about 7 μgauss (Davis and Berge, 1968). The direction of the polarization can, however, give considerable aid in deducing the magnetic field structure in at least the local arm, especially since there are so many polarization measurements available which can be studied as a function of distance through the galactic medium.

Figure 4-9 illustrates the most currently published data of Mathewson and Ford (1970). As is the case for the rotation measure data, there has been considerable controversy in the proper interpretation of these distributions. Without a knowledge of the tangential direction of the field it is not possible to distinguish between helical and linear models. These polarization measurements are not necessarily directly comparable with rotation measures of either extragalactic sources or pulsars. First, the rotation measure determined fields are weighted by the electron density while the stellar polarizaiton determined fields are weighted by the distribution of grains, and the distributions may not be at all correlated. Second, Michel and Yahil (1973) have shown that stellar polarizations could be caused by magnetic field 'wakes' trailing behind the stars. If this were the case, the stellar polarizations could easily give results very different from those obtained from the rotation measure data.

Considering only the polarization of starlight, the most simple and

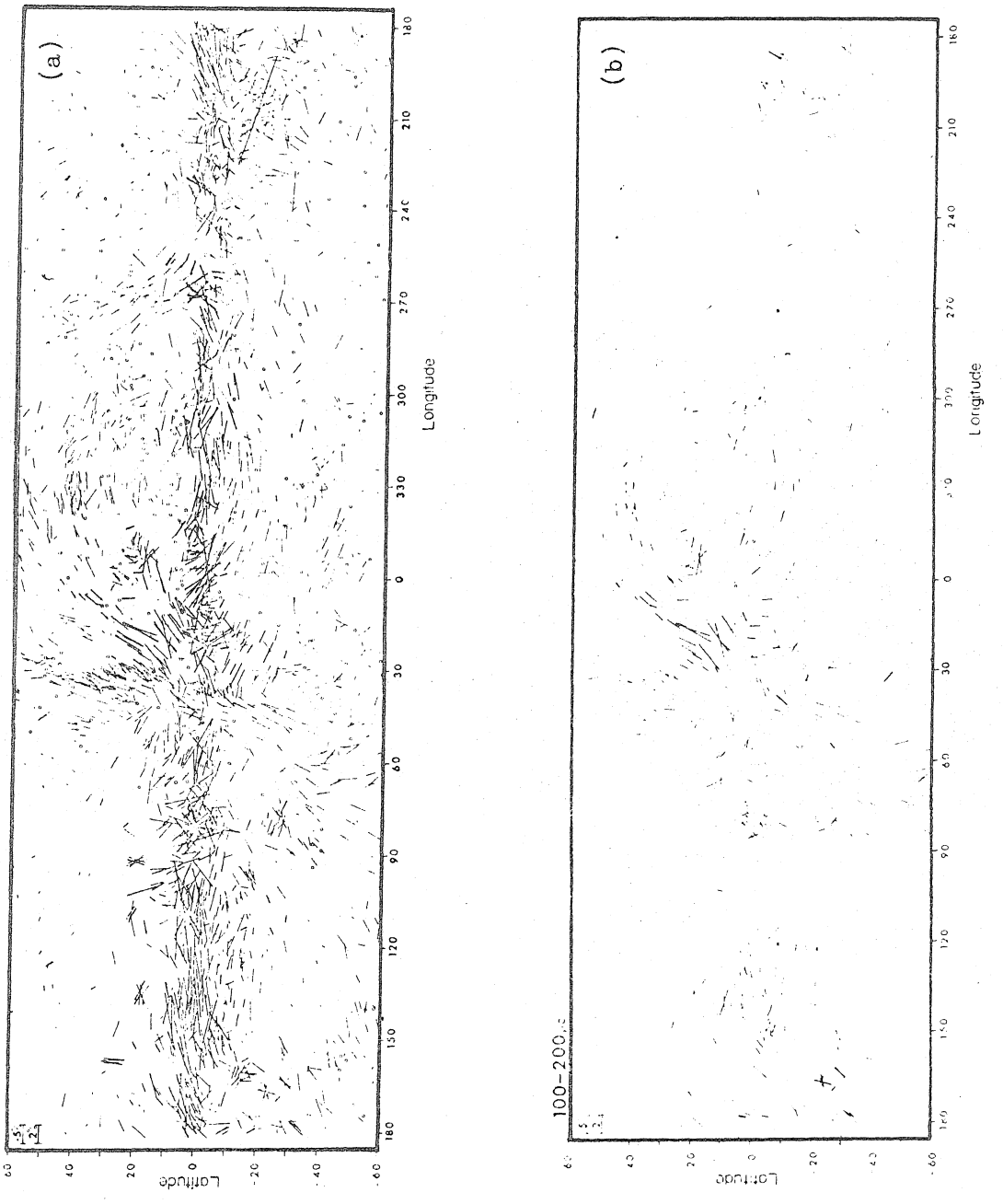

Fig. 4-9(a) and (b).--These figures give the distribution of the stellar polarization measurements with respect to galactic coordinates. The lengths of the individual line-segments indicate the degree of polarization while the direction gives the position angle. From Mathewson and Ford (1970).

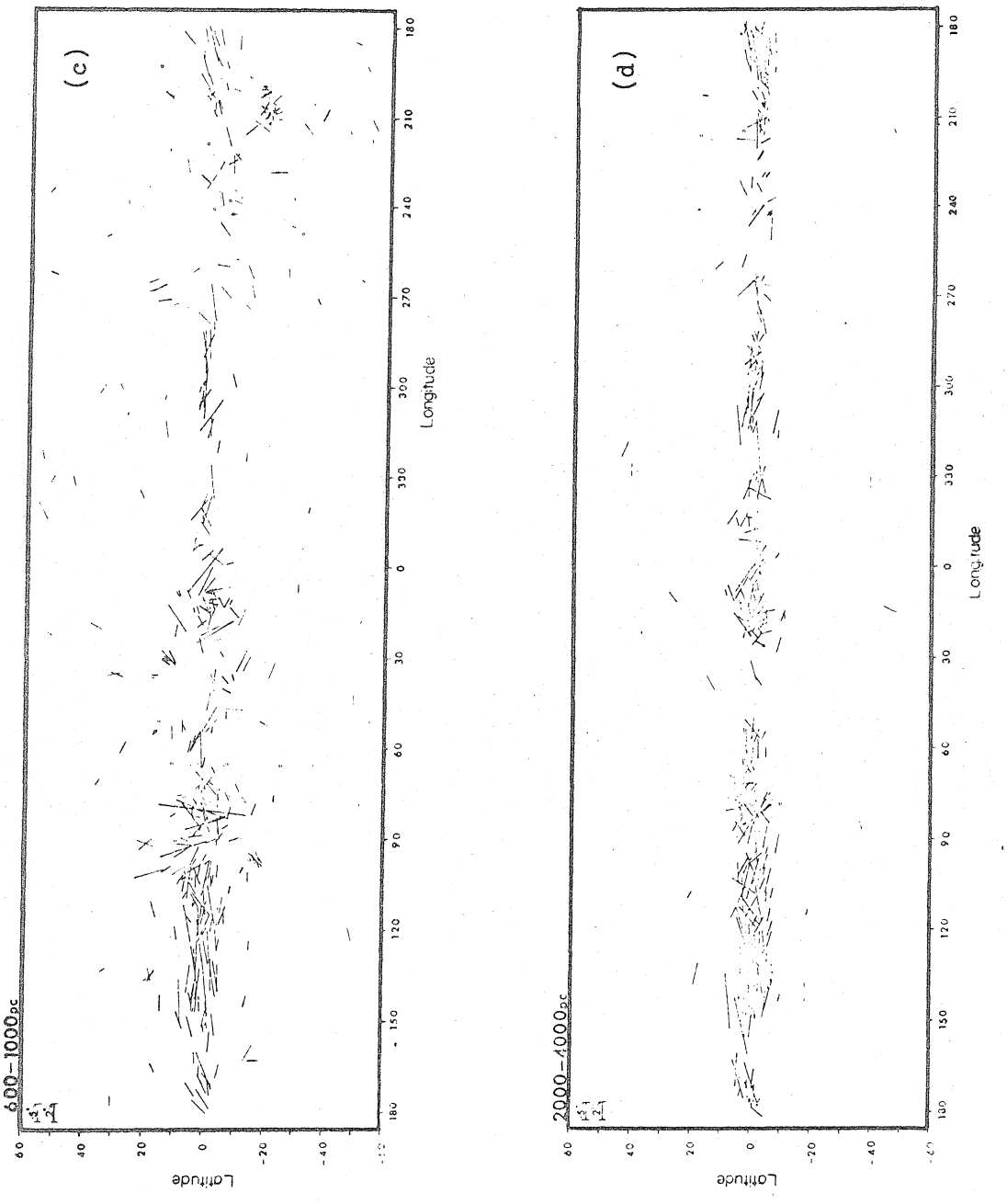

Fig. 4-9(c) and (d).--Figure (a) gives the entire sample of 1800 stellar polarizations while (b) gives those stars between 100 and 200 pc from the sun, (c) gives those between 600 and 100 pc distant, and (d) gives those between 2000 and 4000 pc distant. From Mathewson and Ford (1970).

satisfying model is that of Verschuur (1973) who proposed that the major contribution is from a linear field in the plane directed along the line between $l = 50°$ and $l = 230°$. In addition, there is some sort of anomaly in the direction of Cygnus, $l = 80°$, plus some other minor irregularities.

This disagrees with our model for the rotation measures, which derives a linear field directed towards 94°, or approximately in the direction of the Cygnus 'anomaly'. Verschuur errs here in declaring there is no hydrogen feature in this direction since the Carina-Cygnus arm lies in approximately this direction for several kpc (e.g., see Kerr and Westerhout, 1965). The Cygnus galactic emission maximum is also in this direction (e.g., Berkhuijsen, 1971). The real difficulty here is that of the different distributions of electrons and dust. While the stellar polarizations do show a confused region around $l = 80°$ or 90° indicating a field in that direction, it is minor compared with the overall pattern. Presumably this could be due to the different weighting effects.

We have assumed that the anomalous rotation measures indicating field reversals around the north galactic spur are due to local phenomena. If so, these signs indicate the most probable sense for the longitudinal fields. This could either indicate that the field in the local coherence region is directed towards 230° or that the field is helical or even more complex. In the absence of more extensive pulsar rotation measures the question of the local field structure cannot be uniquely answered. The extragalactic rotation measures rule out any helical structures on a scale of 1 or 2 kpc.

Verschuur raises the possibility that at distances beyond 14 kpc from the galactic center the distribution of matter and fields can extend far beyond the flat disk model generally accepted. If so, the rotation anomalies associated with the spurs are most likely to be unaffected since lines-of-sight directed more-or-less towards the center of the galaxy should pass through little of the material lying out of the plane. The great probability is that the rotation measures of extragalactic sources do provide the sense of the local field at the higher latitudes, and the pulsars can be used to fill in the lower regions.

The field models for both the Faraday rotation of extragalactic sources and the interstellar polarizations are consistent with a large scale (1-2 kpc) linear field directed towards $l = 94°$ plus a more local field, either linear or helical, with an axis most likely along $l = 50°$. This second field is probably inconsequential beyond a few hundred pc since the 2000-4000 pc stars of Figure 4-9(d) seem to favor the 90° field direction.

Zeeman effect

Zeeman splitting of the 21 cm neutral hydrogen emission line has been observed in several regions (Verschuur, 1971). This effect is proportional to the strength of the magnetic field in the emitting or absorbing region and can provide information on the longitudinal sense of the field--toward or away from the observer. Typical observed field strengths are 2 to 7 μgauss and are wholly consistent with the average

total field of 4 to 6 μgauss predicted by the model developed here. Verschuur (1973) has pointed out that the direction of the field in the direction of the Crab Nebula is opposite to that observed for the rotation measures. Such field reversals for various portions of the line-of-sight are a central part of the model developed to explain the deviations in the rotation measures and again confirm that the galactic fields are very complex and not completely explainable by a simple linear or helical model. Field reversals have also been observed in the direction of the Perseus arm.

Zeeman data have a third form of weighting for the magnetic field. Whereas the rotation measures are sensitive to the field in regions where there are electrons and stellar polarizations weight the field by the dust distributions, the Zeeman effect shows only the fields in the hydrogen clouds. The fields in each of these three regions may be very different.

Galactic Synchrotron Radiation

High energy electrons interact with the galactic magnetic field to create synchrotron radiation in the standard fashion. The polarization of this radiation provides information on the transverse field direction and the intensity measures the strength of the magnetic fields present. A good review of the galactic coordinate dependence of the data is given by Berkhuijsen (1971). These data provide the observational base for the existence of the galactic spurs. On the basis of this radiation the galactic field has been assigned upper limits of 20 μgauss for the disk

and 5 for the halo (Davis and Berge, 1968). These values are in no way restrictive upon the field model developed here. A local maximum of this radiation exists along the Carina-Cygnus arm, $l = 80°$, again showing that there is most likely an arm and field in that direction.

Berkhuijsen (1971) also presents highly detailed maps of the distribution of polarization and position angle for the galactic radiation. These distributions are very complex and, while there is a concentration of large polarizations with random position angles near $l = 80°$ or $90°$, the interpretation of the data is not straightforward. Since the radiation is being generated in the same region in which rotation is occurring, there is no reason to expect a linear Faraday rotation curve. Moreover, the high degree of rotation experienced by some of the radiation makes the relationship between the observed position angle and the field direction very doubtful. Some help could be provided if rotation measures for the galactic radiation from all directions could be obtained; but, since most observations have been made at relatively low frequencies, what little information exists is useless for determining rotation.

Hydrogen Absorption Measurements

While observations of the 21 cm emission provide no information on either the fields (except for Zeeman splitting) or the electrons, the data have been used to define the galactic plane and to determine various geometric parameters. In particular, the plane has been observed to be about 220 pc thick by Schmidt (1957) and has subsequently been calculated to be approximately that thickness many times. There is evidence

(Verschuur, 1973) that the disk becomes substantially thicker at 10 kpc or farther from the sun, but locally there is agreement. Additionally, the continuous emission provides an estimate of 200 pc for the thickness of the disk of electrons. Electrons and hydrogen are therefore likely to be distributed in a similar manner. Detailed 21 cm observations indicate that the sun may be located slightly above the plane, the distance being 4 ± 12 pc (Kerr and Westerhout, 1965). On the basis of the model, assuming a 200 pc thick disk of electrons, the distance is given by 100 α = 31 pc above the plane for α = 0.31. The uncertainty of this value is only ±3 pc, but this number is not directly related to the 4 pc value for the hydrogen. The 31 pc figure is based upon the distribution of electrons and field and may be interpreted as the existence of more electrons below the sun, or a stronger field in the lower part of the plane, or both. The separation of the effects is not possible at present. Additional pulsar data may help solve the problem.

C. Intergalactic Magnetic Fields

Much attention has been given to the possibility that extragalactic rotation measure statistics may provide a means of detecting a linear component of any intergalactic magnetic field. This is of considerable interest to those studying the evolution of galaxies, clusters of galaxies and the universe as a whole. Reinhardt (1972) has derived the redshift dependence of the rotation measures due to a uniform linear field throughout the universe as

$$RM = K\, n_{eo} B_o\, 2c\, \Omega^{-1} H_o^{-1} \{\frac{z}{3}(1+\Omega z)^{1/3} + [1-z(3\Omega)^{-1}][(1+\Omega z)^{1/2}-1]\} \cos\theta \qquad (4\text{-}7)$$

where $K = 8.12 \times 10^5$, H_o is the Hubble Constant, and n_{eo} is the electron density at the present epoch. $\Omega = \rho_o/\rho_c$ where ρ_o is the mean matter density and ρ_c is the critical density at the present epoch. The angle between the line-of-sight and the field direction is θ. Reinhardt examined the available rotation data for sources with known redshifts for possible correlations with

$$RM = m\, f(z) \cos\theta + c \qquad (4\text{-}8)$$

where the function of z taken as 1, $(1+z)^{2/3}$, or $(1+z/10)^{1/2}(z/17-1) + 1$, depending on the cosmology. Since the z-dependent functions gave slightly better correlations than the constant for several samples, it was argued that a z dependence and hence an extragalactic field was possible. Unfortunately the direction of the field providing the maximum correlation was about the same as that derived for the present model of the galactic field, suggesting the claimed effect is not extragalactic. Attempts to make the same correlations on what were then thought to be the intrinsic rotation measures failed. The one explanation that comes to mind is that the observed correlations were due entirely to the cos θ term and that the z-functions gave better fits merely due to statistical variations of the data.

On repeating the same analysis on the present set of data, which consists of 128 sources with both redshifts and rotation measures, the opposite results were obtained. That is, taking the best-fitting 70%

of the code 3, 5 and 6 sources with redshifts, correlations were made with the three separate functions tried by Reinhardt. The 83 sources gave maximum correlation coefficients of 0.523, 0.391, and 0.381 for the three functions, respectively. The best field direction was within 10° of that found for the galactic model. Samples were divided on the basis of source type and galactic latitude with essentially the same result. This method gives no evidence of any redshift dependence.

A more sensitive test is the similar examination of the residuals for all the sources after the galactic model has been subtracted. In this case the correlations were 0.166, 0.171, and 0.177, respectively, for field directions towards $l = 90°$, $b = +30°$. These correlations are all at about the 10% level for 83 sources and probably reflect the RM irregularities due to the local region as described in the preceding sections. The differences in the coefficients are not significant. Further attempts using the sources with higher residuals and sources with different quality codes and identifications and latitudes yielded similar results.

Although no linear intergalactic magnetic field was detected, an upper limit on the product of such a field and the intergalactic electron density would prove useful. Such a number is difficult to establish because of the peculiar two-population distribution of the rotation measures and their residuals. However, if the extragalactic RM contribution were as large for $z = 2$ as that of the model at high latitudes, say RM = 10 rad/m^2, some correlation would surely have been noticed. This would correspond to $n_e B$ on the order of 10^{-14} or 10^{-13} gauss cm^{-3},

assuming a Hubble constant of 50 and depending on the particular cosmology used. In any case, it does not seem that a uniform component of an extragalactic magnetic field can be any greater than $2 \times 10^{-13}/n_e$ gauss, although a tangled field could be much stronger. This is not a very restrictive upper limit since cosmologies tend to set maximum values of 10^{-7} or even 10^{-8} gauss for B and n_e is felt to be around 10^{-5} or 10^{-6} cm^{-3} (Reinhardt, 1972). The field could, of course, be even stronger than this limit if positron clouds of about the same abundance as the electrons, existed in intergalactic space. Positrons would cancel the rotation caused by the electrons since they are of opposite charge.

At present the rotation measures of extragalactic sources seem to provide little information on extragalactic fields. This is to be expected since the variations of the rotations due to the galactic field are so great, but should not discourage additional examination of this method of probing intergalactic space.

D. Conclusion and Summary

The knowledge of the rotation measures of extragalactic radio sources in the northern hemisphere has been greatly increased by the measurement of the polarization properties of 206 3C sources at 21, 18 and 6 cm. Combining these new polarization measurements with all available past data has led to 354 known rotation measures. The quality and understanding of the uncertainties for these rotation measures of radio sources is considerably improved over past efforts.

Examination of the 279 extragalactic radio sources with the highest

quality rotation measures has led to a model of the local galactic magnetic field based on a uniform disk of electrons, thickness D, and a uniform linear field. The peculiar distribution of the values of the rotation measure has forced the development of an editing procedure which allows the examination of the central core and broad wings of the rotation distribution separately. The 70% to 90% of the sources which fit the model best show a linear magnetic field in the direction $l = 94° \pm 3°$, $b = -8° \pm 8°$ with magnitude such that 4.06×10^5 nBD = 9.49 ± 0.13 cm^{-3} gauss pc. For $n = 0.06$ cm^{-3} and D = 200 pc, B = 2.0 microgauss. An analysis of the distribution of the residuals with respect to galactic latitude led to the conclusion that there are loops and field reversals, or possibly variations in electron density, on a scale of the order of 100 to 200 pc. The total field strength in these regions is 2 to 3 times the uniform component of 2.0 microgauss.

The largest residuals are concentrated towards the plane indicating that most are not intrinsic to the source but are caused by errors in the rotation measure determination or by small-scale structure in the galaxy. Some sources probably do have high intrinsic rotation measures, but perhaps 90% of the intrinsic Faraday rotations are less than 6 rad/m^2.

The integral of n_eB for lines-of-sight in the southern galactic hemisphere appears to be 1.89 times as great as for those towards positive galactic latitudes. If the field and electrons were uniformly distributed, this would be equivalent to a height above the galactic midplane of 31 ± 3 pc for the sun.

Searches for correlations of the rotation measures with source

characteristics, depolarization measurements, and an extragalactic field failed to yield positive results. An upper limit of 2×10^{-13} gauss cm^{-3} was established for the product of the extragalactic electron density and the field strength of a uniform, linear component of the extragalactic magnetic field.

Almost all of these conclusions are consistent with the other sources of information on the galactic magnetic field: Zeeman effect, cosmic rays, synchrotron radiation, pulsar rotation and dispersion measures, and optical polarizations. The only major discrepancy is that the optical polarizations seem to show a linear or helical field directed towards $l = 50°$ with a minor feature at 80° or 90°. This discrepancy can be explained by differences in the galactic distributions of electrons and dust, and by realizing that a helical or linear field towards 50° within a few hundred parsecs of the sun could be consistent with the high latitude rotation measure data.

REFERENCES

Arp, H.C., et al. 1972, Ap. J. (Letters), 171, L41.

Berkhuijsen, E.M. 1971, Astron. and Astrophys., 14, 359.

Berge, G.L. 1965, Ph.D. Thesis, California Institute of Technology, Pasadena, California.

Berge, G.L., and Seielstad, G.A. 1967, Ap. J., 148, 367.

———. 1972, A. J., 77, 810.

Bologna, J., et al. 1965, Ap. J., 142, 106.

Bologna, J., McClain, E.F., and Sloanaker, R.M. 1969, Ap.J., 156, 815.

Bolton, J.G., Clarke, M.E., and Ekers, J. 1965, Aust. J. Phys., 18, 627.

Bolton, J.G., and Ekers, J. 1966a, Aust. J. Phys., 19, 559.

———. 1966b, ibid., 49, 471.

Bolton, J.G., and Wall, J.V. 1970, Aust. J. Phys., 23, 789.

Burbidge, E.M. 1967a, Ann. Rev. Astr. and Ap., 5, 399.

———. 1967b, Ap. J. (Letters), 149, L51.

———. 1970, ibid., 160, L33.

Burbidge, E.M., and Burbidge, G.R. 1972, Ap. J., 172, 37.

Burbidge, E.M., and Strittmatter, P.A. 1972a, Ap. J. (Letters), 172, L37.

———. 1972b, ibid., 174, L57.

Burn, B.J. 1966, M.N.R.A.S., 133, 67.

CSIRO Radiophysics Staff. 1969, Aust. J. Phys. Astrophys. Supp., 7.

Clarke, M.E., Bolton, J.G., and Shimmins, A.J. 1966, Aust. J. Phys., 19, 375.

Conway, R.G. 1972, private communication.

Conway, R.G., et al. 1972, M.N.R.A.S., 157, 443.

Davies, Kenneth. 1966, Ionospheric Radio Propagation. New York: Dover Publications, Inc.

Davis, L., Jr., and Berge, G.L. 1968, "Evidence for Galactic Magnetic Fields," in Stars and Stellar Systems, Vol. VII. Edited by B.M. Middlehurst and L.H. Aller. Chicago: University of Chicago Press.

Davis, L., Jr., and Greenstein, J.L. 1951, Ap. J., 114, 206.

deVeny, J.B., Osborn, W.H., and Janes, K. 1971, P.A.S.P., 83, 611.

Gardner, F.F., and Davies, R.D. 1966a, Aust. J. Phys., 19, 129.

———. 1966b, ibid., 19, 441.

Gardner, F.F., Morris, D., and Whiteoak, J.B. 1969a, Aust. J. Phys., 22, 79.

———. 1969b, ibid., 22, 813.

Gardner, F.F., and Whiteoak, J.B. 1963, Nature, 197, 1162.

———. 1966, Ann. Revs. Astr. and Ap., 4, 245.

———. 1969, Aust. J. Phys., 22, 107.

Gardner, F.F., Whiteoak, J.B., and Morris, D. 1969, Aust. J. Phys., 22, 821.

Greisen, E.W. 1972, Ph.D. Thesis, California Institute of Technology, Pasadena, California.

Hobbs, R.W., and Haddock, F.T. 1966, Ap. J., 147, 908.

Hobbs, R.W., and Hollinger, J.P. 1968, Ap. J., 154, 423.

Hollinger, J.P., and Hobbs, R.W. 1968, Ap. J., 151, 771.

Hornby, J.M. 1966, M.N.R.A.S., 133, 213.

Jokipii, J.R., and Lerche, I. 1969, Ap. J., 157, 1137.

Kerr, F.J., and Westerhout, G. 1965, "Distribution of Interstellar Hydrogen," in Stars and Stellar Systems, Vol. V. Edited by A. Blauuw and M. Schmidt. Chicago: University of Chicago Press.

Kraus, J.D. 1966, Radio Astronomy. New York: McGraw Hill, Inc.

Kronberg, P.P., and Conway, R.G. 1970, M.N.R.A.S., 147, 149.

Maltby, P., and Seielstad, G.A. 1966, Ap. J., 144, 216.

Manchester, R.N. 1972, Ap. J., 172, 43.

Mathewson, D.S. 1969, Proc. Astron. Soc. Aust., 1, 209.

Mathewson, D.S., and Ford, V.L. 1970, Mem. R.A.S., 74, 139.

Matthews, T.A., Morgan, W.W., and Schmidt, M. 1964, Ap. J., 140, 35.

Michel, F.C., and Yahil, A. 1973, Ap. J., 179, 771.

Mitton, S. 1972, M.N.R.A.S., 155, 373.

Moffet, A.T. 1962, Ap. J. Suppl. No. 67.

Morris, D., and Berge, G.L. 1964a, Ap. J., 139, 1388.

———. 1964b, A. J., 69, 641.

Morris, D., and Radhakrishnan, V. 1963, Ap. J., 137, 147.

Morris, D., Radhakrishnan, V., and Seielstad, G.A. 1964, Ap. J., 139, 551.

Pacholczyk, A.G., and Swihart, T.L. 1967, Ap. J., 150, 647.

———. 1970, ibid., 161, 415.

———. 1971, ibid., 170, 405.

———. 1973, ibid., 179, 21.

Parker, E.N. 1969, Space Sci. Rev., 9, 651.

Ratcliffe, J.A. 1972, An Introduction to the Ionosphere and Magnetosphere. Cambridge: Cambridge University Press.

Read, R.B. 1963, Ap. J., 138, 1.

Reinhardt, M. 1972, M.N.R.A.S., 19, 104.

Reinhardt, M., and Thiel, M.A.F. 1970, Astrophys. Lett., 7, 101.

Sandage, A. 1966, Ap. J., 145, 1.

———. 1967, Ap. J. (Letters), 150, L146.

Sastry, Ch.V., Pauliny-Toth, I.I.K, and Kellermann, K.I. 1967, A. J., 72, 230.

Schmidt, M. 1957, B.A.N., 13, 247.

———. 1965a, Ap. J., 141, 1.

———. 1965b, "Rotation Parameters and Distribution of Mass in the Galaxy," in Stars and Stellar Systems, Vol. V. Edited by A. Blauuw and M. Schmidt. Chicago: University of Chicago Press.

———. 1972, private communication.

Silver, S., ed. 1965, Microwave Antenna Design and Theory. New York: Dover Publications, Inc.

Sofue, Y., et al. 1968, Publ. Astron. Soc. Japan, 20, 388.

Sofue, Y., Fujimoto, M., and Kawabata, K. 1969, Publ. Astron. Soc. Japan, 20, 368.

Spitzer, Lyman, Jr. 1968, Diffuse Matter in Space. New York: John Wiley and Sons.

Tritton, K.P. 1972, M.N.R.A.S., 155, 1P.

Verschuur, G.L. 1971, Ap. J., 165, 651.

———. 1973, IAU Colloquium No. 23.

Woltjer, L. 1965, "Dynamics of Gas and Magnetic Fields; Spiral Structure," in Stars and Stellar Systems, Vol. V. Edited by A. Blauuw and M. Schmidt. Chicago: University of Chicago press.

Wyndham, J.D. 1966, Ap. J., 144, 459.